Tropospheric Ozone Production Pathways with Detailed Chemical Mechanisms

Dissertation zur Erlangung des akademischen Grades
des Doktors der Naturwissenschaftern
am Fachbereich Geowissenschaften
an der Freien Universität Berlin

Vorgelegt von
Jane Coates
im Juli 2016

Freie Universität Berlin

Acknowledgements

Table of Contents

List of Tables

List of Figures

Chapter 1

Introduction

Air pollution is the leading environmental health risk in many areas around the world. The effects of air pollution to the general population range from chronic to less severe health impacts and reduced growth rates of vegetation resulting in economic losses of billions of euros (EEA, 2015). Moreover, the International Agency for Research on Cancer labelled air pollution as carcinogenic (IARC, 2013). Due to these impacts, many governed areas introduced legislation designed to reduce concentrations of many air pollutants.

Tropospheric ozone (O_3) is one of the most problematic air pollutants over Europe with up to 98 % of Europe's urban population exposed to concentrations of ozone above the WHO guidelines (EEA, 2015). Furthermore, in 2011 the EU ozone target value for human health (the EU has no limit value for ozone) was exceeded in 65 % of the EU member states and Europe's ozone target value for vegetation was exceeded in 27 % of the EU-28 agricultural areas (EEA, 2013).

Reducing atmospheric concentrations of tropospheric ozone is a complex problem as ozone is not directly emitted into the troposphere. Tropospheric ozone is produced from the reactions of volatile organic compounds (VOCs) in the presence of nitrogen oxides ($NO_x \equiv NO + NO_2$) and sunlight (Atkinson, 2000). Meteorology and transport also influence tropospheric ozone levels (Jacob and Winner, 2009).

Air quality (AQ) models are an important tool for understanding ozone pollution and predicting future air quality. Many AQ models are available with different scales and dimensions depending on the scope of the modelling experiment. Accurately representing the complexity of ozone production in a computationally efficient model is an ongoing challenge for the modelling community (Russell and Dennis, 2000).

Model intercomparison projects (MIPs) compare the outputs from different models showing differences in tropospheric ozone due to differing representations of key processes. For example, ACCMIP (Atmospheric Chemistry and Climate Model Intercomparison Project) showed different magnitudes of future ozone burden in the same region (Young et al., 2013). A current MIP, CCMI (Chemistry Climate Model Initiative), aims to investigate differences in the representation of chemistry, emissions and transport processes between models to understand the differences between predictions from global models (Eyring et al., 2013).

Detailed process studies are key to understanding differences between simulated ozone levels using different models. This thesis focuses on the influence on ozone production from the representation of VOC degradation chemistry, VOC emissions and the ozone-temperature relationship within models with the research questions framing this work found in Sect. 1.5. This assessment should be beneficial to the modelling community in understanding potential differences between model outputs and improving AQ models. The remainder of this introduction discusses ozone in the atmosphere, the chemistry and sources of ozone as well as the effects of meteorology on ozone production.

1.1   Ozone

Ozone is a atmospheric gas found in the stratosphere and troposphere, however its atmospheric effects are very different in these regions. The stratosphere contains ~ 90 % of the atmospheric ozone with a peak mixing ratio of ~ 12 ppm (Seinfeld and Pandis, 2006). Stratospheric ozone absorbs the sun's ultraviolet radiation which is important due to the adverse effects of excess UV radiation on humans and ecosystems.

In contrast, tropospheric (or surface) ozone is both a pollutant and a greenhouse gas. Increased levels of tropospheric ozone are harmful to humans, plants and other living systems. High ozone exposure may lead to pulmonary problems in humans and can decrease both crop yields and forest growth (World Meteorological Organisation, 2011).

Tropospheric ozone is formed via photochemical production from the reactions between VOCs and NO_x, described in Sect. 1.2, while meteorology and atmospheric transport also influence ozone concentrations. For example, a spring-time peak in tropospheric ozone is common in the Northern Hemisphere (NH)

mid-latitudes, originally attributed to transport of ozone from the stratosphere into the troposphere via the Stratosphere-Troposphere Exchange (STE) (Monks, 2000). However, ozone transported via STE rarely influences surface ozone levels (Lelieveld and Dentener, 2000) and the spring maximum is due to the photochemical reactions occuring in the NH spring after the buildup of reservoir species over winter (Penkett and Brice, 1986). For the rest of this thesis, ozone refers to tropospheric ozone.

Understanding the intracacies of surface ozone pollution requires a combined effort from the modelling, observational and chemical kinetic communities – called the "three-legged stool" approach by Abbatt et al. (2014). Modelling of ozone production helped understand the complexity of atmospheric chemistry, such as the non-linear relationship of ozone production with precursor (VOC and NO_x) emissions. Modelling studies attempt to reproduce observational trends of surface ozone and model predictions may inform new observational studies. Chemical kinetic studies performed by laboratories give insights to missing or incorrect representations of atmospheric chemistry to be included in updated models.

1.2   Ozone Chemistry

Ozone absorbs UV radiation producing either ground-state atomic oxygen ($O(^3P)$) or excited singlet ($O(^1D)$) oxygen atoms.

$$O_3 + h\nu \rightarrow O_2 + O(^3P) \tag{R1}$$

$$O_3 + h\nu \rightarrow O_2 + O(^1D) \tag{R2}$$

Ground-state oxygen quickly reacts with oxygen to reform ozone.

$$O(^3P) + O_2 \xrightarrow{M} O_3 \tag{R3}$$

Thus there is no net loss or production of ozone through (R1) and (R3). $O(^1D)$ may collide with N_2 or O_2 (represented as M in chemical reactions) stabilising to the ground-state. This process again leads to a null cycle with ozone destruction balanced by production. However, $O(^1D)$ can react with water vapour producing hydroxyl (OH) radicals. The OH radical is a highly reactive chemical species reacting with almost all trace chemical species in the troposphere. (Seinfeld and Pandis, 2006; Monks, 2005)

$$O(^1D) + H_2O \rightarrow 2\,OH \tag{R4}$$

The initial oxidation of VOCs by OH initiates a reaction chain which may lead to net production or loss of ozone depending on the atmospheric conditions. For example, when carbon monoxide (CO) reacts with OH in the presence of oxygen, carbon dioxide and the hydroperoxy (HO_2) radical are formed. In polluted areas with high-NO_x concentrations, HO_2 readily reacts with nitrogen oxide (NO) regenerating OH and producing nitrogen dioxide (NO_2).

$$CO + OH \xrightarrow{O_2} HO_2 + CO_2 \tag{R5}$$

$$HO_2 + NO \rightarrow OH + NO_2 \tag{R6}$$
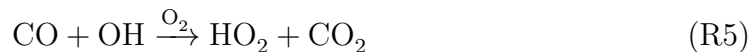
Photolysis of NO_2 produces ground-state atomic oxygen leading to ozone production via (R3).

$$NO_2 + h\nu \rightarrow NO + O(^3P) \tag{R7}$$
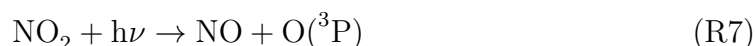
The reaction between OH and NO_2 produces nitric acid (HNO_3) limiting the recycling of OH and NO_2. Nitric acid may be removed through deposition and is a sink for both OH and NO_2.

$$NO_2 + OH \rightarrow HNO_3 \tag{R8}$$
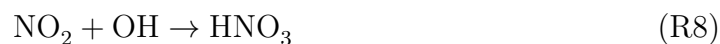
In low-NO_x conditions away from polluted areas, OH and HO_2 are interconverted through reactions with ozone.

$$OH + O_3 \rightarrow HO_2 + O_2 \tag{R9}$$

$$HO_2 + O_3 \rightarrow OH + 2\,O_2 \tag{R10}$$

OH and HO_2 may also react in a termination reaction producing water vapour and oxygen.

$$HO_2 + OH \rightarrow H_2O + O_2 \tag{R11}$$

Other termination reactions involve combination reactions of HO_2 radicals producing hydrogen peroxide (H_2O_2).

$$HO_2 + HO_2 \rightarrow H_2O_2 \tag{R12}$$

Hydrogen peroxide may be removed through deposition (Gunz and Hoffmann, 1990) but may also be a temporary sink for the odd-oxygen species OH and HO_2.

$$H_2O_2 + h\nu \rightarrow 2\,OH \tag{R13}$$

$$H_2O_2 + OH \rightarrow HO_2 + H_2O \tag{R14}$$
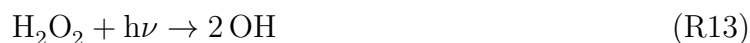
Figure 1.1: Methane degradation pathways in low-NO_x and high-NO_x conditions. Taken from Monks (2005).
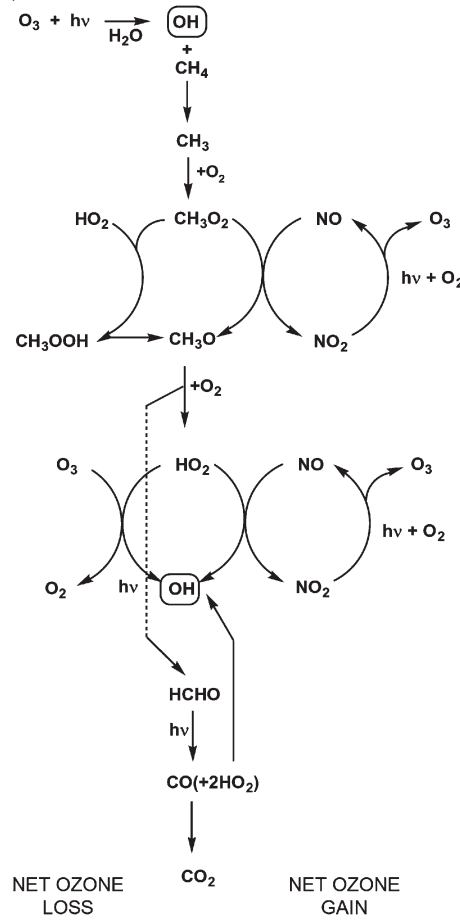
In summary, the secondary degradation of CO produces ozone in high-NO_x conditions while in low-NO_x conditions ozone is destroyed. (Seinfeld and Pandis, 2006; Monks, 2005)

The secondary degradation of more complex VOCs has similar features to that of CO. Methane (CH_4), with a mixing ratio of ~ 1.7 ppmv, is the most abundant VOC in the troposphere. The reaction of CH_4 with OH, in the presence of O_2, produces the methyl peroxy radical (CH_3O_2) – the simplest organic peroxy radical (RO_2).

$$CH_4 + OH \xrightarrow{O_2} CH_3O_2 + H_2O \tag{R15}$$
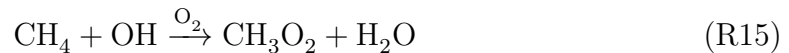
Similar to CO oxidation, NO_x conditions play a crucial role in the fate of CH_3O_2 and whether ozone is produced or destroyed, depicted in Fig. 1.1.

Figure 1.2: Schematic diagram outlining general pathways of the secondary degradation of an emitted VOC.
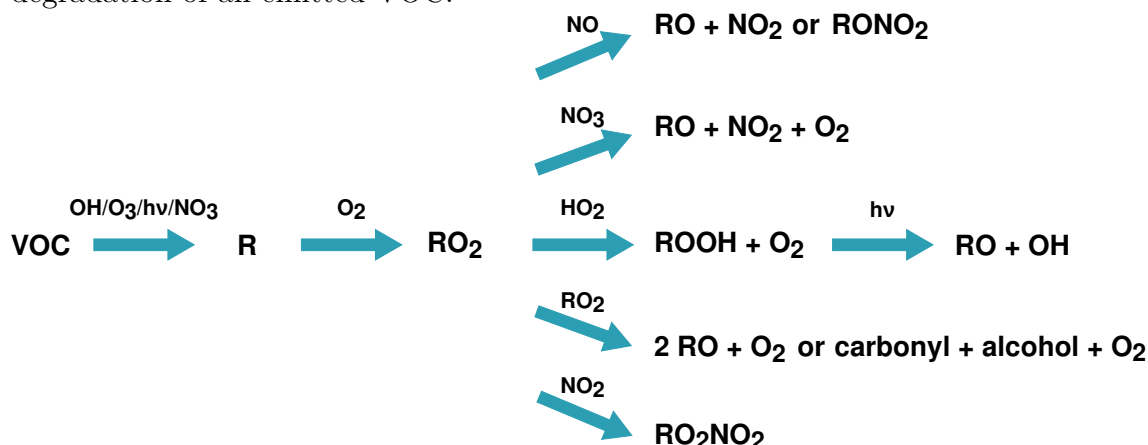
The general types of secondary degradation products formed during CH_4 degradation can be extended to more complex non-methane VOCs (NMVOCs). Initial oxidation pathways of NMVOCs are reaction with OH, while unsaturated VOCs, such as alkenes, may react with ozone and photolysis is important for carbonyl species. During the night-time, reaction with the nitrate (NO_3) radical is typically more important than OH-oxidation due to the relatively higher night-time concentrations of NO_3.

$$VOC + OH/NO_3/O_3/h\nu \xrightarrow{O_2} RO_2 \qquad (R16)$$
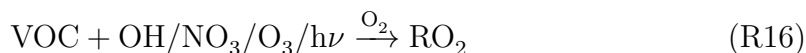
Figure 1.2 represents a general and simplified reaction scheme for VOCs in the troposphere. The initial oxidation of NMVOC produces RO_2 radicals and the fate of the RO_2 determines whether net loss or production of ozone occurs.

$$RO_2 + NO \xrightarrow{M} RONO_2 \qquad (R17)$$

$$RO_2 + NO \rightarrow RO + NO_2 \qquad (R18)$$

$$RO_2 + NO_2 \rightleftharpoons^{M} RO_2NO_2 \qquad (R19)$$

$$RO_2 + NO_3 \rightarrow RO + NO_2 + O_2 \qquad (R20)$$

$$RO_2 + HO_2 \rightarrow ROOH + O_2 \qquad (R21)$$

$$RO_2 + RO_2 \rightarrow 2\,RO + O_2 \qquad (R22)$$

$$RO_2 + RO_2 \rightarrow RCH(OH)R + RC(O)R + O_2 \qquad (R23)$$
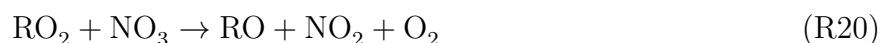
All degradation pathways of RO_2 that produce NO_2 result in O_3 formation due to (R7) and (R3). Reaction with HO_2 forms a hydroperoxide (ROOH) which may either be deposited or photolysed producing an alkoxy (RO) radical and OH. The carbonyl and alcohol products resulting from reactions between RO_2 radicals follows a similar

sequence of reactions and can produce further O_3. Thus the subsequent reactions of secondary degradation products of a VOC may lead to further production of ozone.

Reaction of RO_2 with NO_2 (R19) forms peroxy nitrates (RO_2NO_2) which are a temporary reservoir for RO_2 and NO_x. The thermal decomposition rate of RO_2NO_2 is highly temperature dependent. At lower temperatures, RO_2NO_2 builds up and may be transported away from the region of formation. Thus releasing RO_2 and NO_2 in areas away from large sources of NO_x and fuelling ozone production.

The reaction between NO and ozone is another important reaction in polluted regions.

$$NO + O_3 \rightarrow NO_2 + O_2 \quad\quad\quad\quad\quad\quad (R24)$$

Together with (R7) and (R3), (R24) form a null cycle of ozone production and destruction which limits ozone levels. On the local urban scale close to NO sources, (R24) decreases ozone levels called ozone titration. Ozone titration is also important during the night where the lack of photochemistry does not regenerate ozone. Urban measurement studies have confirmed the importance of ozone titration near sources of NO (Syri et al., 2001).

1.2.1   VOC and NO_x Chemistry

The chemistry in low-NO_x and high-NO_x conditions indicates that ozone production is a non-linear process. Figure 1.3, from Jenkin and Clemitshaw (2000), depicts the non-linear relationship between ozone as a function of VOC and NO_x. This relationship can be divided into distinct regimes of ozone production: *NO_x-sensitive* (or *NO_x-limited*), *NO_x-saturated* (or *VOC-limited*) and *VOC-and-NO_x-sensitive* regimes.
In regions with low-NO_x concentrations, RO_2 are more likely to react with other radicals rather than convert NO to NO_2 leading to ozone production. Increasing NO_x levels increases the number of NO to NO_2 conversions by peroxy radicals leading to ozone production. While, increasing VOC levels has little effect on O_3 production due to increased radical-radical reactions. This is *NO_x-sensitive* chemistry.

On the other hand in regions with high levels of NO_x, reactions between radicals and NO_x are more likely to occur. The production of HNO_3 increases through (R8) removing OH and NO_2. Increasing levels of VOC increase the likelihood of RO_2 converting NO to NO_2 leading to ozone production while increasing NO_x levels will not increase O_3 production. This is *NO_x-saturated* or *VOC-limited* chemistry.

Figure 1.3: Ozone isopleth plots for various initial mixing ratios of NO_x and VOCs. Taken from Jenkin and Clemitshaw (2000).
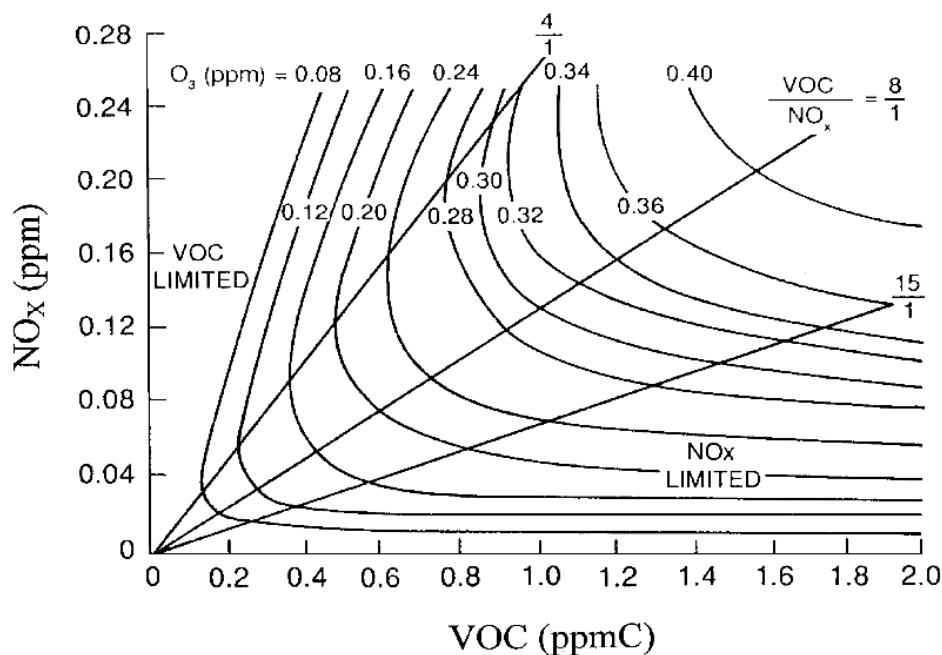
The VOC-and-NO_x-sensitive regime (contour ridges in Fig. 1.3) is characterised by O_3 production being sensitive to both VOC and NO_x levels. Morever, it is in this atmospheric regime that the maximum amount of ozone is produced. Kleinman (1994) showed that this non-linear relationship can be thought of as a titration process between radicals and NO_x with the VOC-and-NO_x-sensitive regime being the turning point.

The non-linear nature of ozone production is one of the challenges in controlling ozone levels. The difficulty is exacerbated by the fact that the troposphere can alternate between these regimes depending on the meteorological conditions. Moreover, fresh emissions tend to occur in NO_x-saturated areas before being transported to VOC-and-NO_x-sensitive and NO_x-sensitive regions.

1.2.2   Representing Atmospheric Chemistry in Models

Representing the degradation chemistry for each VOC in a chemical transport model (CTM) is unrealistic. Even if all the secondary degradation pathways and products were known for every VOC, a CTM would be unable to efficiently solve the differential equations.

The representation of atmospheric chemistry in a CTM is called a chemical mechanism. Chemical mechanisms are developed by simplifying and aggregating VOCs, degradation products and reactions. Less aggressive simplification approaches may result in a chemical mechanism having thousands of species while more aggressive simplification may result in only a hundred species. Chemical mechanisms are verified by comparing the concentrations of field studies or controlled chamber study experiments to model simulations (Stockwell et al., 2012). Section 2.2 includes further details of the simplification techniques used to develop chemical mechanisms.

Chemical mechanism comparison studies, such as Kuhn et al. (1998), Emmerson and Evans (2009) and Archibald et al. (2010), compared the outputs of different chemical mechanisms using the same model setup and initial conditions. These studies showed that the differences between chemical mechanisms led to large differences in simulated ozone concentrations. While these comparisons indicate that chemical mechanisms lead to differences in ozone levels, they do not point out the root cause of the differences.

Determining the source of differences between chemical mechanisms is a difficult task due to the interlinked chemistry of many key species. As part of this study, the ozone production from different chemical mechanisms is compared and differences in the treatment of VOC degradation chemistry is determined. The research questions driving this comparison are presented in Sect. 1.5 and the results are described in Sect. 3.1.

1.3   Source and Sinks of Ozone Precursors

Ozone precursors are emitted from many anthropogenic and biogenic sources with varying emissions throughout the year, month and time of day. In many regions, reduced road transport during the weekend leads to a noticible reduction in NO_x emissions influencing ozone levels. This is called the "weekend-effect". For example, ozone production is NO_x-saturated during weekdays in San Joaquin Valley, California but during the weekend higher ozone levels are recorded as the reduction in NO_x levels leads to VOC-and-NO_x-sensitive chemistry (Pusede et al., 2014). Many sources of NMVOC also have a reduction of activies during the weekend, such as industry and solvent use, and residential combustion is highest during the winter months and lowest during the summer (Denier van der Gon et al., 2011).

Figure 1.4: The sources and sinks of NO_x, adapted from Seinfeld and Pandis (2006).
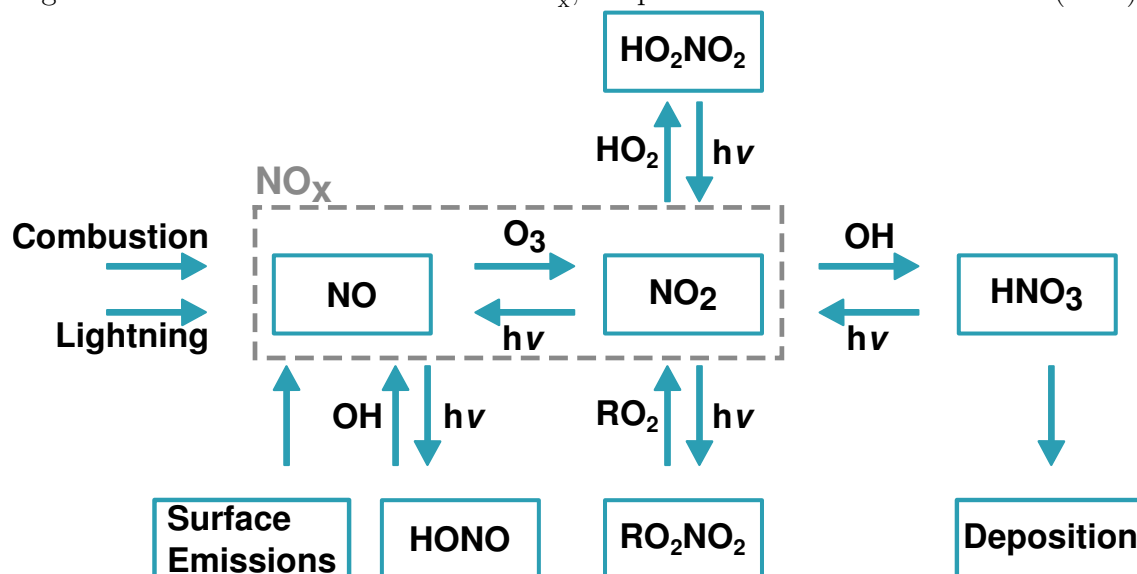
1.3.1 NO_x

Anthropogenic activities are the main source of NO_x emissions into the atmosphere. In the year 2000, almost 52 Tg N were emitted with 65 % fossil fuel combustion (Seinfeld and Pandis, 2006). Examples of fossil fuel combustion are diesel and petrol vehicles, industrial activities and domestic heating (von Schneidemesser et al., 2015).

Up to 95 % of NO_x emissions from combustion are emitted as NO, which is oxidised to form NO_2 through (R24) and (R6). However, the increase in diesel vehicles and the implementation of diesel filters increased the fraction of emitted NO_2 from vehicles. Grice et al. (2009) showed that over Europe, emissions of NO_2 from diesel vehicles have increased from 8.6 % in 2000 to 12.4 % in 2004.

Despite the majority of NO_x emissions coming from human activities, there are also natural sources of NO_x. Lightning is an important source of NO_x in the free troposphere while emissions of NO_x from soils are important in remote regions with little anthropogenic influence. Lightning and soils each contributed ~ 10 % to global NO_x emissions in 2000 (Seinfeld and Pandis, 2006).

The main sink of NO_x is deposition of nitric acid, formed via (R8). Temporary reservoirs, such as peroxy nitrates and HONO, may be transported away from sources into remote areas and their decomposition is an important source of NO_x fuelling ozone production in these areas. These sources and sinks of NO_x are illustrated in Fig. 1.4.

1.3.2   VOCs

This section looks at the sources of sinks of methane, non-methane VOCs and CO. Although CO is not actually a VOC, its photochemistry is important for ozone production. The main sink of VOCs is the oxidation chemistry (Sect. 1.2) leading to CO_2 and H_2O. The degradation of VOCs plays an important role in SOA (secondary organic aerosol) formation as well as ozone production (Hallquist et al., 2009).

The degradation of a VOC yields the maximum possible amount of ozone when every peroxy radical converts NO to NO_2 called the *ozone production potential* (OPP) of a VOC. In reality, the OPP of a VOC is never achieved as other reactions with peroxy radicals occur however the OPP is useful for assessing the amount of ozone produced from emitted VOCs.

Carbon Monoxide

Carbon monoxide is emitted directly into the troposphere through combustion and industrial processes. An equally-important source of CO is its formation during VOC degradation. Hauglustaine et al. (1998) estimated that 881 Tg yr^{-1} of CO was produced globally from chemical oxidation of VOC while 1219 Tg yr^{-1} of CO was directly emitted.

The reaction between CO and OH (R5) is the main sink of CO. The OPP of CO is one as the degradation of CO produces one peroxy radical (HO_2), thus a maximum of one molecule of ozone may be produced during CO degradation.

Methane

Emissions of methane range between 500 and 600 Tg CH_4 yr^{-1} with ~ 60 % of the emissions from anthropogenic sources. The main anthropogenic sources of CH_4 are agriculture, fossil fuels and biomass burning with agriculture contributing 60 % of the anthropogenically emitted CH_4. Emissions from wetlands are the main natural source of methane emissions (Kirschke et al., 2013).

Methane has a lifetime in the atmosphere of about 10 years, significantly longer than other VOCs (Voulgarakis et al., 2013). The lifetime of a chemical species is the time required for the concentration of the species to decrease by $\frac{1}{e}$ (Seinfeld and Pandis, 2006). Thus, methane influences ozone production on the global rather than the regional scale and is important for background levels of ozone.

Reaction with OH (R15) is the main sink of methane and the secondary degradation of CH_4 (Fig. 1.1) produces CO and four peroxy radicals ($1\times$ CH_3O_2, $3\times$ HO_2). Thus the OPP of methane is five as methane degradation can produce a maximum five molecules of O_3 per molecule of CH_4 oxidised.

NMVOCs

A wide variety of NMVOCs are emitted from anthropogenic activities directly into the troposphere. Solvent use, industry, fossil fuel burning and transportation are all major activities emitting NMVOCs of varying functional groups, carbon numbers and reactivity. Emissions of NMVOC from vegetation depends on meteorological variables (such as, temperature and radiation) and biological variables (such as, leaf age and leaf area index) (Guenther et al., 2012).

Lamarque et al. (2010) estimated that in 2000, 130 Tg NMVOC were globally emitted from anthropogenic sources. This amount is dwarfed by emissions from biogenic sources – 1000 Tg NMVOC yr^{-1} (Guenther et al., 2012). Isoprene (C_5H_8) emitted from vegetation dominates at the global scale however emissions of other NMVOC from vegetation, such as monoterpenes and sesquiterpenes, may be significant on the regional scale.

Although isoprene is considered as a biogenic VOC (BVOC), it has been measured in the urban areas of London and Paris away from biogenic emission sources and during times where biogenic emissions are not important, such as freezing conditions in winter. Transport of isoprene is unlikely as isoprene is a highly reactive NMVOC indicating anthropogenic sources of isoprene (von Schneidemesser et al., 2011). Other NMVOC emitted from anthropogenic sources, such as methanol and acetaldehyde, are also emitted from vegetation (Guenther et al., 2012).

The maximum number of molecules of O_3 produced per degradation of an emitted NMVOC depends on the type and the number of carbons of the NMVOC leading to a wide range of OPPs for different NMVOC. Unsaturated NMVOC, such as alkenes, tend to have larger OPPs than alkanes (saturated NMVOC). Even within a functional group of NMVOC different OPPs are calculated. For example, benzene and xylene are both aromatic compounds but as benzene is a more chemically stable molecule it has a lower OPP than xylene (Carter, 1994).

OPPs for complex NMVOCs have been calculated using models by incrementally varying the concentration of an NMVOC and calculating the change in ozone. Different OPP scales have been developed using different NO_x conditions.

The Maximum Incremental Reactivity (MIR) and Maximum Ozone Incremental Reactivity scales of Carter (1994) and the Tagged Ozone Production Potential (TOPP) of Butler et al. (2011) are examples of OPP scales for NMVOCs.

1.3.3   Representing NMVOC Emissions in Models

Emissions of NMVOC species are a critical input in models and emission inventories are used to specify the type and quantity of emissions from source categories. Table 1.1 lists the source sectors of emissions used by the TNO-MACCIII emission inventory (Kuenen et al., 2014). Emission inventories are available for global or regional emissions. For example, EDGAR (Olivier et al., 2001) specifies global emissions while TNO-MACCII (Kuenen et al., 2014) specifies European emissions.

Many uncertainties are associated with emission inventories. For example, Coll et al. (2010) showed that large discrepancies arise between ambient measurements and emission inventories. Often temporal variation of emissions are not captured by emission inventories (Boynard et al., 2014).

BVOC emissions depend on meteorological and biological variables and algorithms estimating BVOC emissions may be calculated as part of the model simulation instead of an emission inventory. Emissions of AVOCs may also depend on meteorological variables, for example, evaporative emissions increase with temperature (Rubin et al., 2006). The Model of Emissions of Gases and Aerosols from Nature (MEGAN) (Guenther et al., 2006, 2012) calculates BVOC emissions using the temperature and radiation values determined from the model. Specifiying BVOC emissions using an algorithm or emission inventory influences modelled ozone concentrations. For example, Curci et al. (2009) noted large differences in summertime ozone concentrations over Europe when using a gridded emission inventory or an on-line algorithm for BVOC emissions.

Emissions of the NMVOCs specified by an emission inventory are mapped to the chemical mechanism species used in the model. This mapping is not standardised throughout the modelling community with the same NMVOC emissions possibly being allocated to different chemical species even if using the same chemical mechanism (Carter, 2015).

The influence of the speciation of NMVOC emissions on modelled ozone production is determined as part of this work. Moreover, the effect of using the same speciations of NMVOC emissions with different chemical mechanisms is also explored. Section 1.5 outlines the research questions and the results are presented in Sect. 3.2.

Table 1.1: Emission source sectors for anthropogenic emissions listed in the TNO-MACCII inventory (Kuenen et al., 2014).

Emission Source Category	Emission Source Category
Public Power	Road Transport: Others
Residential Combustion	Road Transport: Evaporation
Industry	Road Transport: Wear
Fossil Fuel	Non-road Transport
Solvent Use	Waste
Road Transport: Gasoline	Agriculture
Road Transport: Diesel	

1.4   Effects of Meteorology on Ozone Production

Meteorological conditions influence the production of ozone with clear and calm summer days typically having high ozone levels (Dueñas et al., 2002). Comrie (1997) noted a complex relationship between meteorology and ozone due to competing positive and negative effects on ozone production. Table 1.2, taken from Jacob and Winner (2009), details the effects of specific meteorological variables on ozone production.

Climate change is predicted to influence many meteorological variables and increase the number of heatwaves (Karl and Trenberth, 2003). Thus understanding the influence of meteorology on ozone production is particularly important for future predictions of air quality and tackling ozone pollution in a changing climate.

Humidity

Humidity influences ozone production both positively and negatively. When $O(^1D)$, originating from ozone photolysis (R2) reacts with water vapour (R4), the production of OH radicals leads to ozone loss. However, the initiation of VOC degradation through reaction with OH can lead to ozone production (Sect. 1.2). These competing effects of water vapour on ozone production lead to a weak correlation of ozone production with water vapour (Jacob and Winner, 2009).

Wind Speed

High wind speeds transport ozone precursors away from their sources leading to a generally negative effect on ozone pollution over a region. Model projections of Doherty et al. (2013) showed that while climate change is expected to change large-scale atmospheric transport there is little influence on the spatial patterns of mean concentrations of ozone.

Table 1.2: Influence of meteorological variables on ozone production, taken from Jacob and Winner (2009).

Meteorological Variable	Influence on Ozone
Temperature	Consistently positive
Stagnation	Consistently positive
Wind Speed	Generally negative
Mixing Height	Weak or variable
Humidity	Weak or variable
Cloud Cover	Generally negative
Precipitation	Weak or variable

Stagnation

During periods of low wind speeds, emissions of ozone precursors remain close to their sources. These stagnant conditions over polluted urban areas are highly correlated with increased ozone production over urban areas (Jacob and Winner, 2009). Heatwaves result from stagnant conditions along with high temperatures enhancing the ozone pollution over a region.

Mixing Height

The effects of the mixing height of the planetary boundary layer (PBL) with the free troposphere depend on the region. For example, Dawson et al. (2007) found that over the Eastern U.S., regions with low ozone are positively correlated with a higher mixing height whereas regions with high ozone levels are negatively affected. This spatial effect of mixing height on ozone production depends on the difference between ozone levels within the PBL and the free troposphere (Jacob and Winner, 2009).

Mixing between the PBL and free troposphere into regions with levels of surface ozone lower than the free troposphere is an additional source of ozone. Conversely, mixing of the elevated levels of ozone from polluted areas into the free troposphere reduces the burden of surface ozone.

Cloud Cover

Cloud cover negatively affects the photochemistry of ozone production with increased cloud cover reducing the amount of sunlight reaching the troposphere. Korsog and Wolff (1991) showed a negative correlation between cloud cover and ozone and ozone levels in the study of Dawson et al. (2007) were not significantly influenced by changes in cloud cover.

Precipitation

Precipiation influences the wet deposition rates of ozone and other chemical species. The studies of Dawson et al. (2007) and Murazaki and Hess (2006) noted a minor influence of precipitation on ozone levels.

Temperature

Temperature is positively correlated with ozone in many areas. Otero et al. (2016) showed that temperature was the main driver of summertime ozone values over many areas of central Europe while Camalier et al. (2007) correlated ozone with temperature over the Eastern US. Sillman and Samson (1995) illustrated that only ozone pollution produced from the chemistry described in Sect. 1.2 is correlated with temperature rather than background ozone, the ozone levels without the influence of local emissions of anthropogenic NMVOCs.

Temperature directly influences ozone levels in two ways: increasing the emissions of VOCs from vegetation and speeding up the rates of chemical reactions. The review of Pusede et al. (2015) showed that the temperature dependence of radical production, organic reactivity, the shorter lifetime of RO_2NO_2 and the formation of alkyl nitrates (R18) affects ozone production.

There is a lack of detailed process studies separating the direct effects of temperature on ozone over differing NO_x conditions despite observational and regional modelling studies correlating temperature with ozone production. The final part of this work addresses whether the increase in BVOC emissions or faster reaction rates with temperature is more important for ozone production. The research questions for this study are detailed in Sect. 1.5 and results are presented in Sect. 3.3.

1.5   Research Questions and Objectives of this Thesis

The detailed chemistry producing ozone cannot be fully represented in models for reasons of computational efficiency. Thus models select a particular representation of atmospheric chemistry raising the overarching research questions for this thesis:

- How do representations of detailed atmospheric chemistry influence simulated ozone production?
- What are the most important chemical processes when simulating ozone production?

These questions are addressed in this work through detailed modelling studies highlighting the chemical processes having the largest impact on simulated ozone production under three different conditions.

Firstly, different simplified versions of the ozone production chemistry are available to the modelling community with comparison studies showing that ozone concentrations vary between chemical mechanisms. These chemical mechanism comparison studies do not determine the root causes of the differences between chemical mechanisms, leading to the research questions:

- How do the simplification techniques used by different chemical mechanisms affect ozone production?
- Which processes are responsible for differences in ozone production with different chemical mechanisms?

Secondly, NMVOC emissions are a known source of uncertainty in modelling experiments. The choice of emission inventory influences the speciation of individual NMVOC emissions possibly influencing ozone production. By comparing the ozone produced using different emission inventories, the following research questions are addressed:

- What is the influence on modelled ozone production when using different speciations of emitted NMVOCs?
- Does this influence change when using different chemical mechanisms?

Finally, meteorology influences ozone production with temperature having the strongest positive correlation with ozone. Temperature directly influences ozone production through increasing biogenic emissions and speeding up the reaction rates of chemical reactions.

- Are temperature-dependent emissions or chemical processes more important for ozone production with increasing temperature?
- How is the ozone-temperature relationship treated by different chemical mechanisms?

Detailed processed studies were performed using a box model to address these research questions, details of the experimental setup are presented in Chap. 2. The results of the experiments are found in Chap. 3, the general discussion and conclusions of the thesis are in Chap. 4.

Chapter 2

Methodology

This chapter details the methodology used to address the research questions of this work (Sect. 1.5). A brief description of AQ modelling is followed by the model set-up used in the separate studies (Sect. 2.1). The chemical mechanisms used in this work are introduced in Sect. 2.2 and the required initial and boundary conditions are described in Sect. 2.3

2.1   Air Quality Modelling

AQ models are mathematical representations of the atmosphere designed to produce continuous output fields that aid in explaining sources of air pollution. All models numerically solve the system of differential equations describing the conservation of chemical species used by the model (Russell and Dennis, 2000).

Solving the system of differential equations requires initial and boundary conditions for each chemical species. Initial conditions fix the starting concentrations of each species in every grid-box. Boundary conditions require knowledge of the concentration and transport of each species at the boundary edges of the model grid.

Eulerian models are the most common type of AQ model (Russell and Dennis, 2000). These models describe the atmosphere by fixed grid-boxes where species are transported in and out of the boxes (Seinfeld and Pandis, 2006). Box models are the simplest type of model (zero-dimensional) having uniform atmospheric concentrations that are a function of time. Whereas 3-D models describe atmospheric concentrations as a function of time, latitude, longitude and height requiring more computing power than a box model (Seinfeld and Pandis, 2006). Box models may

Table 2.1: MECCA box model settings.

Model Parameter	Setting
Pressure	1013 hPa
Relative Humidity	81 %
Starting Date and Time	27th March 06:00
Model Time Step	20 mins

lack realism but are useful for studying detailed processes influencing air quality.

2.1.1   Model Description and Setup

The MECCA (Module Efficiently Calculating the Chemistry of the Atmosphere) box model was used throughout this work. MECCA was developed by Sander et al. (2005) and adapted to include MCM v3.1 chemistry by Butler et al. (2011). MECCA was used in the published studies of Kubistin et al. (2010) and Lourens et al. (2016).

MECCA is written in Fortran code and runs on UNIX/Linux platforms. The Kinetic Pre-Processor (KPP, Damian et al. (2002)) processed the chemical mechanism and generated Fortran code further compiled within MECCA. KPP has many choices of numerical solver for solving the differential equations, a Rosenbrock solver (ros3 option) was used throughout this work.

Emissions of species into the box and deposition of species out of the box were handled by KPP. The chemical mechanism included pseudo-unimolecular reactions specifying the emissions and dry deposition of chemical species with the relevant rate. The emitted chemical species and emission rates were read into the model using a namelist file. Namelist files also specified the initial and boundary conditions of chemical species.

The physical parameters used in MECCA throughout this work are detailed in Table 2.1. In the first two studies, temperature was held constant at 293 K (20°C) and the boundary layer height was fixed at 1000 m. In the final study, MECCA was updated to include a variable diurnal boundary layer height and temperature was systematically varied between 288 and 313 K (15–40 °C). These changes to the model setup for the final study are outlined in Paper III (Chap. 9).

Photolysis rates were paramaterised as a function of the solar zenith angle based on the approach of the MCM (Jenkin et al., 1997). This paramaterisation

Table 2.2: Chemical mechanisms used in this work.

Chemical Mechanism	Lumping Type	Reference
MCM v3.1 and v3.2	No lumping	Jenkin et al. (1997), Jenkin et al. (2003) Saunders et al. (2003), Bloss et al. (2005) Rickard et al. (2015)
CRIv2	Lumped intermediate	Jenkin et al. (2008)
MOZART-4	Lumped molecule	Emmons et al. (2010)
RADM2	Lumped molecule	Stockwell et al. (1990)
RACM	Lumped molecule	Stockwell et al. (1997)
RACM2	Lumped molecule	Goliff et al. (2013)
CBM-IV	Lumped structure	Gery et al. (1989)
CB05	Lumped structure	Yarwood et al. (2005)

utilises the degree of latitude and in the first two studies 34 °N, roughly the city of Los Angeles, was used. In the final study, the latitude was set to 51 °N simulating central European conditions.

2.2   Chemical Mechanisms

The chemical mechanisms used in this study are listed in Table 2.2 with more details found in Paper I (Sect. 3.1). These chemical mechanisms were chosen as they are commonly used by the AQ modelling community as outlined by the review of European modelling groups by Baklanov et al. (2014).

The Master Chemical Mechanism (MCM, Jenkin et al. (1997, 2003); Saunders et al. (2003); Bloss et al. (2005); Rickard et al. (2015)) is a near-explicit chemical mechanism with a high level of detail making it ideal as the reference chemical mechanism in each study of this work. The Common Representative Intermediates (CRI) chemical mechanism (Jenkin et al., 2008) is a lumped-intermediate mechanism where the degradation productions are aggregated (lumped) rather than emitted VOC.

Lumped molecule chemical mechanisms aggregate primary VOC into mechanism species and is the most commonly used simplification technique. The lumped-molecule chemical mechanisms used in this work were Model for OZone and Related chemical Tracers (MOZART, Emmons et al. (2010)), Regional Acid Deposition Model (RADM2, Stockwell et al. (1990)), Regional Atmospheric Chemistry Mechanism (RACM, Stockwell et al. (1997)) and RACM2 Goliff et al. (2013). Lumped structure chemical mechanism represent emissions of NMVOC through emissions of mechanism species representing the bonds present in the NMVOC. The Carbon Bond mechanisms CBM-IV (Gery et al., 1989) and CB05 (Yarwood et al., 2005)

were the lumped-structure chemical mechanisms used in this work.

2.2.1 Implementing Chemical Mechanisms in MECCA

Each chemical mechanism listed in Table 2.2 was adapted to the KPP format used in the MECCA box model. The WRF-Chem model (Grell et al., 2005) includes KPP versions of RADM2, RACM and CBM-IV and this was the source for these chemical mechanisms. The full version of the CRI v2 was obtained from `http://mcm.leeds.ac.uk/CRI` while the original reference was the source for all other chemical mechanisms in Table 2.2.

In order to focus on the differences in the representation of VOC degradation between the chemical mechanisms, a number of harmonisations between the chemical mechanisms were implemented. For these harmonisations, the approaches used by the reference chemical mechanism (MCM v3.2) were implemented in the reduced chemical mechanisms. These changes are detailed in Paper I (Chap. 7).

2.2.2 Tagging of Chemical Mechanisms

AQ models can be used to allocate the effects of different precursors or emission sources on ozone production. For example, source removal studies perform separate model simulations with and without emissions from a sector to quantify the effect of the sector on ozone production, such as the quantification of megacity emissions on ozone production in Butler and Lawrence (2009). Tagging is another approach where the chemical mechanism includes additional chemical species labelled (tagged) with source information. For example, Emmons et al. (2012) tagged the MOZART-4 chemistry to attribute ozone production to emission sources of NO_x.

In Butler et al. (2011), tagged VOC chemistry allows allocation of ozone production to emitted VOC. Tagging involves labelling every organic degradation product produced during the degradation of a VOC with the name of the VOC. This labelling is repeated for every degradation product until the final degradation products (CO_2 and H_2O) are produced, thus every VOC has a separate set of reactions fully describing its degradation. This tagging approach uses O_x production as a proxy for O_3 production and is only valid for NO_x-limited and VOC-and-NO_x sensitive chemistry not NO_x-saturated conditions. The O_x family includes O_3, NO_2, $O(^1D)$, $O(^3P)$, NO_3, N_2O_5 and other species involved in fast production and loss cycles with NO_2.

All chemical mechanisms in Table 2.2 were tagged using the approach of Butler et al. (2011). In the first study, the tagging approach was the basis for comparing the respresentations of VOC degradation chemistry and their effects on ozone production. The second study used VOC-and-NO_x-sensitive conditions and simulations using the tagged chemical mechanisms determined sources of differences in ozone production from the solvent sector emission inventories of Table 2.3. Variable NO_x conditions were used in the third study hence using the tagging approach was not possible. Thus all model simulations assessing the ozone-temperature relationship with different NO_x conditions were performed with non-tagged versions of the chemical mechanisms.

2.3   Initial and Boundary Conditions

In all simulations of this work, methane (CH_4) was fixed to 1.75 ppmv while carbon monoxide (CO) and O_3 were initialised at 200 ppbv and 40 ppbv and then allowed to evolve freely. The initial conditions for NMVOC emissions were held constant until noon of the first day of simulations to simulate a fresh emissions plume.

NMVOC Initial Conditions

The initial conditions for NMVOC species differed in each experiment, a brief summary is given below and details are found in the respective publications (Chaps. 7–9). The first study used the initial conditions of the Los Angeles simulation in Butler et al. (2011) to determine the emissions needed for constant mixing ratios of the initial NMVOCs. These emissions were mapped to the appropriate chemical species of each chemical mechanism in Table 2.2 keeping the amount of emitted NMVOC constant between model runs.

The second study used NMVOC emissions specified by the emission inventories for the solvent sector listed in Table 2.3 over a theoretical urban area of 1000 km^2 with total NMVOC emissions of 1000 tons/day. The solvent sector contributes $\sim$ 43 % by mass of total emissions (EEA, 2011), thus total NMVOC emissions of 430 tons/day were used. Further simulations used emissions from all other sectors (remaining 570 tons/day) while varying the solvent sector NMVOC emissions. Additional simulations included BVOC emissions of isoprene and monoterpenes while varying the speciation of NMVOC emissions from the solvent sector.

Table 2.3: Solvent sector emission inventories compared in this work.

Speciation	Comment	Reference
TNO	European average	Builtjes et al. (2002)
IPCC	Model Specific	Ehhalt et al. (2001)
EMEP	Model Specific	Simpson et al. (2012)
DE94	Country Specific	Friedrich et al. (2002)
GR95	Country Specific	Sidiropoulos and Tsilingiridis (2007)
GR05	Country Specific	Sidiropoulos and Tsilingiridis (2007)
UK98	Country Specific	Goodwin (2000)
UK08	Country Specific	Murrells et al. (2010)

The NMVOC emissions of the solvent sector were assigned to MCM v3.2 species based on the speciations of each emission inventory. Model simulations were repeated using MOZART-4 and RADM2 to investigate whether changing the chemical mechanism affected the differences in ozone concentrations between the solvent sector emission inventories.

The final study looked at the ozone-temperature relationship over central Europe and used the emissions of NMVOC from Benelux (Belgium, Netherlands and Luxembourg). The TNO_MACCIII emissions for the year 2011 were used as anthropogenic NMVOC emissions and mapped to MCM v3.2 species. Temperature-independent emissions of biogenic species (isoprene and monoterpenes) were taken from the EMEP speciation (Simpson et al., 2012). Simulations using temperature-dependent emissions of isoprene used the MEGAN2.1 (Guenther et al., 2012) algorithm. All simulations were repeated using the CRI v2, MOZART-4, RADM2 and CB05 chemical mechanisms.

NO$_x$ Initial Conditions

NO$_x$ conditions generating VOC-and-NO$_x$ sensitive chemistry were used in the first two studies. This was achieved by emitting the amount of NO required to balance the source of radicals at each time step. While the final study assessed the relationship between ozone and temperature with different NO$_x$ conditions. For these simulations, a constant source of NO emissions was systematically varied between 5.0×10^9 and 1.5×10^{12} molecules (NO) cm^{-2} s^{-1} at each temperature used in this study ($15 - 40$ °C).

Boundary Conditions

No chemical boundary conditions were used in the first two studies as the experiments considered a contained box. In the final study, MECCA included a diurnal profile of the PBL with vertical mixing into the free troposphere using the PBL heights from the BAERLIN2014 campaign (Bonn et al., 2016). The boundary conditions for the free troposphere mixing ratios for O_3, CH_4 and CO were set to 50 ppbv, 1.8 ppmv and 116 ppbv respectively. These mixing ratios were taken from the 700 hPa height using the MATCH-MPIC chemical weather forecast data (`http://cwf.iass-potsdam.de/`) from March 21st, 2014.

Chapter 3

Presentation of Papers

This chapter outlines the main findings in each scientific paper published as part of this thesis. These publications, found in Chaps. 7–9, addressed the research questions framed in Sect. 1.5.

3.1 Paper I: A comparison of chemical mechanisms using tagged ozone production potential (TOPP) analysis

Published: J. Coates and T. M. Butler. A comparison of chemical mechanisms using tagged ozone production potential (TOPP) analysis. *Atmospheric Chemistry and Physics*, 15(15):8795–8808, 2015.

This paper compared the effects of VOC degradation on ozone production described by the reduced chemical mechanisms of Table 2.2 to the detailed MCM v3.2 chemical mechanism. This chemical mechanism comparison used the tagging approach described in Sect. 2.2.2 to obtain insights into the influences of the simplified representations of VOC degradation by chemical mechanisms on ozone production.

The time series of ozone mixing ratios on the first two days of simulations using reduced chemical mechanisms were generally lower than the time series of ozone mixing ratios using the MCM v3.2. The difference in peak ozone on the first day between all chemical mechanisms was 21 ppbv when including the outlier RACM chemical mechanism and 8 ppbv when not including RACM. The representation of the degradation of aromatic VOC in RACM led to lower ozone mixing ratios than all other chemical mechanisms.

The VOC degradation described in CRI v2, a lumped-intermediate chemical mechanism, produced the most similar amounts of O_x to the MCM v3.2 for each VOC. On the other hand, the VOC degradation in all other reduced chemical mechanisms led to differences in O_x production with the largest differences occuring after the first day of simulations. The degradation of aromatic VOC in the reduced chemical mechanisms led to the largest differences in O_x production from the MCM v3.2.

Many VOC were broken down into smaller-sized degradation products faster on the first day in reduced chemical mechanisms than the MCM v3.2. The faster breakdown of VOC leads to lower amounts of larger-sized degradation products that may further degrade and produce O_x. Thus, many VOC in reduced chemical mechanisms produced a lower peak of O_x than the MCM v3.2 leading to lower ozone mixing ratios from the reduced chemical mechanisms compared to the MCM v3.2.

Reactive VOC, such as alkenes and aromatic VOC, produced peak O_x on the first day of simulations. Alkenes produced similar amounts of O_x on the first day between chemical mechanisms with differences in O_x production arising when mechanism species represented individual VOC. Large inter-mechanism differences in O_x production resulted from the degradation of aromatic VOC on the first day due to the faster break down of the mechanism species representing aromatic VOC in reduced chemical mechanisms. The less-reactive alkanes produced peak O_x on the second day of simulations with peak O_x lower in each reduced chemical mechanism than the MCM v3.2 due to the faster break down of alkanes into smaller sized degradation products on the first day by the reduced chemical mechanisms.

3.2 Paper II: Variation of the NMVOC Speciation in the Solvent Sector and the Sensitivity of Modelled Tropospheric Ozone

The second publication compared ozone production using different emission inventories (EIs) of NMVOC emissions for the solvent sector. The MCM v3.2, MOZART-4 and RADM2 chemical mechanisms were used to ascertain whether the representation of tropospheric chemistry affected the differences in ozone production

when using the different solvent sector EIs. Simulations using the tagged approach were performed to allocate O_x production to the emitted NMVOC specified by each EI.

A maximum difference in peak ozone mixing ratios ranged between 11 and 15 ppbv with different EIs using a single chemical mechanism. When using the same EI, a maximum difference of 7 ppbv in peak ozone mixing ratios was determined between simulations with different chemical mechanisms. Thus both the choice of chemical mechanism and EI influenced ozone production.

A lower maximum difference in peak ozone (6 – 9 ppbv) was produced from simulations using emissions from all other non-solvent emission sectors while varying the emissions from the solvent sector with each chemical mechanism. Including emissions from biogenic sources further reduced the maximum differences in peak ozone mixing ratios (5 – 8 ppbv) with each chemical mechanism.

Reactive VOC, such as alkenes and aromatics, contributed the most to O_x production on the first day. While less-reactive VOC, such as alkanes and oxygenated VOC, contributed the most to the cumulative O_x production after seven days of simulations.

A positive correlation was determined between O_x production and the contribution of alkane species by the EI. While a negative correlation was determined between cumulative O_x production and the contribution of oxygenated species by the EIs. No correlation was found between the specification of aromatic species by EIs and O_x production and as not all solvent sector EIs specify alkene emissions no correlation was calculated between specified alkene emissions and O_x production.

3.3 Paper III: The Influence of Temperature on Ozone Production under varying NO_x Conditions – a modelling study

The final publication looked at the ozone-temperature relationship with different NO_x conditions simulated by a box model. A series of box model simulations varying temperature and NO_x conditions were performed using NMVOC emissions

representative of central Europe, first using a temperature-independent source of isoprene emissions followed by simulations using a temperature-dependent source of isoprene emissions. All simulations were repeated using the MCM v3.2, CRI v2, MOZART-4, RADM2 and CB05 chemical mechanisms.

Each chemical mechanism produced a non-linear relationship between ozone, temperature and NO_x. This non-linear relationship was similar to that previously determined by observational studies. With each chemical mechanism, the absolute increase in ozone with temperature was slightly higher for temperature-dependent chemistry than the increase in ozone with temperature due to isoprene emissions. The largest increases in ozone mixing ratios with temperature were obtained with moderate NO_x conditions and the lowest increase in ozone mixing ratios was achieved with low NO_x conditions.

The O_x production normalised by the total loss rate of emitted NMVOC was roughly constant with temperature showing that the production of O_x with temperature was controlled by the loss rate of VOCs. The increased loss rate of VOCs with temperature was mainly due to the increased OH-reactivity of the emitted NMVOC with temperature. Net production of normalised O_x increased with temperature in all NO_x conditions due the temperature dependent chemistry of RO_2NO_2 species. At higher temperatures the equilibrium of RO_2NO_2 (R19) shifts towards decomposition to RO_2 and NO_2 thus at higher temperatures more RO_2 is available to produce O_x via (R18).

The box model results were also compared to observational data and output from the WRF-Chem model. The rate of increase of ozone with temperature from the box model was about half the rate of increase of ozone with temperature using observational and WRF-Chem output. Observational data and the output of 3-D models such as WRF-Chem include additional effects of temperature on ozone such as stagnantion where low wind speeds lead to the accumulation of reactants promoting ozone production. Box model simulations without mixing were performed to approximate stagnant conditions which increased the rate of increase in ozone with temperature than the box model simulations including mixing. These results indicated that the modelled relationship between ozone, temperature and NO_x was more sensitive to mixing than the choice of chemical mechanism.

Chapter 4

Overall Discussion and Conclusions

The research questions of Sect. 1.5 were addressed by the box modelling studies of Chap. 3 and these questions are answered in this chapter. In each study the near-explicit MCM v3.2 was the reference chemical mechanism with the simulations were repeated using reduced chemical mechanisms typically used by modelling groups for regional and global studies.

The first study compared the effects of different simplification techniques used by chemical mechanisms on ozone production. The reduced chemical mechanisms used in the comparison were developed through lumping VOC degradation intermediates (CRI v2), aggregating emitted NMVOCs into lumped molecules (MOZART-4, RADM2, RACM, RACM2) and expressing the emitted NMVOCs by lumped structure species (CBM-IV, CB05). Out of these three simplification techniques, the lumped-intermediate approach produced the most similar amounts of ozone from each VOC to the MCM v3.2 while the lumped-molecule and lumped-structure approaches generally produced less ozone than the MCM v3.2 from the degradation of the VOC. Thus the technique of lumping intermediate species rather than lumping VOCs appears promising for representing ozone production in future chemical mechanisms.

The second objective of the first study was to determine the processes responsible for the differences in ozone production using the different reduced chemical mechanisms. The largest differences in ozone production from the reduced chemical mechanisms to the MCM v3.2 were obtained for VOC represented by lumped mechanism species than those with VOC explicitly represented. In particular, the

representation of aromatic VOC consistently produced lower ozone in all the reduced chemical mechanisms. These differences in ozone production from aromatic VOC are not surprising as the degradation of aromatic VOC is an area of uncertainty (Atkinson and Arey, 2003). Even the detailed degradation chemistry of aromatic VOC in the MCM v3.2 was unable to reproduce the results from chamber experiments (Bloss et al., 2005).

Another process leading to lower ozone production from VOC degradation than the MCM v3.2 was the faster break down of emitted VOC into smaller sized degradation products by lumped-molecule and lumped-structure chemical mechanisms. In particular, the faster break down of alkanes in lumped-molecule and lumped-structure chemical mechanisms led to a lower peak of ozone production than the MCM v3.2. As alkanes are less-reactive VOC, they are more likely to be transported downwind of emission sources affecting ozone production in urban background areas. Thus underestimating the ozone production from alkanes may impact simulated ozone levels of urban background areas.

The second study looked at the influence of varying the speciation of NMVOC emissions from the solvent sector on ozone production. In box model experiments using the MCM v3.2, differences in ozone production resulted from the different speciations of NMVOC emissions. Ozone production on the first day was influenced by the amounts of alkenes and aromatic VOC specified by the solvent sector emission inventory (EI). While the contribution of alkanes and oxygenated VOC by the solvent sector EI determined ozone production at the end of the simulations.

Similar differences in ozone production were obtained when repeating the box model simulations using reduced chemical mechanisms (MOZART-4, RADM2). Thus although the emissions of NMVOC were represented by fewer species in the reduced chemical mechanisms than the MCM v3.2, the differences in ozone production were not dampened by reducing the complexity of the chemical mechanism.

This study was designed as a scoping study to determine whether updating the speciation of an EI influenced model predictions of ozone levels. Given the results of this study, further modelling studies using different atmospheric conditions and more complex models are warranted to obtain a complete picture of how varying the speciation of NMVOC emissions influences modelled ozone levels.

The final study modelled the relationship between ozone, temperature and NO_x using central European conditions. In order to verify whether temperature-dependent increases in reaction rates or isoprene emissions from nature are more important for the increase in ozone with temperature, separate simulations

using a temperature-independent and temperature-dependent source of isoprene emissions were performed. From these simulations, the absolute increase in ozone with temperature due to faster reaction rates was slightly higher than the increase in ozone with temperature due to increased isoprene emissions with temperature regardless of NO_x conditions. This result was surprising as studies (e.g. Racherla and Adams (2008), Doherty et al. (2013)) attributed the increase of ozone with temperature to increased isoprene emissions from vegetation.

The increase in ozone with temperature in all NO_x conditions was principally due to the faster loss rates of the emitted VOC with temperature as the OH-reactivity of the emitted VOC increased with temperature. As expected, peroxy nitrate (RO_2NO_2) chemistry also played a role in the increase of ozone production with temperature with increased RO_2NO_2 decomposition at higher temperatures leading to more RO_2 available to produce ozone. Thus the initial oxidation of emitted VOC and RO_2NO_2 chemistry are critical to modelling the relationship between ozone, temperature and NO_x.

Simulations were performed using reduced chemical mechanisms (CRI v2, RADM2, MOZART-4, CB05) to determine whether the relationship between ozone, temperature and NO_x differed between representations of atmospheric chemistry. Each chemical mechanism reproduced the non-linear relationship between ozone, temperature and NO_x with the choice of chemical mechanism not significantly changing this relationship. The rate of increase of ozone with temperature was found to be more sensitive to the amount of mixing rather than the choice of chemical mechanism when comparing the box model simulations to observational and 3D model output.

Overall, the representation of detailed atmospheric chemistry influenced ozone production as in each of the studies differences between ozone levels were obtained when repeating model simulations with different chemical mechanisms. Thus the choice of chemical mechanism is important for AQ modelling studies predicting future ozone levels. The representation of emitted NMVOC by the different chemical mechanisms was critical leading to differences in ozone production in each study. The secondary degradation processes of RO_2NO_2 chemistry and the rate of break down of emitted NMVOC by reduced chemical mechanisms also had implications for ozone production.

Chapter 5

Outlook

Although ozone pollution is a major problem in Europe, there is currently no legally binding limit value for ozone. The EU Directive 2008/50/EG sets a target value for human health requiring the mean eight hourly ozone concentration not to exceed 120 μg m^{-3} (= 60 ppbv) on more than 25 calendar days. The same EU Directive also sets an AOT40 target value for the exposure of vegetation to ozone of less than $18,000$ μg m^{-3} · h. AOT40 is the sum of the differences between the mean hourly ozone values above 80 μg m^{-3} (= 40 ppbv) and the value of 80 μg m^{-3} between 8 am and 8 pm from May to July.

The EU has laws regulating the emissions of ozone precursors (NO$_x$ and VOC). While these laws have reduced the emissions of both NO$_x$ and VOC over Europe, the target value for ozone is regularly exceeded throughout Europe. The non-linear relationship between ozone, NO$_x$ and VOC as well as intercontinental transport of ozone and its precursors impact the response of ozone pollution despite reductions in precursor emissions. The European Environmental Agency (EEA) recommends further mitigation efforts on the local, regional and global scales to reduce ambient ozone levels.

Setting a legally binding limit value for ambient ozone over Europe should inspire mitigation strategies at the local and regional scales in a bid to meet this limit. Meeting a limit value requires assessing different mitigation approaches and here AQ modelling will be a vital tool in determining the efficacy of a mitigation strategy for reducing ambient ozone. Thus research aiming to improve model performance would also aid in increasing the confidence of AQ predictions from models, an asset for judging different mitigation strategies.

The detailed process studies performed as part of this work were designed

to ultimately improve model performance increasing the confidence of the predictions of AQ models for mitigation strategies. A number of recommendations to the AQ modelling community are listed based on these studies. AQ modelling groups should use up-to-date chemical mechanisms to incorporate the findings and recommendations from the chemical kinetics community. This is undoubtably more work for a modelling group as further work such as testing the model with a new chemical mechanism and translating emissions into the new chemical species would need to be performed. However as shown in the first study, updated versions of the same chemical mechanism produced more similar amounts of ozone to the near-explicit MCM v3.2 chemical mechanism. Thus using an updated chemical mechanism should increase the confidence of the modelled ozone production from the degradation of emitted VOCs.

As the lumped-intermediate chemical mechanism produced the most similar amounts of ozone to the MCM v3.2, the approach of using a highly detailed chemical mechanism and lumping the degradation products appears promising for developing future chemical mechanisms. This approach did not break down the emitted VOC into smaller degradation products as fast as the lumped-molecule and lumped-structure chemical mechanisms, which was the main cause for the lower ozone production using these chemical mechanisms compared to the MCM v3.2. Lumped-intermediate chemical mechanisms include more chemical species than lumped-molecule and lumped-structure chemical mechanisms making their use less appealling from a computational efficiency perspective. However gains in computational speed with modern computing centres might reduce this concern and facilitate the use of more complex chemical mechanisms as part of 3D models.

One feature of future mitigation strategies could be to substitute the emissions of a more-reactive NMVOC with a less-reactive NMVOC thus changing the NMVOC speciation profile from emission sectors. Such mitigation strategies require updating emission inventories and assessing how the change in speciation could influence ambient ozone levels. The results of the second study indicate that ozone production close to emission sources would be reduced using such mitigation strategies but ozone production downwind may increase.

A warmer climate is predicted in the future as a result of climate change and this may affect ozone production chemistry in future emission scenarios. The influence of meteorological variables on ozone production is extremely important with the third study demonstrating an increase in ozone production with temperature. A deeper understanding of the effects of meteorology on ozone production is required to ensure that mitigation strategies are robust enough to still reduce ambient ozone

in the future.

The oxidation of emitted NMVOC determined the increase of ozone with temperature further emphasising the importance of adequately representing both the speciation and initial degradation of emitted NMVOC. The increase of ozone with temperature was sensitive to atmospheric mixing with less atmospheric mixing allowing the secondary degradation of NMVOC to proceed further than situations with enhanced atmospheric mixing. Thus stressing the importance of representing the secondary degradation of NMVOC by the chemical mechanism used by an AQ model.

The results from the detailed process studies performed in this work were all performed using a box model and further work using 3D models is required to verify how additional processes, such as regional transport, also influence ozone production under these conditions. The use of a box model was ideal for the scope of the studies of this thesis allowing a deeper insight into the chemical processes requiring a sharper focus when using more realistic 3-D models.

Chapter 6

Summary and Zusammenfassung

6.1 Summary

Tropospheric ozone is a short-lived climate forcing pollutant that is hazardous to human health and impacts deleteriously on vegetation. Ozone is not emitted directly into the troposphere but formed from the photochemical reactions of VOCs and NO_x with meteorological conditions strongly influencing ozone production. This thesis assessed the chemical mechanisms of ozone production represented within air quality models by determining the influence of VOC degradation, the speciation of VOC emissions and temperature on modelled ozone production. All modelling experiments in this work used a box model to perform detailed process studies focusing on the representation of tropospheric chemistry impacting ozone production. Model simulations used the highly-detailed MCM v3.2 chemical mechanism as a reference and repeated using reduced chemical mechanisms typically used by regional and global models determining the sensitivity of ozone production to the choice of chemical mechanism.

The effects of different simplification approaches used by chemical mechanisms on ozone production were determined by comparing the ozone produced during VOC degradation between different chemical mechanisms. The lumped-intermediate (CRI v2) chemical mechanism produced the most similar amounts of ozone to the MCM v3.2 from the degradation of each VOC. While VOC degradation described by lumped-molecule (MOZART-4, RADM2, RACM and RACM2) and lumped-structure (CBM-IV and CB05) chemical mechanisms generally produced less ozone than the MCM v3.2. A faster breakdown of the emitted VOC into smaller sized degradation products in the lumped-molecule and lumped-structure

chemical mechanisms caused the lower ozone production during VOC degradation. Also, larger differences in ozone production were produced from VOC represented by mechanism species than VOCs represented by explicit species.

The influence on ozone production from the speciation of VOC emissions by an emission inventory was established by comparing the ozone produced from different emission inventories of the solvent sector. In these experiments, the different emission inventories of VOC emissions led to differences in peak ozone mixing ratios and ozone production. The ozone production on the first day was influenced by the specified contributions of alkene and aromatic VOC. Emission inventories specifying larger amounts of alkane emissions produced the largest amounts of ozone at the end of simulations than those specifying a larger contribution of emissions of oxygenated VOC. Repeating the simulations with reduced chemical mechanisms (MOZART-4 and RADM2) reproduced the differences in ozone production obtained with the MCM v3.2 chemical mechanism. These results indicated a sensitivity of ozone production to both the choice of chemical mechanism and emission inventory speciation.

The final study of this work considered the relationship between ozone, temperature and NO_x. The increase of ozone with temperature due to temperature-dependent chemistry was slightly larger than the increase of ozone with temperature due to increased isoprene emissions with temperature in all NO_x conditions. A non-linear relationship between ozone, temperature and NO_x was obtained with each chemical mechanism used in this study (MCM v3.2, CRI v2, MOZART-4, RADM2 and CB05). With each chemical mechanism, the increase in ozone production with temperature was due to the increased loss of the emitted VOC with temperature mainly caused by the increased OH-reactivity of VOC with temperature. The temperature-dependent chemistry of peroxy nitrate compounds, such as PANs, also led to an increase of ozone production with temperature.

The detailed processes studies of this work will help improve model performance and the confidence in predictions of future ozone levels from air quality modelling studies. The representation of VOC degradation and secondary processes such as the rate of breakdown of the emitted VOC and peroxy nitrate chemistry by a chemical mechanism are particularly important processes for the predictions of ozone levels with different mitigation strategies.

6.2   Zusammenfassung

Troposphärisches Ozon ist ein kurzlebiger klimawirksamer Schadstoff, der für die menschliche Gesundheit gefährlich ist und sich auf schädliche Weise auf die Vegetation auswirkt. Ozon wird nicht direkt in die Troposphäre ausgestoßen, sondern entsteht aus den photochemischen Reaktionen von VOCs und NOx, wobei meteorologische Bedingungen die Ozonproduktion stark beeinflussen. Die vorliegende Arbeit untersuchte die chemischen Mechanismen der Ozonproduktion innerhalb von Luftqualitätsmodellen, indem der Einfluss von VOC-Abbau, der Speziation von VOC-Ausstößen und der Temperatur auf modellierte Ozonproduktion untersucht wurde. Alle Modellierungsexperimente in dieser Arbeit verwendeten ein Box-Modell, um detaillierte Prozessstudien mit dem Fokus auf der Darstellung der Auswirkung troposphärischer Chemie auf die Ozonproduktion durchzuführen. Modellsimulationen verwendeten den hochdetaillierten, chemischen Mechanismus MCM v3.2 als Referenz. Die Modellsimulation wurden dann mit reduzierten chemischen Mechanismen wiederholt, die in der Regel von regionalen und globalen Modellen verwendet werden, um zu bestimmen wie die Wahl der chemischen Mechanismen sich auf die Empfindlichkeit der Ozonproduktion auswirkt.

Die Auswirkungen der verschiedenen Vereinfachungsansätze, die die chemischen Mechanismen bezüglich der Ozonproduktion verwenden, wurden durch einen Vergleich der Ozonproduktion während des VOC-Abbaus zwischen verschiedenen chemischen Mechanismen bestimmt. Der chemische Mechanismus CRI v2 hat im Vergleich zu MCM v3.2 die vergleichbarste Ozonmenge aus dem Abbau jedes VOC erzeugt. Der VOC-Abbau welcher in den xxx (M-4, R2, R und R2) und yyy (C-IV und CB) chemischen Mechanismen beschrieben ist, produzierte jedoch gemeinhin weniger Ozon als MCM v3.2. Ein schnellerer Abbau des ausgestoßenen VOC in kleinere Abbauprodukte in den xxx und yyy chemischen Mechanismen verursachte die geringere Ozonproduktion während des VOC-Abbaus. Des Weiteren wurden größere Unterschiede in der Ozonproduktion durch VOCs erzeugt, welche durch Mechanismusspezien repräsentiert waren, als solche die durchexplizite Spezien dargestellt wurden.

—

Der Einfluss auf die Ozonproduktion von der Speziation von VOC-Ausstöße durch ein Emissionsinventar wurde durch Vergleich der Ozon aus verschiedenen Emissionsinventaren des Lösungsmittels Sektor produziert etabliert. In diesen Experimenten führte die unterschiedlichen Emissionsinventare der VOC-Ausstöße von Unterschieden in der Mischungsverhältnisse von Spitzozon und die Ozonproduktion.

Die Ozonproduktion am ersten Tag wurde von den angegebenen Beiträgen von Alken und aromatischen VOC beeinflußt. Emissionsinventar größere Mengen an Alkanausstöße Angabe erzeugt die größten Mengen an Ozon am Ende der Simulation als die einen größeren Beitrag der Ausstößen von oxygeniertem VOC angibt. Durch Wiederholung der Simulationen mit reduzierten chemischen Mechanismen (MOZART-4 und RADM2) wiedergegeben, die Unterschiede in der Ozonproduktion mit dem MCM v3.2 chemischen Mechanismus erhalten. Diese Ergebnisse zeigten eine Sensitivität von Ozonproduktion sowohl die Wahl der chemischen Mechanismus und Emissionsinventar Speziation.

Die letzte Studie dieser Arbeit betrachtet die Beziehung zwischen Ozon, Temperatur und NO_x. Der Anstieg des Ozons mit der Temperatur aufgrund der temperaturabhängigen Chemie war geringfügig größer als der Anstieg des Ozons mit der Temperatur aufgrund der erhöhten Isopren-Ausstöße mit der Temperatur in allen NO_x Bedingungen. Eine nicht-lineare Zusammenhang zwischen Ozon, Temperatur und NO_x wurde mit jeder chemischen Mechanismus in dieser Studie (MCM v3.2, CRI v2, MOZART-4, RADM2 und CB05) verwendet wird, erhalten. Bei jeder chemischen Mechanismus, war der Anstieg der Ozonproduktion mit der Temperatur aufgrund der erhöhten Verlust des ausgestoßenen VOC mit der Temperatur hauptsächlich verursacht durch die erhöhte OH-Reaktivität von VOC mit der Temperatur. Die temperaturabhängige Chemie von Peroxynitraten, wie PANs, führte auch zu einer Erhöhung der Ozonproduktion mit der Temperatur.

Die detaillierten Prozesse Studien dieser Arbeit wird dazu beitragen, Modellleistung und das Vertrauen in die Prognosen zukünftiger Ozonwerte von Luftqualitätsmodellierungsstudien zu verbessern. Die Darstellung von VOC-Abbau und sekundären Prozesse wie die Abbaugeschwindigkeit der emittierten VOC und Peroxynitratchemie durch einen chemischen Mechanismus sind besonders wichtige Prozesse für den Vorhersagen der Ozonwerte mit unterschiedlichen Minderungsstrategien.

References

J. Abbatt, C. George, M. Melamed, P. Monks, S. Pandis, and Y. Rudich. New directions: Fundamentals of atmospheric chemistry: Keeping a three-legged stool balanced. *Atmospheric Environment*, 84:390 – 391, 2014.

A. Archibald, M. Jenkin, and D. Shallcross. An isoprene mechanism intercomparison. *Atmospheric Environment*, 44(40):5356 – 5364, 2010.

R. Atkinson. Atmospheric chemistry of VOCs and NO_x. *Atmospheric Environment*, 34(12-14):2063–2101, 2000.

R. Atkinson and J. Arey. Atmospheric Degradation of Volatile Organic Compounds. *Chemical Reviews*, 103:4605–4638, 2003.

A. Baklanov, K. Schlünzen, P. Suppan, J. Baldasano, D. Brunner, S. Aksoyoglu, G. Carmichael, J. Douros, J. Flemming, R. Forkel, S. Galmarini, M. Gauss, G. Grell, M. Hirtl, S. Joffre, O. Jorba, E. Kaas, M. Kaasik, G. Kallos, X. Kong, U. Korsholm, A. Kurganskiy, J. Kushta, U. Lohmann, A. Mahura, A. Manders-Groot, A. Maurizi, N. Moussiopoulos, S. T. Rao, N. Savage, C. Seigneur, R. S. Sokhi, E. Solazzo, S. Solomos, B. Sørensen, G. Tsegas, E. Vignati, B. Vogel, and Y. Zhang. Online coupled regional meteorology chemistry models in Europe: current status and prospects. *Atmospheric Chemistry and Physics*, 14(1):317–398, 2014.

C. Bloss, V. Wagner, M. E. Jenkin, R. Vollamer, W. J. Bloss, J. D. Lee, D. E. Heard, K. Wirtz, M. Martin-Reviejo, G. Rea, J. C. Wenger, and M. J. Pilling. Development of a detailed chemical mechanism (MCMv3.1) for the atmospheric oxidation of aromatic hydrocarbons. *Atmospheric Chemistry and Physics*, 5:641–664, 2005.

B. Bonn, E. von Schneidemesser, D. Andrich, J. Quedenau, H. Gerwig, A. Lüdecke, J. Kura, A. Pietsch, C. Ehlers, D. Klemp, C. Kofahl, R. Nothard, A. Kerschbaumer, W. Junkermann, R. Grote, T. Pohl, K. Weber, B. Lode, P. Schönberger, G. Churkina, T. M. Butler, and M. G. Lawrence. BAERLIN2014 - The influence of land surface types on and the horizontal heterogeneity of air pollutant levels in Berlin. *Atmospheric Chemistry and Physics Discussions*, 2016:1–62, 2016.

A. Boynard, A. Borbon, T. Leonardis, B. Barletta, S. Meinardi, D. R. Blake, and N. Locoge. Spatial and seasonal variability of measured anthropogenic non-methane hydrocarbons in urban atmospheres: Implication on emission ratios. *Atmospheric Environment*, 82(0):258–267, 2014.

P. Builtjes, M. Loon, M. Schaap, S. Teeuwisse, A. Visschedijk, and J. Bloos. The development of an emission data base over Europe and further contributions of TNO-MEP. Technical report, TNO Environment, 2002.

T. Butler, M. Lawrence, D. Taraborrelli, and J. Lelieveld. Multi-day ozone production potential of volatile organic compounds calculated with a tagging approach. *Atmospheric Environment*, 45(24):4082 – 4090, 2011.

T. M. Butler and M. G. Lawrence. The influence of megacities on global atmospheric chemistry: a modelling study. *Environmental Chemistry*, 6:219–225, 2009.

L. Camalier, W. Cox, and P. Dolwick. The effects of meteorology on ozone in urban areas and their use in assessing ozone trends. *Atmospheric Environment*, 41(33):7127 – 7137, 2007.

W. P. Carter. Development of ozone reactivity scales for volatile organic compounds. *Air & Waste*, 44(7):881–899, 1994.

W. P. L. Carter. Development of a Database for Chemical Mechanism Assignments for Volatile Organic Emissions. *Journal of the Air & Waste Management Association*, 0, 2015.

J. Coates and T. M. Butler. A comparison of chemical mechanisms using tagged ozone production potential (TOPP) analysis. *Atmospheric Chemistry and Physics*, 15(15):8795–8808, 2015.

J. Coates, K. A. Mar, N. Ojha, and T. M. Butler. The influence of temperature on ozone production under varying NO_x conditions – a modelling study. *Atmospheric Chemistry and Physics Discussions*, Submitted, 2016.

I. Coll, C. Rousseau, B. Barletta, S. Meinardi, and D. R. Blake. Evaluation of an urban NMHC emission inventory by measurements and impact on CTM results. *Atmospheric Environment*, 44(31):3843 – 3855, 2010.

A. C. Comrie. Comparing neural networks and regression models for ozone forecasting. *Journal of the Air & Waste Management Association*, 47(6):653–663, 1997.

G. Curci, M. Beekmann, R. Vautard, G. Smiatek, R. Steinbrecher, J. Theloke, and R. Friedrich. Modelling study of the impact of isoprene and terpene biogenic

emissions on European ozone levels. *Atmospheric Environment*, 43(7):1444 – 1455, 2009.

V. Damian, A. Sandu, M. Damian, F. Potra, and G. R. Carmichael. The kinetic preprocessor KPP-a software environment for solving chemical kinetics. *Computers & Chemical Engineering*, 26(11):1567 – 1579, 2002.

J. P. Dawson, P. J. Adams, and S. N. Pandis. Sensitivity of ozone to summertime climate in the eastern USA: A modeling case study . *Atmospheric Environment*, 41 (7):1494 – 1511, 2007.

H. Denier van der Gon, C. Hendriks, J. Kuenen, A. Segers, and A. Visschedijk. Description of current temporal emission patterns and sensitivity of predicted AQ for temporal emission patterns. Technical Report EU FP7 MACC report: D_D-EMIS_1.3, TNO, 2011.

R. M. Doherty, O. Wild, D. T. Shindell, G. Zeng, I. A. MacKenzie, W. J. Collins, A. M. Fiore, D. S. Stevenson, F. J. Dentener, M. G. Schultz, P. Hess, R. G. Derwent, and T. J. Keating. Impacts of climate change on surface ozone and intercontinental ozone pollution: A multi-model study. *Journal of Geophysical Research: Atmospheres*, 118(9):3744–3763, 2013.

C. Dueñas, M. Fernández, S. Cañete, J. Carretero, and E. Liger. Assessment of ozone variations and meteorological effects in an urban area in the Mediterranean Coast. *Science of The Total Environment*, 299(1–3):97 – 113, 2002.

EEA. Air quality in Europe - 2011 report. Technical Report 12/2011, European Environmental Agency, 2011.

EEA. Air quality in Europe - 2013 report. Technical Report 9/2013, European Environmental Agency, 2013.

EEA. Air quality in Europe - 2015 report. Technical Report 5/2015, European Environmental Agency, 2015.

Ehhalt, D., Prather, M., Dentener, F., Derwent, R., Dlugokencky, E., Holland, E., Isaksen, I., Katima, J., Kirchhoff, V., Matson, P., Midgley, P., Wang, and M. Climate Change 2001: The Scientific Basis. Contribution of Working Group I to the Third Assessment Report of the Intergovernmental Panel on Climate Change. Technical report, IPCC, 2001.

K. M. Emmerson and M. J. Evans. Comparison of tropospheric gas-phase chemistry schemes for use within global models. *Atmospheric Chemistry and Physics*, 9(5): 1831–1845, 2009.

L. K. Emmons, S. Walters, P. G. Hess, J.-F. Lamarque, G. G. Pfister, D. Fillmore, C. Granier, A. Guenther, D. Kinnison, T. Laepple, J. Orlando, X. Tie, G. Tyndall, C. Wiedinmyer, S. L. Baughcum, and S. Kloster. Description and evaluation of the Model for Ozone and Related chemical Tracers, version 4 (MOZART-4). *Geoscientific Model Development*, 3(1):43–67, 2010.

L. K. Emmons, P. G. Hess, J.-F. Lamarque, and G. G. Pfister. Tagged ozone mechanism for mozart-4, cam-chem and other chemical transport models. *Geoscientific Model Development*, 5(6):1531–1542, 2012.

V. Eyring, J.-F. Lamarque, P. Hess, F. Arfeuille, K. Bowman, M. P. Chipperfield, B. Duncan, A. Fiore, A. Gettelman, M. A. Giorgetta, C. Granier, M. Hegglin, D. Kinnison, M. Kunze, U. Langematz, B. Luo, R. Martin, K. Matthes, P. A. Newman, T. Peter, A. Robock, T. Ryerson, A. Saiz-Lopez, R. Salawitch, M. Schultz, T. G. Shepherd, D. Shindell, J. Staehelin, S. Tegtmeier, L. Thomason, S. Tilmes, J.-P. Vernier, D. W. Waugh, , and P. J. Young. Overview of IGAC/SPARC Chemistry-Climate Model Initiative (CCMI) Community Simulations in Support of Upcoming Ozone and Climate Assessments. *SPARC Newsletter*, 40:48–66, 2013.

R. Friedrich, B. Wickert, P. Blank, S. Emeis, W. Engewald, D. Hassel, H. Hoffmann, H. Michael, A. Obermeier, K. Schäfer, T. Schmitz, A. Sedlmaier, M. Stockhause, J. Theloke, and F.-J. Weber. Development of Emission Models and Improvement of Emission Data for Germany. *Journal of Atmospheric Chemistry*, 42(1):179–206, 2002.

M. W. Gery, G. Z. Whitten, J. P. Killus, and M. C. Dodge. A photochemical kinetics mechanism for urban and regional scale computer modeling. *Journal of Geophysical Research*, 94(D10):12,925–12,956, 1989.

W. S. Goliff, W. R. Stockwell, and C. V. Lawson. The regional atmospheric chemistry mechanism, version 2. *Atmospheric Environment*, 68:174 – 185, 2013.

J. Goodwin. UK Emissions of Air Pollutants 1970 to 1998. Technical report, DEFRA, 2000.

G. Grell, S. Peckham, R. Schmitz, S. McKeen, G. Frost, W. Skamarock, and B. Eder. Fully coupled "online" chemistry within the WRF model. *Atmospheric Environment*, 39(37):6957–6975, 2005.

S. Grice, J. Stedman, A. Kent, M. Hobson, J. Norris, J. Abbott, and S. Cooke. Recent trends and projections of primary NO2 emissions in Europe. *Atmospheric Environment*, 43(13):2154 – 2167, 2009.

A. Guenther, T. Karl, P. Harley, C. Wiedinmyer, P. I. Palmer, and C. Geron. Estimates of global terrestrial isoprene emissions using MEGAN (Model of Emissions of Gases and Aerosols from Nature). *Atmospheric Chemistry and Physics*, 6(11): 3181–3210, 2006.

A. B. Guenther, X. Jiang, C. L. Heald, T. Sakulyanontvittaya, T. Duhl, L. K. Emmons, and X. Wang. The Model of Emissions of Gases and Aerosols from Nature version 2.1 (MEGAN2.1): an extended and updated framework for modeling biogenic emissions. *Geoscientific Model Development*, 5(6):1471–1492, 2012.

D. W. Gunz and M. R. Hoffmann. Atmospheric chemistry of peroxides: a review. *Atmospheric Environment. Part A. General Topics*, 24(7):1601 – 1633, 1990.

M. Hallquist, J. C. Wenger, U. Baltensperger, Y. Rudich, D. Simpson, M. Claeys, J. Dommen, N. M. Donahue, C. George, A. H. Goldstein, J. F. Hamilton, H. Herrmann, T. Hoffmann, Y. Iinuma, M. Jang, M. E. Jenkin, J. L. Jimenez, A. Kiendler-Scharr, W. Maenhaut, G. McFiggans, T. F. Mentel, A. Monod, A. S. H. Prévôt, J. H. Seinfeld, J. D. Surratt, R. Szmigielski, and J. Wildt. The formation, properties and impact of secondary organic aerosol: current and emerging issues. *Atmospheric Chemistry and Physics*, 9(14):5155–5236, 2009.

D. A. Hauglustaine, G. P. Brasseur, S. Walters, P. J. Rasch, J.-F. Müller, L. K. Emmons, and M. A. Carroll. MOZART, a global chemical transport model for ozone and related chemical tracers 2. Model results and evaluation. *Journal of Geophysical Research*, 103(D21):28,291–28,335, 1998.

IARC. Outdoor air pollution a leading environmental cause of cancer deaths. `https://www.iarc.fr/en/media-centre/iarcnews/pdf/pr221_E.pdf`, 2013. [Online; accessed 31-December-2015].

D. J. Jacob and D. A. Winner. Effect of climate change on air quality. *Atmospheric Environment*, 43(1):51 – 63, 2009. Atmospheric Environment - Fifty Years of Endeavour.

M. Jenkin, L. Watson, S. Utembe, and D. Shallcross. A Common Representative Intermediates (CRI) mechanism for VOC degradation. Part 1: Gas phase mechanism development. *Atmospheric Environment*, 42(31):7185 – 7195, 2008.

M. E. Jenkin and K. C. Clemitshaw. Ozone and other secondary photochemical pollutants: Chemical processes governing their formation in the planetary boundary layer. *Atmospheric Environment*, 34(16):2499–2527, 2000.

M. E. Jenkin, S. M. Saunders, and M. J. Pilling. The tropospheric degradation of volatile organic compounds: a protocol for mechanism development. *Atmospheric Environment*, 31(1):81 – 104, 1997.

M. E. Jenkin, S. M. Saunders, V. Wagner, and M. J. Pilling. Protocol for the development of the Master Chemical Mechanism, MCM v3 (Part B): tropospheric degradation of aromatic volatile organic compounds. *Atmospheric Chemistry and Physics*, 3(1):181–193, 2003.

T. R. Karl and K. E. Trenberth. Modern global climate change. *Science*, 302(5651): 1719–1723, 2003.

S. Kirschke, P. Bousquet, P. Ciais, M. Saunois, J. G. Canadell, E. J. Dlugokencky, P. Bergamaschi, D. Bergmann, D. R. Blake, L. Bruhwiler, P. Cameron-Smith, S. Castaldi, F. Chevallier, L. Feng, A. Fraser, M. Heimann, E. L. Hodson, S. Houweling, B. Josse, P. J. Fraser, P. B. Krummel, J.-F. Lamarque, R. L. Langenfelds, C. Le Quere, V. Naik, S. O'Doherty, P. I. Palmer, I. Pison, D. Plummer, B. Poulter, R. G. Prinn, M. Rigby, B. Ringeval, M. Santini, M. Schmidt, D. T. Shindell, I. J. Simpson, R. Spahni, L. P. Steele, S. A. Strode, K. Sudo, S. Szopa, G. R. van der Werf, A. Voulgarakis, M. van Weele, R. F. Weiss, J. E. Williams, and G. Zeng. Three decades of global methane sources and sinks. *Nature Geoscience*, 6 (10):813–823, 2013.

L. I. Kleinman. Low and high NO_x tropospheric photochemistry. *Journal of Geophysical Research*, 99(D8):16,831–16,838, 1994.

P. E. Korsog and G. T. Wolff. An examination of urban ozone trends in the Northeastern U.S. (1973–1983) using a robust statistical method. *Atmospheric Environment. Part B. Urban Atmosphere*, 25(1):47 – 57, 1991.

D. Kubistin, H. Harder, M. Martinez, M. Rudolf, R. Sander, H. Bozem, G. Eerdekens, H. Fischer, C. Gurk, T. Klüpfel, R. Königstedt, U. Parchatka, C. L. Schiller, A. Stickler, D. Taraborrelli, J. Williams, and J. Lelieveld. Hydroxyl radicals in the tropical troposphere over the Suriname rainforest: comparison of measurements with the box model MECCA. *Atmospheric Chemistry and Physics*, 10(19):9705–9728, 2010.

J. J. P. Kuenen, A. J. H. Visschedijk, M. Jozwicka, and H. A. C. Denier van der Gon. TNO-MACC_II emission inventory; a multi-year (2003–2009) consistent high-resolution european emission inventory for air quality modelling. *Atmospheric Chemistry and Physics*, 14(20):10963–10976, 2014.

M. Kuhn, P. Builtjes, D. Poppe, D. Simpson, W. Stockwell, Y. Andersson-Sko¨ld, A. Baart, M. Das, F. Fiedler, Ø. Hov, F. Kirchner, P. Makar, J. Milford, M. Roemer, R. Ruhnke, A. Strand, B. Vogel, and H. Vogel. Intercomparison of the gas-phase chemistry in several chemistry and transport models. *Atmospheric Environment*, 32 (4):693 – 709, 1998.

J.-F. Lamarque, T. C. Bond, V. Eyring, C. Granier, A. Heil, Z. Klimont, D. Lee, C. Liousse, A. Mieville, B. Owen, M. G. Schultz, D. Shindell, S. J. Smith, E. Stehfest, J. Van Aardenne, O. R. Cooper, M. Kainuma, N. Mahowald, J. R. McConnell, V. Naik, K. Riahi, and D. P. van Vuuren. Historical (1850–2000) gridded anthropogenic and biomass burning emissions of reactive gases and aerosols: methodology and application. *Atmospheric Chemistry and Physics*, 10(15):7017–7039, 2010.

J. Lelieveld and F. J. Dentener. What controls tropospheric ozone? *Journal of Geophysical Research: Atmospheres*, 105(D3):3531–3551, 2000.

A. S. M. Lourens, T. M. Butler, J. P. Beukes, P. G. van Zyl, G. D. Fourie, and M. G. Lawrence. Investigating atmospheric photochemistry in the Johennesburg-Pretoria megacity using a box model. *South African Journal of Science*, 112(1/2), 2016.

P. S. Monks. A review of the observations and origins of the spring ozone maximum. *Atmospheric Environment*, 34(21):3545 – 3561, 2000.

P. S. Monks. Gas-phase radical chemistry in the troposphere. *Chem. Soc. Rev.*, 34: 376–395, 2005.

K. Murazaki and P. Hess. How does climate change contribute to surface ozone change over the united states? *Journal of Geophysical Research: Atmospheres*, 111 (D5), 2006. D05301.

T. P. Murrells, N.R.P., G. Thistlethwaite, A. Wagner, Y. Li, T.B., J. Norris, C. Walker, R. A. Stewart, I. Tsagatakis, R. Whiting, C.C., S. Okamura, M. Peirce, S. Sneddon, J. Webb, J.T., J. MacCarthy, S. Choudrie, and N. Brophy. UK Emissions of Air Pollutants 1970 to 2008. Technical report, DEFRA, Didcot, UK, 2010.

J. Olivier, J. Berdowski, J. Bakker, A. Visschedijk, and J. Bloos. Applications of EDGAR. Including a description of EDGAR 3.0: reference database with trend data for 1970–1995. Technical Report RIVM report No. 773301 001/NOP report no. 410200 051, RIVM, 2001.

N. Otero, J. Sillmann, J. L. Schnell, H. W. Rust, and T. Butler. Synoptic and meteorological drivers of extreme ozone concentrations over europe. *Environmental Research Letters*, 11(2):024005, 2016.

S. A. Penkett and K. A. Brice. The spring maximum of photo-oxidants in the Northern Hemisphere troposphere. *Nature*, 319:655–657, 1986.

S. E. Pusede, D. R. Gentner, P. J. Wooldridge, E. C. Browne, A. W. Rollins, K.-E. Min, A. R. Russell, J. Thomas, L. Zhang, W. H. Brune, S. B. Henry, J. P. DiGangi, F. N. Keutsch, S. A. Harrold, J. A. Thornton, M. R. Beaver, J. M. St. Clair, P. O. Wennberg, J. Sanders, X. Ren, T. C. VandenBoer, M. Z. Markovic, A. Guha, R. Weber, A. H. Goldstein, and R. C. Cohen. On the temperature dependence of organic reactivity, nitrogen oxides, ozone production, and the impact of emission controls in San Joaquin Valley, California. *Atmospheric Chemistry and Physics*, 14 (7):3373–3395, 2014.

S. E. Pusede, A. L. Steiner, and R. C. Cohen. Temperature and Recent Trends in the Chemistry of Continental Surface Ozone. *Chemical Reviews*, 115(10):3898–3918, 2015.

P. N. Racherla and P. J. Adams. The response of surface ozone to climate change over the eastern united states. *Atmospheric Chemistry and Physics*, 8(4):871–885, 2008.

A. Rickard, J. Young, M. J. Pilling, M. E. Jenkin, S. Pascoe, and S. M. Saunders. The Master Chemical Mechanism Version MCM v3.2. `http://mcm.leeds.ac.uk/ MCMv3.2/`, 2015. [Online; accessed 25-March-2015].

J. I. Rubin, A. J. Kean, R. A. Harley, D. B. Millet, and A. H. Goldstein. Temperature dependence of volatile organic compound evaporative emissions from motor vehicles. *Journal of Geophysical Research: Atmospheres*, 111(D3), 2006. D03305.

A. Russell and R. Dennis. NARSTO critical review of photochemical models and modeling. *Atmospheric Environment*, 34(12–14):2283 – 2324, 2000.

R. Sander, A. Kerkweg, P. Jöckel, and J. Lelieveld. Technical note: The new comprehensive atmospheric chemistry module mecca. *Atmospheric Chemistry and Physics*, 5(2):445–450, 2005.

S. M. Saunders, M. E. Jenkin, R. G. Derwent, and M. J. Pilling. Protocol for the development of the Master Chemical Mechanism, MCM v3 (Part A): tropospheric degradation of non-aromatic volatile organic compounds. *Atmospheric Chemistry and Physics*, 3(1):161–180, 2003.

J. H. Seinfeld and S. N. Pandis. *Atmospheric Chemistry and Physics: From Air Pollution to Climate Change*. John Wiley & Sons Inc, New York, second edition, 2006.

C. Sidiropoulos and G. Tsilingiridis. Composition changes of NMVOC emissions from solvent use in Greece for the period 1990-2005. *Fresenius Environmental Bulletin*, 16(9):1108–1112, 2007.

S. Sillman and P. J. Samson. Impact of temperature on oxidant photochemistry in urban, polluted rural and remote environments. *Journal of Geophysical Research: Atmospheres*, 100(D6):11497–11508, 1995.

D. Simpson, A. Benedictow, H. Berge, R. Bergström, L. D. Emberson, H. Fagerli, C. R. Flechard, G. D. Hayman, M. Gauss, J. E. Jonson, M. E. Jenkin, A. Nyíri, C. Richter, V. S. Semeena, S. Tsyro, J.-P. Tuovinen, Á. Valdebenito, and P. Wind. The EMEP MSC-W chemical transport model – technical description. *Atmospheric Chemistry and Physics*, 12(16):7825–7865, 2012.

W. R. Stockwell, P. Middleton, J. S. Chang, and X. Tang. The second generation regional acid deposition model chemical mechanism for regional air quality modeling. *Journal of Geophysical Research: Atmospheres*, 95(D10):16343–16367, 1990.

W. R. Stockwell, F. Kirchner, M. Kuhn, and S. Seefeld. A new mechanism for regional atmospheric chemistry modeling. *Journal of Geophysical Research: Atmospheres*, 102(D22):25847–25879, 1997.

W. R. Stockwell, C. V. Lawson, E. Saunders, and W. S. Goliff. A review of tropospheric atmospheric chemistry and gas-phase chemical mechanisms for air quality modeling. *Atmosphere*, 3(1):1, 2012.

S. Syri, M. Amann, W. Schöpp, and C. Heyes. Estimating long-term population exposure to ozone in urban areas of Europe. *Environmental Pollution*, 113(1):59 – 69, 2001.

E. von Schneidemesser, P. S. Monks, V. Gros, J. Gauduin, and O. Sanchez. How important is biogenic isoprene in an urban environment? a study in london and paris. *Geophysical Research Letters*, 38(19), 2011. L19804.

E. von Schneidemesser, P. S. Monks, J. D. Allan, L. Bruhwiler, P. Forster, D. Fowler, A. Lauer, W. T. Morgan, P. Paasonen, M. Righi, K. Sindelarova, and M. A. Sutton. Chemistry and the Linkages between Air Quality and Climate Change. *Chemical Reviews*, 2015. PMID: 25926133.

E. von Schneidemesser, J. Coates, H. D. van der Gon, A. Visschedijk, and T. Butler. Variation of the NMVOC speciation in the solvent sector and the sensitivity of modelled tropospheric ozone. *Atmospheric Environment*, 135:59 – 72, 2016.

A. Voulgarakis, V. Naik, J.-F. Lamarque, D. T. Shindell, P. J. Young, M. J. Prather, O. Wild, R. D. Field, D. Bergmann, P. Cameron-Smith, I. Cionni, W. J. Collins, S. B. Dalsøren, R. M. Doherty, V. Eyring, G. Faluvegi, G. A. Folberth, L. W. Horowitz, B. Josse, I. A. MacKenzie, T. Nagashima, D. A. Plummer, M. Righi, S. T. Rumbold, D. S. Stevenson, S. A. Strode, K. Sudo, S. Szopa, and G. Zeng. Analysis of present day and future OH and methane lifetime in the ACCMIP simulations. *Atmospheric Chemistry and Physics*, 13(5):2563–2587, 2013.

World Meteorological Organisation. Scientific Assessment of Ozone Depletion: 2010. Technical Report 516 pp., World Meteorological Organisation, Geneva, Switzerland, March 2011.

G. Yarwood, S. Rao, M. Yocke, and G. Z. Whitten. Updates to the Carbon Bond Chemical Mechanism: CB05. Technical report, U. S Environmental Protection Agency, 2005.

P. J. Young, A. T. Archibald, K. W. Bowman, J.-F. Lamarque, V. Naik, D. S. Stevenson, S. Tilmes, A. Voulgarakis, O. Wild, D. Bergmann, P. Cameron-Smith, I. Cionni, W. J. Collins, S. B. Dalsøren, R. M. Doherty, V. Eyring, G. Faluvegi, L. W. Horowitz, B. Josse, Y. H. Lee, I. A. MacKenzie, T. Nagashima, D. A. Plummer, M. Righi, S. T. Rumbold, R. B. Skeie, D. T. Shindell, S. A. Strode, K. Sudo, S. Szopa, and G. Zeng. Pre-industrial to end 21st century projections of tropospheric ozone from the Atmospheric Chemistry and Climate Model Intercomparison Project (ACCMIP). *Atmospheric Chemistry and Physics*, 13(4):2063–2090, 2013.

Chapter 7

Paper I: A comparison of chemical mechanisms using tagged ozone production potential (TOPP) analysis

**Atmospheric
Chemistry
and Physics**

A comparison of chemical mechanisms using tagged ozone production potential (TOPP) analysis

J. Coates and T. M. Butler

Institute for Advanced Sustainability Studies, Potsdam, Germany

Correspondence to: J. Coates (jane.coates@iass-potsdam.de)

Abstract. Ground-level ozone is a secondary pollutant produced photochemically from reactions of NO_x with peroxy radicals produced during volatile organic compound (VOC) degradation. Chemical transport models use simplified representations of this complex gas-phase chemistry to predict O_3 levels and inform emission control strategies. Accurate representation of O_3 production chemistry is vital for effective prediction. In this study, VOC degradation chemistry in simplified mechanisms is compared to that in the near-explicit Master Chemical Mechanism (MCM) using a box model and by "tagging" all organic degradation products over multi-day runs, thus calculating the tagged ozone production potential (TOPP) for a selection of VOCs representative of urban air masses. Simplified mechanisms that aggregate VOC degradation products instead of aggregating emitted VOCs produce comparable amounts of O_3 from VOC degradation to the MCM. First-day TOPP values are similar across mechanisms for most VOCs, with larger discrepancies arising over the course of the model run. Aromatic and unsaturated aliphatic VOCs have the largest inter-mechanism differences on the first day, while alkanes show largest differences on the second day. Simplified mechanisms break VOCs down into smaller-sized degradation products on the first day faster than the MCM, impacting the total amount of O_3 produced on subsequent days due to secondary chemistry.

1 Introduction

Ground-level ozone (O_3) is both an air pollutant and a climate forcer that is detrimental to human health and crop growth (Stevenson et al., 2013). O_3 is produced from the reactions of volatile organic compounds (VOCs) and nitro-

gen oxides ($NO_x = NO + NO_2$) in the presence of sunlight (Atkinson, 2000).

Background O_3 concentrations have increased during the last several decades due to the increase of overall global anthropogenic emissions of O_3 precursors (HTAP, 2010). Despite decreases in emissions of O_3 precursors over Europe since 1990, EEA (2014) reports that 98 % of Europe's urban population are exposed to levels exceeding the WHO air quality guideline of $100 \, \mu g \, m^{-3}$ over an 8 h mean. These exceedances result from local and regional O_3 precursor gas emissions, their intercontinental transport and the non-linear relationship of O_3 concentrations to NO_x and VOC levels (EEA, 2014).

Effective strategies for emission reductions rely on accurate predictions of O_3 concentrations using chemical transport models (CTMs). These predictions require adequate representation of gas-phase chemistry in the chemical mechanism used by the CTM. For reasons of computational efficiency, the chemical mechanisms used by global and regional CTMs must be simpler than the nearly explicit mechanisms which can be used in box modelling studies. This study compares the impacts of different simplification approaches of chemical mechanisms on O_3 production chemistry focusing on the role of VOC degradation products.

$$NO + O_3 \rightarrow NO_2 + O_2 \tag{R1}$$
$$NO_2 + h\nu \rightarrow NO + O(^3P) \tag{R2}$$
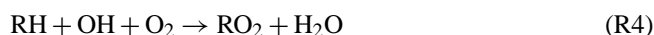$$O_2 + O(^3P) + M \rightarrow O_3 + M \tag{R3}$$

The photochemical cycle (Reactions R1–R3) rapidly produces and destroys O_3. NO and NO_2 reach a near-steady state via Reactions (R1) and (R2) which is disturbed in two cases. Firstly, via O_3 removal (deposition or Reaction R1 during night-time and near large NO sources) and secondly,

when O_3 is produced through VOC–NO_x chemistry (Sillman, 1999).

VOCs (RH) are mainly oxidised in the troposphere by the hydroxyl radical (OH) forming peroxy radicals (RO_2) in the presence of O_2. For example, Reaction (R4) describes the OH oxidation of alkanes proceeding though abstraction of an H from the alkane. In high-NO_x conditions, typical of urban environments, RO_2 react with NO (Reaction R5) to form alkoxy radicals (RO), which react quickly with O_2 (Reaction R6) producing a hydroperoxy radical (HO_2) and a carbonyl species ($R'CHO$). The secondary chemistry of these first-generation carbon-containing oxidation products is analogous to the sequence of Reactions (R4–R6), producing further HO_2 and RO_2 radicals. Subsequent-generation oxidation products can continue to react, producing HO_2 and RO_2 until they have been completely oxidised to CO_2 and H_2O. Both RO_2 and HO_2 react with NO to produce NO_2 (Reactions R5 and R7) leading to O_3 production via Reactions (R2) and (R3). Thus, the amount of O_3 produced from VOC degradation is related to the number of NO to NO_2 conversions by RO_2 and HO_2 radicals formed during VOC degradation (Atkinson, 2000).

$$RH + OH + O_2 \rightarrow RO_2 + H_2O \tag{R4}$$
$$RO_2 + NO \rightarrow RO + NO_2 \tag{R5}$$
$$RO + O_2 \rightarrow R'CHO + HO_2 \tag{R6}$$
$$HO_2 + NO \rightarrow OH + NO_2 \tag{R7}$$

Three atmospheric regimes with respect to O_3 production can be defined (Jenkin and Clemitshaw, 2000). In the NO_x-sensitive regime, VOC concentrations are much higher than those of NO_x, and O_3 production depends on NO_x concentrations. On the other hand, when NO_x concentrations are much higher than those of VOCs (VOC-sensitive regime), VOC concentrations determine the amount of O_3 produced. Finally, the NO_x–VOC-sensitive regime produces maximal O_3 and is controlled by both VOC and NO_x concentrations.

These atmospheric regimes remove radicals through distinct mechanisms (Kleinman, 1991). In the NO_x-sensitive regime, radical concentrations are high relative to NO_x leading to radical removal by radical combination (Reaction R8) and bimolecular destruction (Reaction R9) (Kleinman, 1994).

$$RO_2 + HO_2 \rightarrow ROOH + O_2 \tag{R8}$$
$$HO_2 + OH \rightarrow H_2O + O_2 \tag{R9}$$

However, in the VOC-sensitive regime, radicals are removed by reacting with NO_2 leading to nitric acid (HNO_3) (Reaction R10) and PAN species (Reaction R11).

$$NO_2 + OH \rightarrow HNO_3 \tag{R10}$$
$$RC(O)O_2 + NO_2 \rightarrow RC(O)O_2NO_2 \tag{R11}$$
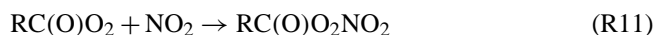
The NO_x–VOC-sensitive regime has no dominant radical removal mechanism as radical and NO_x amounts are compara-

ble. This chemistry results in O_3 concentrations being a nonlinear function of NO_x and VOC concentrations.

Individual VOCs impact O_3 production differently through their diverse reaction rates and degradation pathways. These impacts can be quantified using ozone production potentials (OPPs), which can be calculated through incremental reactivity (IR) studies using photochemical models. In IR studies, VOC concentrations are changed by a known increment and the change in O_3 production is compared to that of a standard VOC mixture. Examples of IR scales are the maximum incremental reactivity (MIR) and maximum ozone incremental reactivity (MOIR) scales in Carter (1994), as well as the photochemical ozone creation potential (POCP) scale of Derwent et al. (1996, 1998). The MIR, MOIR and POCP scales were calculated under different NO_x conditions, thus calculating OPPs in different atmospheric regimes.

Butler et al. (2011) calculate the maximum potential of a number of VOCs to produce O_3 by using NO_x conditions inducing NO_x–VOC-sensitive chemistry over multi-day scenarios using a "tagging" approach – the tagged ozone production potential (TOPP). Tagging involves labelling all organic degradation products produced during VOC degradation with the name of the emitted VOCs. Tagging enables the attribution of O_3 production from VOC degradation products back to the emitted VOCs, thus providing detailed insight into VOC degradation chemistry. Butler et al. (2011), using a near-explicit chemical mechanism, showed that some VOCs, such as alkanes, produce maximum O_3 on the second day of the model run; in contrast to unsaturated aliphatic and aromatic VOCs which produce maximum O_3 on the first day. In this study, the tagging approach of Butler et al. (2011) is applied to several chemical mechanisms of reduced complexity, using conditions of maximum O_3 production (NO_x–VOC-sensitive regime), to compare the effects of different representations of VOC degradation chemistry on O_3 production in the different chemical mechanisms.

A near-explicit mechanism, such as the Master Chemical Mechanism (MCM) (Jenkin et al., 2003; Saunders et al., 2003; Bloss et al., 2005), includes detailed degradation chemistry making the MCM ideal as a reference for comparing chemical mechanisms. Reduced mechanisms generally take two approaches to simplifying the representation of VOC degradation chemistry: lumped-structure approaches and lumped-molecule approaches (Dodge, 2000).

Lumped-structure mechanisms speciate VOCs by the carbon bonds of the emitted VOCs (e.g. the Carbon Bond mechanisms, CBM-IV (Gery et al., 1989) and CB05 (Yarwood et al., 2005)). Lumped-molecule mechanisms represent VOCs explicitly or by aggregating (lumping) many VOCs into a single mechanism species. Mechanism species may lump VOCs by functionality (MOdel for Ozone and Related chemical Tracers, MOZART-4, Emmons et al., 2010) or OH reactivity (Regional Acid Deposition Model, RADM2 (Stockwell et al., 1990), Regional Atmospheric Chemistry

Mechanism, RACM (Stockwell et al., 1997) and RACM2 (Goliff et al., 2013)). The Common Representative Intermediates mechanism (CRI) lumps the degradation products of VOCs rather than the emitted VOCs (Jenkin et al., 2008).

Many comparison studies of chemical mechanisms consider modelled time series of O_3 concentrations over varying VOC and NO_x concentrations. Examples are Dunker et al. (1984), Kuhn et al. (1998) and Emmerson and Evans (2009). The largest discrepancies between the time series of O_3 concentrations in different mechanisms from these studies arise when modelling urban rather than rural conditions and are attributed to the treatment of radical production, organic nitrate and night-time chemistry. Emmerson and Evans (2009) also compare the inorganic gas-phase chemistry of different chemical mechanisms; differences in inorganic chemistry arise from inconsistencies between IUPAC and JPL reaction rate constants.

Mechanisms have also been compared using OPP scales. OPPs are a useful comparison tool as they relate O_3 production to a single value. Derwent et al. (2010) compared the near-explicit MCM v3.1 and SAPRC-07 mechanisms using first-day POCP values calculated under VOC-sensitive conditions. The POCP values were comparable between the mechanisms. Butler et al. (2011) compared first-day TOPP values to the corresponding published MIR, MOIR and POCP values. TOPP values were most comparable to MOIR and POCP values due to the similarity of the chemical regimes used in their calculation.

In this study, we compare TOPP values of VOCs using a number of mechanisms to those calculated with the MCM v3.2, under standardised conditions which maximise O_3 production. Differences in O_3 production are explained by the differing treatments of secondary VOC degradation in these mechanisms.

2 Methodology

2.1 Chemical mechanisms

The nine chemical mechanisms compared in this study are outlined in Table 1 with a brief summary below. We used a subset of each chemical mechanism containing all the reactions needed to fully describe the degradation of the VOCs in Table 2. The reduced mechanisms in this study were chosen as they are commonly used in 3-D models and apply different approaches to representing secondary VOC chemistry. The recent review by Baklanov et al. (2014) shows that each chemical mechanism used in this study are actively used by modelling groups.

The MCM (Jenkin et al., 1997, 2003; Saunders et al., 2003; Bloss et al., 2005; Rickard et al., 2015) is a near-explicit mechanism which describes the degradation of 125 primary VOCs. The MCM v3.2 is the reference mechanism in this study due to its level of detail (16 349 organic reac-

tions). Despite this level of detail, the MCM had difficulties in reproducing the results of chamber study experiments involving aromatic VOCs (Bloss et al., 2005).

The CRI (Jenkin et al., 2008) is a reduced chemical mechanism with 1145 organic reactions describing the oxidation of the same primary VOCs as the MCM v3.1 (12 691 organic reactions). VOC degradation in the CRI is simplified by lumping the degradation products of many VOCs into mechanism species whose overall O_3 production reflects that of the MCM v3.1. The CRI v2 is available in more than one reduced variant, described in Watson et al. (2008). We used a subset of the full version of the CRI v2 (http://mcm.leeds.ac.uk/CRI). Differences in O_3 production between the CRI v2 and MCM v3.2 may be due to changes in the MCM versions rather than the CRI reduction techniques, hence the MCM v3.1 is also included in this study.

MOZART-4 represents global tropospheric and stratospheric chemistry (Emmons et al., 2010). Explicit species exist for methane, ethane, propane, ethene, propene, isoprene and α-pinene. All other VOCs are represented by lumped species determined by the functionality of the VOCs. Tropospheric chemistry is described by 145 organic reactions in MOZART-4.

RADM2 (Stockwell et al., 1990) describes regional-scale atmospheric chemistry using 145 organic reactions with explicit species representing methane, ethane, ethene and isoprene. All other VOCs are assigned to lumped species based on OH reactivity and molecular weight. RADM2 was updated to RACM (Stockwell et al., 1997) with more explicit and lumped species representing VOCs as well as revised chemistry (193 organic reactions). RACM2 is the updated RACM version (Goliff et al., 2013) with substantial updates to the chemistry, including more lumped and explicit species representing emitted VOCs (315 organic reactions).

CBM-IV (Gery et al., 1989) uses 46 organic reactions to simulate polluted urban conditions and represents ethene, formaldehyde and isoprene explicitly while all other emitted VOCs are lumped by their carbon bond types. All primary VOCs were assigned to lumped species in CBM-IV as described in Hogo and Gery (1989). For example, the mechanism species PAR represents the C–C bond. Pentane, having five carbon atoms, is represented as 5 PAR. A pentane mixing ratio of 1200 pptv is assigned to 6000 (= 1200 × 5) pptv of PAR in CBM-IV. CBM-IV was updated to CB05 (Yarwood et al., 2005) by including further explicit species representing methane, ethane and acetaldehyde, and has 99 organic reactions. Other updates include revised allocation of primary VOCs and updated rate constants.

2.2 Model set-up

The modelling approach and set-up follows the original TOPP study of Butler et al. (2011). The approach is summarised here; further details can be found in the Supplement and in Butler et al. (2011). We use the MECCA box model,

Table 1. The chemical mechanisms used in the study are shown here. MCM v3.2 is the reference mechanism. The number of organic species and reactions needed to fully oxidise the VOCs in Table 2 for each mechanism are also included.

Chemical mechanism	Number of organic species	Number of organic reactions	Type of lumping	Reference	Recent study
MCM v3.2	1884	5621	No lumping	Rickard et al. (2015)	Koss et al. (2015)
MCM v3.1	1677	4862	No lumping	Jenkin et al. (1997) Saunders et al. (2003) Jenkin et al. (2003) Bloss et al. (2005)	Lidster et al. (2014)
CRI v2	189	559	Lumped intermediates	Jenkin et al. (2008)	Derwent et al. (2015)
MOZART-4	61	135	Lumped molecule	Emmons et al. (2010)	Hou et al. (2015)
RADM2	42	105	Lumped molecule	Stockwell et al. (1990)	Li et al. (2014)
RACM	51	152	Lumped molecule	Stockwell et al. (1997)	Ahmadov et al. (2015)
RACM2	92	244	Lumped molecule	Goliff et al. (2013)	Goliff et. al. (2015)
CBM-IV	19	47	Lumped structure	Gery et al. (1989)	Foster et al. (2014)
CB05	33	86	Lumped structure	Yarwood et al. (2005)	Dunker et al. (2015)

originally described by Sander et al. (2005), and as subsequently modified by Butler et al. (2011) to include MCM chemistry. In this study, the model is run under conditions representative of 34° N at the equinox (broadly representative of the city of Los Angeles, USA).

Maximum O_3 production is achieved in each model run by balancing the chemical source of radicals and NO_x at each time step by emitting the appropriate amount of NO. These NO_x conditions induce NO_x–VOC-sensitive chemistry. Ambient NO_x conditions are not required as this study calculates the maximum potential of VOCs to produce O_3. Future work should verify the extent to which the maximum potential of VOCs to produce O_3 is reached under ambient NO_x conditions.

VOCs typical of Los Angeles and their initial mixing ratios are taken from Baker et al. (2008), listed in Table 2. Following Butler et al. (2011), the associated emissions required to keep the initial mixing ratios of each VOC constant until noon of the first day were determined for the MCM v3.2. These emissions are subsequently used for each mechanism, ensuring the amount of each VOC emitted was the same in every model run. Methane (CH_4) was fixed at 1.8 ppmv while CO and O_3 were initialised at 200 and 40 ppbv and then allowed to evolve freely.

The VOCs used in this study are assigned to mechanism species following the recommendations from the literature of each mechanism (Table 1), the representation of each VOC in the mechanisms is found in Table 2. Emissions of lumped species are weighted by the carbon number of the mechanism species ensuring the total amount of emitted reactive carbon was the same in each model run.

The MECCA box model is based upon the Kinetic Pre-Processor (KPP) (Damian et al., 2002). Hence, all chemical mechanisms were adapted into modularised KPP format. The inorganic gas-phase chemistry described in the MCM v3.2 was used in each run to remove any differences between treatments of inorganic chemistry in each mechanism. Thus, differences between the O_3 produced by the mechanisms are due to the treatment of organic degradation chemistry.

The MCM v3.2 approach to photolysis, dry deposition of VOC oxidation intermediates and $RO_2 - RO_2$ reactions was used for each mechanism; details of these adaptations can be found in the Supplement. Some mechanisms include reactions which are only important in the stratosphere or free troposphere. For example, PAN photolysis is only important in the free troposphere (Harwood et al., 2003) and was removed from MOZART-4, RACM2 and CB05 for the purpose of the study, as this study considers processes occurring within the planetary boundary layer.

2.3 Tagged ozone production potential (TOPP)

This section summarises the tagging approach described in Butler et al. (2011) which is applied in this study.

2.3.1 O_x family and tagging approach

O_3 production and loss is dominated by rapid photochemical cycles, such as Reactions (R1)–(R3). The effects of rapid production and loss cycles can be removed by using chemical families that include rapidly inter-converting species. In this study, we define the O_x family to include O_3, $O(^3P)$, $O(^1D)$, NO_2 and other species involved in fast cycling with NO_2, such as HO_2NO_2 and PAN species. Thus, production of O_x can be used as a proxy for production of O_3.

The tagging approach follows the degradation of emitted VOCs through all possible pathways by labelling every organic degradation product with the name of the emitted VOCs. Thus, each emitted VOC effectively has its own set of degradation reactions. Butler et al. (2011) showed that O_x production can be attributed to the VOCs by following the tags of each VOC.

Table 2. Non-methane volatile organic compounds (NMVOCs) present in Los Angeles. Mixing ratios are taken from Baker et al. (2008) and their representation in each chemical mechanism. The representation of the VOCs in each mechanism is based upon the recommendations of the literature for each mechanism (Table 1).

NMVOCs	Mixing ratio (pptv)	MCM v3.1, v3.2, CRI v2	MOZART-4	RADM2	RACM	RACM2	CBM-IV	CB05
Alkanes								
Ethane	6610	C2H6	C2H6	ETH	ETH	ETH	0.4 PAR	ETHA
Propane	6050	C3H8	C3H8	HC3	HC3	HC3	1.5 PAR	1.5 PAR
Butane	2340	NC4H10	BIGALK	HC3	HC3	HC3	4 PAR	4 PAR
2-Methylpropane	1240	IC4H10	BIGALK	HC3	HC3	HC3	4 PAR	4 PAR
Pentane	1200	NC5H12	BIGALK	HC5	HC5	HC5	5 PAR	5 PAR
2-Methylbutane	2790	IC5H12	BIGALK	HC5	HC5	HC5	5 PAR	5 PAR
Hexane	390	NC6H14	BIGALK	HC5	HC5	HC5	6 PAR	6 PAR
Heptane	160	NC7H16	BIGALK	HC5	HC5	HC5	7 PAR	7 PAR
Octane	80	NC8H18	BIGALK	HC8	HC8	HC8	8 PAR	8 PAR
Alkenes								
Ethene	2430	C2H4	C2H4	OL2	ETE	ETE	ETH	ETH
Propene	490	C3H6	C3H6	OLT	OLT	OLT	OLE + PAR	OLE + PAR
Butene	65	BUT1ENE	BIGENE	OLT	OLT	OLT	OLE + 2 PAR	OLE + 2 PAR
2-Methylpropene	130	MEPROPENE	BIGENE	OLI	OLI	OLI	PAR + FORM + ALD2	FORM + 3 PAR
Isoprene	270	C5H8	ISOP	ISO	ISO	ISO	ISOP	ISOP
Aromatics								
Benzene	480	BENZENE	TOLUENE	TOL	TOL	BEN	PAR	PAR
Toluene	1380	TOLUENE	TOLUENE	TOL	TOL	TOL	TOL	TOL
m-Xylene	410	MXYL	TOLUENE	XYL	XYL	XYM	XYL	XYL
p-Xylene	210	PXYL	TOLUENE	XYL	XYL	XYP	XYL	XYL
o-Xylene	200	OXYL	TOLUENE	XYL	XYL	XYO	XYL	XYL
Ethylbenzene	210	EBENZ	TOLUENE	TOL	TOL	TOL	TOL + PAR	TOL + PAR

O_x production from lumped-mechanism species are reassigned to the VOCs of Table 2 by scaling the O_x production of the mechanism species by the fractional contribution of each represented VOC. For example, TOL in RACM2 represents toluene and ethylbenzene with fractional contributions of 0.87 and 0.13 to TOL emissions. Scaling the O_x production from TOL by these factors gives the O_x production from toluene and ethylbenzene in RACM2.

Many reduced mechanisms use an operator species as a surrogate for RO_2 during VOC degradation enabling these mechanisms to produce O_x while minimising the number of RO_2 species represented. O_x production from operator species is assigned as O_x production from the organic degradation species producing the operator. This allocation technique is also used to assign O_x production from HO_2 via Reaction (R7).

2.3.2 Definition of TOPP

Attributing O_x production to individual VOCs using the tagging approach is the basis for calculating the TOPP of a VOC, which is defined as the number of O_x molecules produced per emitted molecule of VOC. The TOPP value of

a VOC that is not represented explicitly in a chemical mechanism is calculated by multiplying the TOPP value of the mechanism species representing the VOCs by the ratio of the carbon numbers of the VOCs to the mechanism species. For example, CB05 represents hexane as 6 PAR, so the TOPP value of hexane in the CB05 is 6 times the TOPP of PAR. MOZART-4 represents hexane with the five carbon species BIGALK. Thus, hexane emissions are represented molecule for molecule as $\frac{6}{5}$ of the equivalent number of molecules of BIGALK, and the TOPP value of hexane in MOZART-4 is calculated by multiplying the TOPP value of BIGALK by $\frac{6}{5}$.

3 Results

3.1 Ozone time series and O_x production budgets

Figure 1 shows the time series of O_3 mixing ratios obtained with each mechanism. There is an 8 ppbv difference in O_3 mixing ratios on the first day between RADM2, which has the highest O_3, and RACM2, which has the lowest O_3 mixing ratios when not considering the outlier time series of RACM. The difference between RADM2 and RACM, the low outlier, was 21 ppbv on the first day. The O_3 mixing ratios in
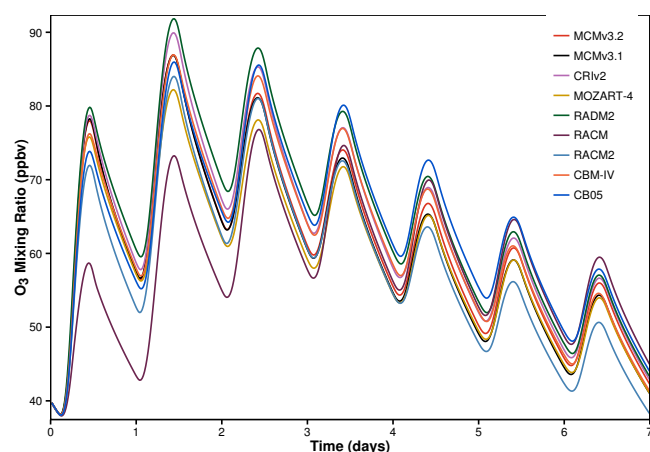
Figure 1. Time series of O_3 mixing ratios obtained using each mechanism.

Figure 2. Day-time O_x production budgets in each mechanism allocated to individual VOCs.

the CRI v2 are larger than those in the MCM v3.1, which is similar to the results in Jenkin et al. (2008) where the O_3 mixing ratios of the CRI v2 and MCM v3.1 are compared over a 5-day period.

The O_3 mixing ratios in Fig. 1 are influenced by the approaches used in developing the chemical mechanisms and not a function of the explicitness of the chemical mechanism. For example, the O_3 mixing ratios obtained using the Carbon Bond mechanisms (CBM-IV and CB05) compare well with the MCM despite both Carbon Bond mechanisms having $\sim 1\,\%$ of the number of reactions in the MCM v3.2. Also, the O_3 mixing ratios from RACM2 and RADM2 show similar absolute differences from that of the MCM despite RACM2 having more than double the number of reactions of RADM2.

The day-time O_x production budgets allocated to individual VOCs for each mechanism are shown in Fig. 2. The relationships between O_3 mixing ratios in Fig. 1 are mirrored in Fig. 2 where mechanisms producing high amounts of O_x also have high O_3 mixing ratios. The conditions in the box model lead to a daily maximum of OH that increases with each day leading to an increase on each day in both the reaction rate of the OH oxidation of CH_4 and the daily contribution of CH_4 to O_x production.

The first-day mixing ratios of O_3 in RACM are lower than other mechanisms due to a lack of O_x production from aromatic VOCs on the first day in RACM (Fig. 2). Aromatic degradation chemistry in RACM results in net loss of O_x on the first day, described later in Sect. 3.2.1.

RADM2 is the only reduced mechanism that produces higher O_3 mixing ratios than the more detailed mechanisms (MCM v3.2, MCM v3.1 and CRI v2). Higher mixing ratios of O_3 in RADM2 are produced due to increased O_x production from propane compared to the MCM v3.2; on the first day, the O_x production from propane in RADM2 is triple that of the MCM v3.2 (Fig. 2). Propane is represented as HC3 in
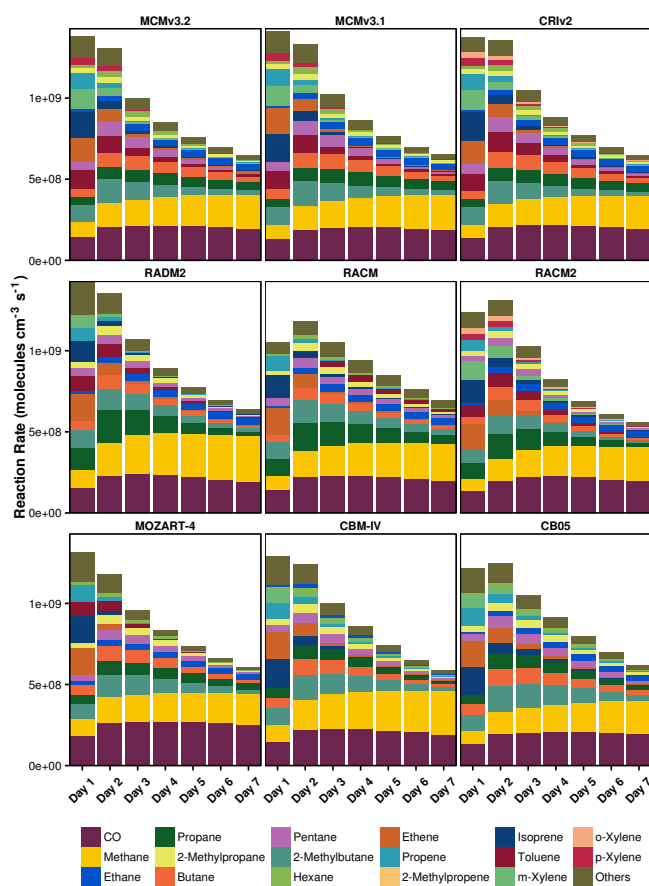
RADM2 (Stockwell et al., 1990) and the degradation of HC3 has a lower yield of the less-reactive ketones compared to the MCM. The further degradation of ketones hinders O_x production due to the low OH reactivity and photolysis rate of ketones. Secondary degradation of HC3 proceeds through the degradation of acetaldehyde (CH_3CHO) propagating O_x production through the reactions of CH_3CO_3 and CH_3O_2 with NO. Thus, the lower ketone yields lead to increased O_x production from propane degradation in RADM2 compared to the MCM v3.2.

3.2 Time-dependent O_x production

Time series of daily TOPP values for each VOC are presented in Fig. 3 and the cumulative TOPP values at the end of the model run obtained for each VOC using each of the mechanisms, normalised by the number of atoms of C in each VOC are presented in Table 3. In the MCM and CRI v2, the cumulative TOPP values obtained for each VOC show that by the end of the model run, larger alkanes have produced more O_x per unit of reactive C than alkenes or aromatic VOCs. By the end of the runs using the lumped-structure mechanisms (CBM-IV and CB05), alkanes produce similar
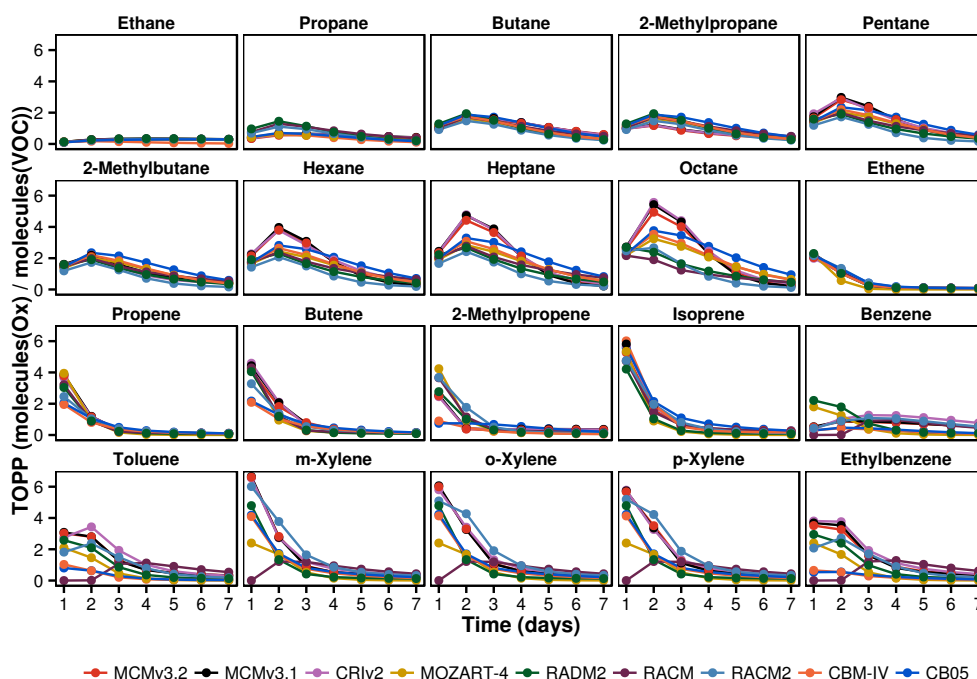
Figure 3. TOPP value time series using each mechanism for each VOC.

Table 3. Cumulative TOPP values at the end of the model run for all VOCs with each mechanism, normalised by the number of C atoms in each VOC.

NMVOCs	MCM v3.2	MCM v3.1	CRI v2	MOZART-4	RADM2	RACM	RACM2	CBM-IV	CB05
				Alkanes					
Ethane	0.9	1.0	0.9	0.9	1.0	1.0	0.9	0.3	0.9
Propane	1.1	1.2	1.2	1.1	1.8	1.8	1.4	0.9	1.0
Butane	2.0	2.0	2.0	1.7	1.8	1.8	1.4	1.7	2.1
2-Methylpropane	1.3	1.3	1.3	1.7	1.8	1.8	1.4	1.7	2.1
Pentane	2.1	2.1	2.2	1.7	1.5	1.6	1.1	1.7	2.1
2-Methylbutane	1.6	1.6	1.5	1.7	1.5	1.6	1.1	1.7	2.1
Hexane	2.1	2.1	2.2	1.7	1.5	1.6	1.1	1.7	2.1
Heptane	2.0	2.1	2.2	1.7	1.5	1.6	1.1	1.7	2.1
Octane	2.0	2.0	2.2	1.7	1.2	1.0	1.0	1.7	2.1
				Alkenes					
Ethene	1.9	1.9	1.9	1.4	2.0	2.0	2.2	1.9	2.2
Propene	1.9	2.0	1.9	1.7	1.5	1.6	1.5	1.2	1.4
Butene	1.9	2.0	2.0	1.5	1.5	1.6	1.5	0.8	0.9
2-Methylpropene	1.1	1.2	1.2	1.5	1.1	1.5	1.6	0.5	0.5
Isoprene	1.8	1.8	1.8	1.3	1.2	1.6	1.7	1.9	2.1
				Aromatics					
Benzene	0.8	0.8	1.1	0.6	0.9	0.6	0.9	0.3	0.3
Toluene	1.3	1.3	1.5	0.6	0.9	0.6	1.0	0.3	0.3
m-Xylene	1.5	1.5	1.6	0.6	0.9	0.6	1.7	0.9	1.0
p-Xylene	1.5	1.5	1.6	0.6	0.9	0.6	1.7	0.9	1.0
o-Xylene	1.5	1.5	1.6	0.6	0.9	0.6	1.7	0.9	1.0
Ethylbenzene	1.3	1.4	1.5	0.6	0.9	0.6	1.0	0.2	0.3

amounts of O_x per reactive C, while aromatic VOCs and some alkenes produce less O_x per reactive C than the MCM. However, in lumped-molecule mechanisms (MOZART-4, RADM2, RACM, RACM2), practically all VOCs produce less O_x per reactive C than the MCM by the end of the run. This lower efficiency of O_x production from many individual VOCs in lumped-molecule and lumped-structure mechanisms would lead to an underestimation of O_3 levels downwind of an emission source, and a smaller contribution to background O_3 when using lumped-molecule and lumped-structure mechanisms.

The lumped-intermediate mechanism (CRI v2) produces the most similar O_x to the MCM v3.2 for each VOC, seen in Fig. 3 and Table 3. Higher variability in the time-dependent O_x production is evident for VOCs represented by lumped-mechanism species. For example, 2-methylpropene, represented in the reduced mechanisms by a variety of lumped species, has a higher spread in time-dependent O_x production than ethene, which is explicitly represented in each mechanism.

In general, the largest differences in O_x produced by aromatic and alkene species are on the first day of the simulations, while the largest inter-mechanism differences in O_x produced by alkanes are on the second and third days of the simulations. The reasons for these differences in behaviour will be explored in Sect. 3.2.1, which examines differences in first day O_x production between the chemical mechanisms, and Sect. 3.2.2, which examines the differences in O_x production on subsequent days.

3.2.1 First-day ozone production

The first-day TOPP values of each VOC from each mechanism, representing O_3 production from freshly emitted VOCs near their source region, are compared to those obtained with the MCM v3.2 in Fig. 4. The root mean square error (RMSE) of all first-day TOPP values in each mechanism relative to those in the MCM v3.2 are also included in Fig. 4. The RMSE value of the CRI v2 shows that first-day O_x production from practically all the individual VOC matches that in the MCM v3.2. All other reduced mechanisms have much larger RMSE values indicating that the first-day O_x production from the majority of the VOCs differs from that in the MCM v3.2.

The reduced complexity of reduced mechanisms means that aromatic VOCs are typically represented by one or two mechanism species leading to differences in O_x production of the actual VOCs compared to the MCM v3.2. For example, all aromatic VOCs in MOZART-4 are represented as toluene, thus less-reactive aromatic VOCs, such as benzene, produce higher O_x whilst more-reactive aromatic VOCs, such as the xylenes, produce less O_x in MOZART-4 than the MCM v3.2. RACM2 includes explicit species representing benzene, toluene and each xylene resulting in O_x production
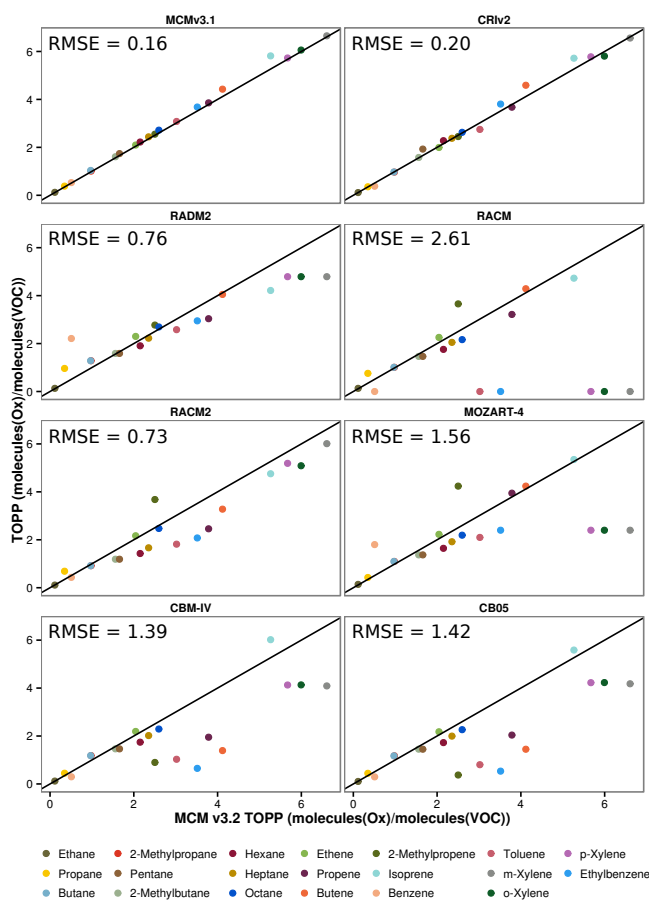

Figure 4. The first-day TOPP values for each VOC calculated using MCM v3.2 and the corresponding values in each mechanism. The root mean square error (RMSE) of each set of TOPP values is also displayed. The black line is the 1 : 1 line.

that is the most similar to the MCM v3.2 than other reduced mechanisms.

Figure 3 shows a high spread in O_x production from aromatic VOCs on the first day indicating that aromatic degradation is treated differently between mechanisms. Toluene degradation is examined in more detail by comparing the reactions contributing to O_x production and loss in each mechanism, shown in Fig. 5. These reactions are determined by following the "toluene" tags in the tagged version of each mechanism.

Toluene degradation in RACM includes several reactions consuming O_x that are not present in the MCM, resulting in net loss of O_x on the first 2 days. Ozonolysis of the cresol OH adduct mechanism species, ADDC, contributes significantly to O_x loss in RACM. This reaction was included in RACM due to improved cresol product yields when comparing RACM predictions with experimental data (Stockwell et al., 1997). Other mechanisms that include cresol OH adduct species do not include ozonolysis and these reactions are not included in the updated RACM2.
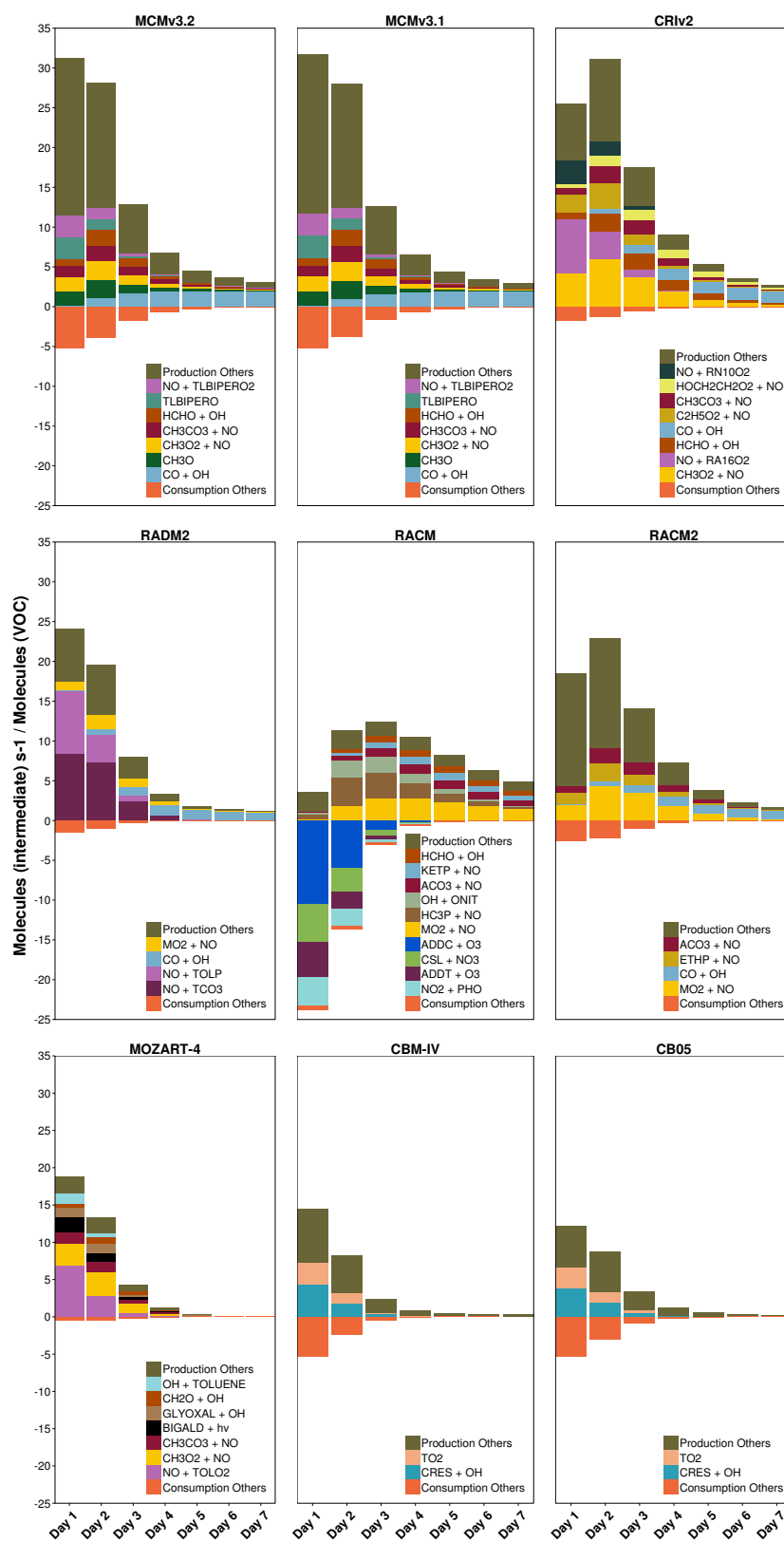
Figure 5. Day-time O_x production and loss budgets allocated to the responsible reactions during toluene degradation in all mechanisms. These reactions are presented using the species defined in each mechanism in Table 1.

The total O_x produced on the first day during toluene degradation in each reduced mechanism is less than that in the MCM v3.2 (Fig. 5). Less O_x is produced in all reduced mechanisms due to a faster breakdown of the VOCs into smaller fragments than the MCM, described later in Sect. 3.3. Moreover, in CBM-IV and CB05, less O_x is produced during toluene degradation as reactions of the toluene degradation products CH_3O_2 and CO do not contribute to the O_x production budgets, which is not the case in any other mechanism (Fig. 5).

Maximum O_x production from toluene degradation in CRI v2 and RACM2 is reached on the second day in contrast to the MCM v3.2 which produces peak O_x on the first day. The second-day maximum of O_x production in CRI v2 and RACM2 from toluene degradation results from more efficient production of unsaturated dicarbonyls than the MCM v3.2. The degradation of unsaturated dicarbonyls produces peroxy radicals such as $C_2H_5O_2$ which promote O_x production via reactions with NO.

Unsaturated aliphatic VOCs generally produce similar amounts of O_x between mechanisms, especially explicitly represented VOCs, such as ethene and isoprene. On the other hand, unsaturated aliphatic VOCs that are not explicitly represented produce differing amounts of O_x between mechanisms (Fig. 3). For example, the O_x produced during 2-methylpropene degradation varies between mechanisms; differing rate constants of initial oxidation reactions and non-realistic secondary chemistry lead to these differences; further details are found in the Supplement.

Non-explicit representations of aromatic and unsaturated aliphatic VOCs coupled with differing degradation chemistry and a faster breakdown into smaller-size degradation products results in different O_x production in lumped-molecule and lumped-structure mechanisms compared to the MCM v3.2.

3.2.2 Ozone production on subsequent days

Alkane degradation in CRI v2 and both MCMs produces a second-day maximum in O_x that increases with alkane carbon number (Fig. 3). The increase in O_x production on the second day is reproduced for each alkane by the reduced mechanisms, except octane in RADM2, RACM and RACM2. However, larger alkanes produce less O_x than the MCM on the second day in all lumped-molecule and lumped-structure mechanisms.

The lumped-molecule mechanisms (MOZART-4, RADM2, RACM and RACM2) represent many alkanes by mechanism species which may lead to unrepresentative secondary chemistry for alkane degradation. For example, 3 times more O_x is produced during the degradation of propane in RADM2 than the MCM v3.2 on the first day (Fig. 2). Propane is represented in RADM2 by the mechanism species HC3 which also represents other classes of VOCs, such as alcohols. The secondary chemistry of HC3 is
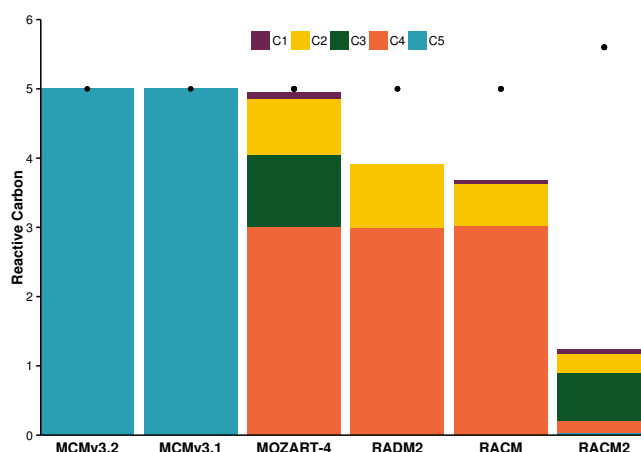

Figure 6. The distribution of reactive carbon in the products of the reaction between NO and the pentyl peroxy radical in lumped-molecule mechanisms compared to the MCM. The black dot represents the reactive carbon of the pentyl peroxy radical.

tailored to produce O_x from these different VOCs and differs from alkane degradation in the MCM v3.2 by producing less ketones in RADM2.

As will be shown in Sect. 3.3, another feature of reduced mechanisms is that the breakdown of emitted VOCs into smaller-sized degradation products is faster than the MCM. Alkanes are broken down quicker in CBM-IV, CB05, RADM2, RACM and RACM2 through a higher rate of reactive carbon loss than the MCM v3.2 (shown for pentane and octane in Fig. 8); reactive carbon is lost through reactions not conserving carbon. Despite many degradation reactions of alkanes in MOZART-4 almost conserving carbon, the organic products have less reactive carbon than the organic reactant also speeding up the breakdown of the alkane compared to the MCM v3.2.

For example, Fig. 6 shows the distribution of reactive carbon in the reactants and products from the reaction of NO with the pentyl peroxy radical in both MCMs and each lumped-molecule mechanism. In all the lumped-molecule mechanisms, the individual organic products have less reactive carbon than the organic reactant. Moreover, in RADM2, RACM and RACM2, this reaction does not conserve reactive carbon leading to faster loss rates of reactive carbon.

The faster breakdown of alkanes in lumped-molecule and lumped-structure mechanisms on the first day limits the amount of O_x produced on the second day, as less of the larger-sized degradation products are available for further degradation and O_x production.

3.3 Treatment of degradation products

The time-dependent O_x production of the different VOCs in Fig. 3 results from the varying rates at which VOCs break up into smaller fragments (Butler et al., 2011). Varying breakdown rates of the same VOCs between mechanisms could
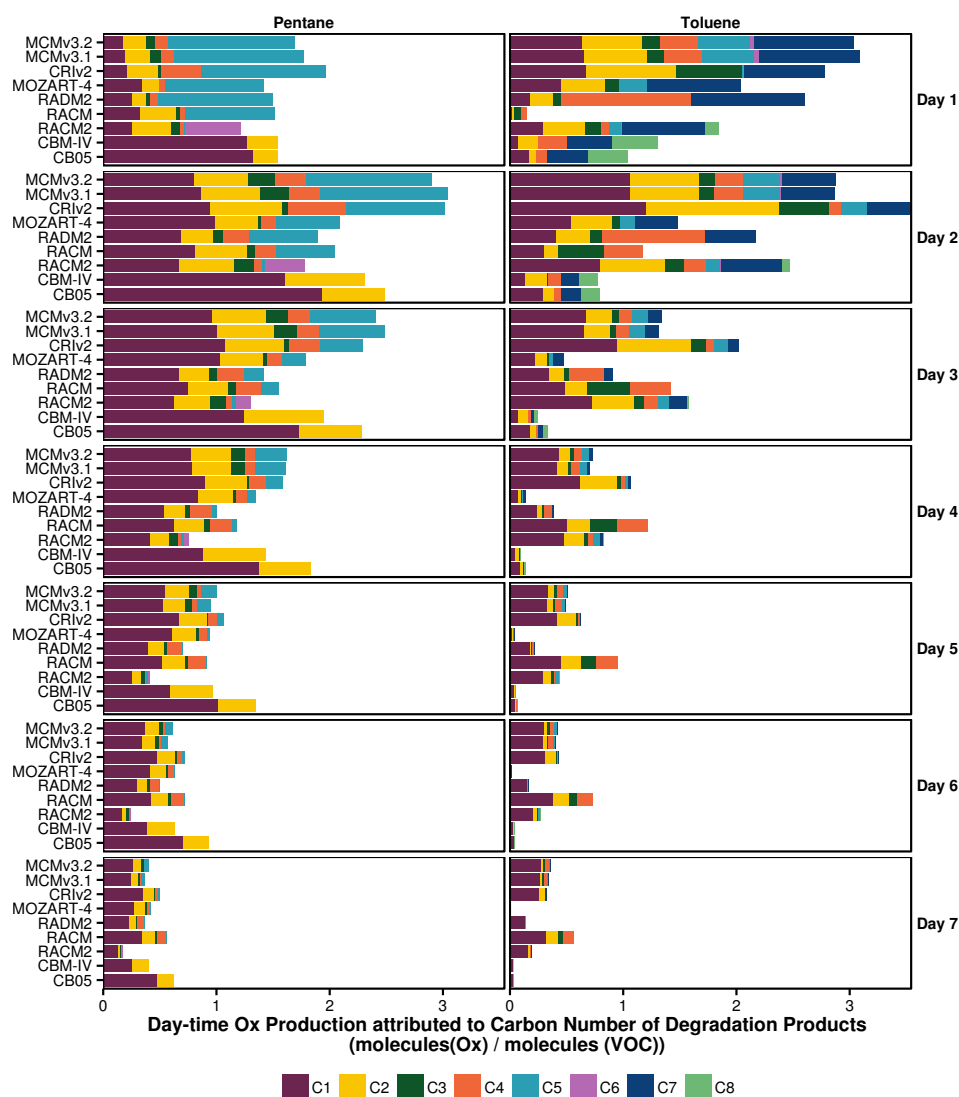
Figure 7. Day-time O_x production during pentane and toluene degradation is attributed to the number of carbon atoms of the degradation products for each mechanism.

explain the different time-dependent O_x production between mechanisms. The breakdown of pentane and toluene between mechanisms is compared in Fig. 7 by allocating the O_x production to the number of carbon atoms in the degradation products responsible for O_x production on each day of the model run in each mechanism. Some mechanism species in RADM2, RACM and RACM2 have fractional carbon numbers (Stockwell et al., 1990, 1997; Goliff et al., 2013) and O_x production from these species was reassigned as O_x production of the nearest integral carbon number.

The degradation of pentane, a five-carbon VOC, on the first day in the MCM v3.2 produces up to 50 % more O_x from degradation products also having five carbon atoms than any reduced mechanism. Moreover, the contribution of the degradation products having five carbon atoms in the MCM v3.2 is consistently higher throughout the model run than in re-

duced mechanisms (Fig. 7). Despite producing less total O_x, reduced mechanisms produce up to double the amount of O_x from degradation products with one carbon atom than in the MCM v3.2. The lower contribution of larger degradation products indicates that pentane is generally broken down faster in reduced mechanisms, consistent with the specific example shown for the breakdown of the pentyl peroxy radical in Fig. 6.

The rate of change in reactive carbon during pentane, octane and toluene degradation was determined by multiplying the rate of each reaction occurring during pentane, octane and toluene degradation by its net change in carbon, shown in Fig. 8. Pentane is broken down faster in CBM-IV, CB05, RADM2, RACM and RACM2 by losing reactive carbon more quickly than the MCM v3.2. MOZART-4 also breaks pentane down into smaller-sized products quicker
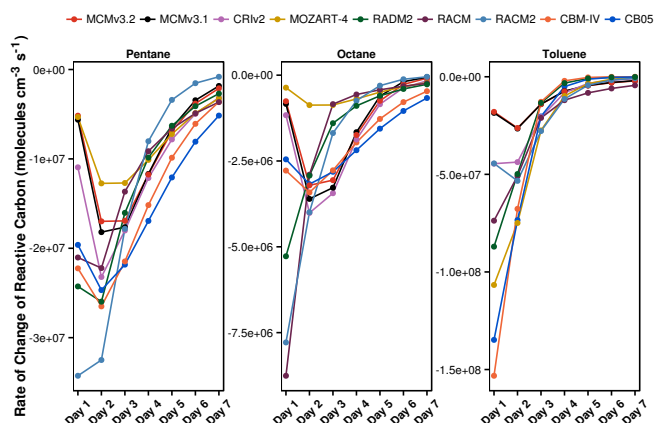
Figure 8. Daily rate of change in reactive carbon during pentane, octane and toluene degradation. Octane is represented by the five carbon species, BIGALK, in MOZART-4.

than the MCM v3.2 as reactions during pentane degradation in MOZART-4 have organic products whose carbon number is less than the organic reactant, described in Sect. 3.2.2. The faster breakdown of pentane on the first day limits the amount of reactive carbon available to produce further O_x on subsequent days leading to lower O_x production after the first day in reduced mechanisms.

Figure 3 showed that octane degradation produces peak O_x on the first day in RADM2, RACM and RACM2 in contrast to all other mechanisms where peak O_x is produced on the second day. Octane degradation in RADM2, RACM and RACM2 loses reactive carbon much faster than any other mechanism on the first day so that there are not enough degradation products available to produce peak O_x on the second day (Fig. 8). This loss of reactive carbon during alkane degradation leads to the lower accumulated ozone production from these VOCs shown in Table 3.

As seen in Fig. 3, O_x produced during toluene degradation has a high spread between the mechanisms. Figure 7 shows differing distributions of the sizes of the degradation products that produce O_x. All reduced mechanisms omit O_x production from at least one degradation fragment size which produces O_x in the MCM v3.2, indicating that toluene is also broken down more quickly in the reduced mechanisms than the more explicit mechanisms. For example, toluene degradation in RACM2 does not produce O_x from degradation products with six carbons, as is the case in the MCM v3.2. Figure 8 shows that all reduced mechanisms lose reactive carbon during toluene degradation faster than the MCM v3.2. Thus, the degradation of aromatic VOCs in reduced mechanisms are unable to produce similar amounts of O_x as the explicit mechanisms.

4 Conclusions

Tagged ozone production potentials (TOPPs) were used to compare O_x production during VOC degradation in reduced chemical mechanisms to the near-explicit MCM v3.2. First-day mixing ratios of O_3 are similar to the MCM v3.2 for most mechanisms; the O_3 mixing ratios in RACM were much lower than the MCM v3.2 due to a lack of O_x production from the degradation of aromatic VOCs. Thus, RACM may not be the appropriate chemical mechanism when simulating atmospheric conditions having a large fraction of aromatic VOCs.

The lumped-intermediate mechanism, CRI v2, produces the most similar amounts of O_x to the MCM v3.2 for each VOC. The largest differences between O_x production in CRI v2 and MCM v3.2 were obtained for aromatic VOCs; however, overall these differences were much lower than any other reduced mechanism. Thus, when developing chemical mechanisms, the technique of using lumped-intermediate species whose degradation are based upon more detailed mechanism should be considered.

Many VOCs are broken down into smaller-sized degradation products faster on the first day in reduced mechanisms than the MCM v3.2 leading to lower amounts of larger-sized degradation products that can further degrade and produce O_x. Thus, many VOCs in reduced mechanisms produce a lower maximum of O_x and lower total O_x per reactive C by the end of the run than the MCM v3.2. This lower O_x production from many VOCs in reduced mechanisms leads to lower O_3 mixing ratios compared to the MCM v3.2.

Alkanes produce maximum O_3 on the second day of simulations and this maximum is lower in reduced mechanisms than the MCM v3.2 due to the faster breakdown of alkanes into smaller-sized degradation products on the first day. The lower maximum in O_3 production during alkane degradation in reduced mechanisms leads to an underestimation of the O_3 levels downwind of VOC emissions and an underestimation of the VOC contribution to tropospheric background O_3 when using reduced mechanisms in regional or global modelling studies.

This study has determined the maximum potential of VOCs represented in reduced mechanisms to produce O_3; this potential may not be reached as ambient NO_x conditions may not induce NO_x–VOC-sensitive chemistry. Moreover, the maximum potential of VOCs to produce O_3 may not be reached when using these reduced mechanisms in 3-D models due to the influence of additional processes, such as mixing and meteorology. Future work shall examine the extent to which the maximum potential of VOCs to produce O_3 in reduced chemical mechanisms is reached using ambient NO_x conditions and including processes found in 3-D models.

The Supplement related to this article is available online at doi:10.5194/acp-15-8795-2015-supplement.

References

Ahmadov, R., McKeen, S., Trainer, M., Banta, R., Brewer, A., Brown, S., Edwards, P. M., de Gouw, J. A., Frost, G. J., Gilman, J., Helmig, D., Johnson, B., Karion, A., Koss, A., Langford, A., Lerner, B., Olson, J., Oltmans, S., Peischl, J., Pétron, G., Pichugina, Y., Roberts, J. M., Ryerson, T., Schnell, R., Senff, C., Sweeney, C., Thompson, C., Veres, P. R., Warneke, C., Wild, R., Williams, E. J., Yuan, B., and Zamora, R.: Understanding high wintertime ozone pollution events in an oil- and natural gas-producing region of the western US, Atmos. Chem. Phys., 15, 411–429, doi:10.5194/acp-15-411-2015, 2015.

Atkinson, R.: Atmospheric chemistry of VOCs and NO_x, Atmos. Environ., 34, 2063–2101, 2000.

Baker, A. K., Beyersdorf, A. J., Doezema, L. A., Katzenstein, A., Meinardi, S., Simpson, I. J., Blake, D. R., and Rowland, F. S.: Measurements of nonmethane hydrocarbons in 28 United States cities, Atmos. Environ., 42, 170–182, 2008.

Baklanov, A., Schlünzen, K., Suppan, P., Baldasano, J., Brunner, D., Aksoyoglu, S., Carmichael, G., Douros, J., Flemming, J., Forkel, R., Galmarini, S., Gauss, M., Grell, G., Hirtl, M., Joffre, S., Jorba, O., Kaas, E., Kaasik, M., Kallos, G., Kong, X., Korsholm, U., Kurganskiy, A., Kushta, J., Lohmann, U., Mahura, A., Manders-Groot, A., Maurizi, A., Moussiopoulos, N., Rao, S. T., Savage, N., Seigneur, C., Sokhi, R. S., Solazzo, E., Solomos, S., Sørensen, B., Tsegas, G., Vignati, E., Vogel, B., and Zhang, Y.: Online coupled regional meteorology chemistry models in Europe: current status and prospects, Atmos. Chem. Phys., 14, 317–398, doi:10.5194/acp-14-317-2014, 2014.

Bloss, C., Wagner, V., Jenkin, M. E., Volkamer, R., Bloss, W. J., Lee, J. D., Heard, D. E., Wirtz, K., Martin-Reviejo, M., Rea, G., Wenger, J. C., and Pilling, M. J.: Development of a detailed chemical mechanism (MCMv3.1) for the atmospheric oxidation of aromatic hydrocarbons, Atmos. Chem. Phys., 5, 641–664, doi:10.5194/acp-5-641-2005, 2005.

Butler, T. M., Lawrence, M. G., Taraborrelli, D., and Lelieveld, J.: Multi-day ozone production potential of volatile organic compounds calculated with a tagging approach, Atmos. Environ., 45, 4082–4090, 2011.

Carter, W. P. L.: Development of ozone reactivity scales for volatile organic compounds, J. Air Waste Manage., 44, 881–899, 1994.

Damian, V., Sandu, A., Damian, M., Potra, F., and Carmichael, G.: The kinetic preprocessor KPP – a software environment for solving chemical kinetics, Comput. Chem. Eng., 26, 1567–1579, 2002.

Derwent, R. G., Jenkin, M. E., and Saunders, S. M.: Photochemical ozone creation potentials for a large number of reactive hydrocarbons under European conditions, Atmos. Environ., 30, 181–199, 1996.

Derwent, R. G., Jenkin, M. E., Saunders, S. M., and Pilling, M. J.: Photochemical ozone creation potentials for organic compounds

in Northwest Europe calculated with a master chemical mechanism, Atmos. Environ., 32, 2429–2441, 1998.

Derwent, R. G., Jenkin, M. E., Pilling, M. J., Carter, W. P. L., and Kaduwela, A.: Reactivity scales as comparative tools for chemical mechanisms, J. Air Waste Manage., 60, 914–924, 2010.

Derwent, R. G., Utember, S. R., Jenkin, M. E., and Shallcross, D. E.: Tropospheric ozone production regions and the intercontinental origins of surface ozone over Europe, Atmos. Environ., 112, 216–224, 2015

Dodge, M.: Chemical oxidant mechanisms for air quality modeling: critical review, Atmos. Environ., 34, 2103–2130, 2000.

Dunker, A. M., Kumar, S., and Berzins, P. H.: A comparison of chemical mechanisms used in atmospheric models, Atmos. Environ., 18, 311–321, 1984.

Dunker, A. M., Koo, B., and Yarwood, G.: Source Apportionment of the Anthropogenic Increment to Ozone, Formaldehyde, and Nitrogen Dioxide by the Path- Integral Method in a 3D Model, Environ. Sci. Technol., 49, 6751–6759, 2015.

EEA: Air quality in Europe – 2014 report, Tech. Rep. 5/2014, European Environmental Agency, Publications Office of the European Union, doi:10.2800/22847, 2014.

Emmerson, K. M. and Evans, M. J.: Comparison of tropospheric gas-phase chemistry schemes for use within global models, Atmos. Chem. Phys., 9, 1831–1845, doi:10.5194/acp-9-1831-2009, 2009.

Emmons, L. K., Walters, S., Hess, P. G., Lamarque, J.-F., Pfister, G. G., Fillmore, D., Granier, C., Guenther, A., Kinnison, D., Laepple, T., Orlando, J., Tie, X., Tyndall, G., Wiedinmyer, C., Baughcum, S. L., and Kloster, S.: Description and evaluation of the Model for Ozone and Related chemical Tracers, version 4 (MOZART-4), Geosci. Model Dev., 3, 43–67, doi:10.5194/gmd-3-43-2010, 2010.

Foster, P. N., Prentice, I. C., Morfopoulos, C., Siddall, M., and van Weele, M.: Isoprene emissions track the seasonal cycle of canopy temperature, not primary production: evidence from remote sensing, Biogeosciences, 11, 3437–3451, doi:10.5194/bg-11-3437-2014, 2014.

Gery, M. W., Whitten, G. Z., Killus, J. P., and Dodge, M. C.: A photochemical kinetics mechanism for urban and regional scale computer modeling, J. Geophys. Res., 94, 12925–12956, 1989.

Goliff, W. S., Stockwell, W. R., and Lawson, C. V.: The regional atmospheric chemistry mechanism, version 2, Atmos. Environ., 68, 174–185, 2013.

Goliff, W. S., Luria, M., Blake, D. R., Zielinska, B., Hallar, G., Valente, R. J., Lawson, C. V., and Stockwell, W. R.: Nighttime air quality under desert conditions, Atmos. Environ., 114, 102–111, 2015.

Harwood, M., Roberts, J., Frost, G., Ravishankara, A., and Burkholder, J.: Photochemical studies of $CH_3C(O)OONO_2$ (PAN) and $CH_3CH_2C(O)OONO_2$ (PPN): NO_3 quantum yields, J. Phys. Chem. A, 107, 1148–1154, 2003.

Hogo, H. and Gery, M.: User's guide for executing OZIPM-4 (Ozone Isopleth Plotting with Optional Mechanisms, Version 4) with CBM-IV (Carbon-Bond Mechanisms-IV) or optional mechanisms. Volume 1. Description of the ozone isopleth plotting package. Version 4, Tech. rep., US Environmental Protection Agency, Durham, North Carolina, USA, 1989.

Hou, X., Zhu, B., Fei, D., and Wang, D.: The impacts of summer monsoons on the ozone budget of the atmospheric boundary

layer of the Asia-Pacific region, Sci. Total Environ., 502, 641–649, 2015.

HTAP: Hemispheric Transport of Air Pollution 2010, Part A: Ozone and Particulate Matter, Air Pollution Studies No.17, Geneva, Switzerland, 2010.

Jenkin, M. E. and Clemitshaw, K. C.: Ozone and other secondary photochemical pollutants: chemical processes governing their formation in the planetary boundary layer, Atmos. Environ., 34, 2499–2527, 2000.

Jenkin, M. E., Saunders, S. M., and Pilling, M. J.: The tropospheric degradation of volatile organic compounds: a protocol for mechanism development, Atmos. Environ., 31, 81–104, 1997.

Jenkin, M. E., Saunders, S. M., Wagner, V., and Pilling, M. J.: Protocol for the development of the Master Chemical Mechanism, MCM v3 (Part B): tropospheric degradation of aromatic volatile organic compounds, Atmos. Chem. Phys., 3, 181–193, doi:10.5194/acp-3-181-2003, 2003.

Jenkin, M. E., Watson, L. A., Utembe, S. R., and Shallcross, D. E.: A Common Representative Intermediates (CRI) mechanism for VOC degradation. Part 1: Gas phase mechanism development, Atmos. Environ., 42, 7185–7195, 2008.

Kleinman, L. I.: Seasonal dependence of boundary layer peroxide concentration: the low and high NO_x regimes, J. Geophys. Res., 96, 20721–20733, 1991.

Kleinman, L. I.: Low and high NO_x tropospheric photochemistry, J. Geophys. Res., 99, 16831–16838, 1994.

Koss, A. R., de Gouw, J., Warneke, C., Gilman, J. B., Lerner, B. M., Graus, M., Yuan, B., Edwards, P., Brown, S. S., Wild, R., Roberts, J. M., Bates, T. S., and Quinn, P. K.: Photochemical aging of volatile organic compounds associated with oil and natural gas extraction in the Uintah Basin, UT, during a wintertime ozone formation event, Atmos. Chem. Phys., 15, 5727–5741, doi:10.5194/acp-15-5727-2015, 2015.

Kuhn, M., Builtjes, P. J. H., Poppe, D., Simpson, D., Stockwell, W. R., Andersson-Sköld, Y., Baart, A., Das, M., Fiedler, F., Hov, Ø., Kirchner, F., Makar, P. A., Milford, J. B., Roemer, M. G. M., Ruhnke, R., Strand, A., Vogel, B., and Vogel, H.: Intercomparison of the gas-phase chemistry in several chemistry and transport models, Atmos. Environ., 32, 693–709, 1998.

Li, J., Georgescu, M., Hyde, P., Mahalov, A., and Moustaoui, M.: Achieving accurate simulations of urban impacts on ozone at high resolution, Environ. Res. Lett., 9, 114019, doi:10.1088/1748-9326/9/11/114019, 2014.

Lidster, R. T., Hamilton, J. F., Lee, J. D., Lewis, A. C., Hopkins, J. R., Punjabi, S., Rickard, A. R., and Young, J. C.: The impact of monoaromatic hydrocarbons on OH reactivity in the coastal UK boundary layer and free troposphere, Atmos. Chem. Phys., 14, 6677–6693, doi:10.5194/acp-14-6677-2014, 2014.

Rickard, A., Young, J., Pilling, M., Jenkin. M., Pascoe, S., and Saunders S.: The Master Chemical Mechanism Version MCM v3.2, available at: http://mcm.leeds.ac.uk/MCMv3.2/, last access: 15 July 2015.

Sander, R., Kerkweg, A., Jöckel, P., and Lelieveld, J.: Technical note: The new comprehensive atmospheric chemistry module MECCA, Atmos. Chem. Phys., 5, 445–450, doi:10.5194/acp-5-445-2005, 2005.

Saunders, S. M., Jenkin, M. E., Derwent, R. G., and Pilling, M. J.: Protocol for the development of the Master Chemical Mechanism, MCM v3 (Part A): tropospheric degradation of non-aromatic volatile organic compounds, Atmos. Chem. Phys., 3, 161–180, doi:10.5194/acp-3-161-2003, 2003.

Sillman, S.: The relation between ozone, NO_x and hydrocarbons in urban and polluted rural environments, Atmos. Environ., 33, 1821–1845, 1999.

Stevenson, D. S., Young, P. J., Naik, V., Lamarque, J.-F., Shindell, D. T., Voulgarakis, A., Skeie, R. B., Dalsoren, S. B., Myhre, G., Berntsen, T. K., Folberth, G. A., Rumbold, S. T., Collins, W. J., MacKenzie, I. A., Doherty, R. M., Zeng, G., van Noije, T. P. C., Strunk, A., Bergmann, D., Cameron-Smith, P., Plummer, D. A., Strode, S. A., Horowitz, L., Lee, Y. H., Szopa, S., Sudo, K., Nagashima, T., Josse, B., Cionni, I., Righi, M., Eyring, V., Conley, A., Bowman, K. W., Wild, O., and Archibald, A.: Tropospheric ozone changes, radiative forcing and attribution to emissions in the Atmospheric Chemistry and Climate Model Intercomparison Project (ACCMIP), Atmos. Chem. Phys., 13, 3063–3085, doi:10.5194/acp-13-3063-2013, 2013.

Stockwell, W. R., Middleton, P., Chang, J. S., and Tang, X.: The second generation regional acid deposition model chemical mechanism for regional air quality modeling, J. Geophys. Res., 95, 16343–16367, 1990.

Stockwell, W. R., Kirchner, F., Kuhn, M., and Seefeld, S.: A new mechanism for regional atmospheric chemistry modeling, J. Geophys. Res.-Atmos., 102, 25847–25879, 1997.

Watson, L. A., Shallcross, D. E., Utembe, S. R., and Jenkin, M. E.: A Common Representative Intermediates (CRI) mechanism for VOC degradation. Part 2: Gas phase mechanism reduction, Atmos. Environ., 42, 7196–7204, 2008.

Yarwood, G., Rao, S., Yocke, M., and Whitten, G. Z.: Updates to the Carbon Bond Chemical Mechanism: CB05, Tech. rep., US Environmental Protection Agency, Novato, California, USA, 2005.

Atmospheric
Chemistry
and Physics

Open Access

Supplement of

A comparison of chemical mechanisms using tagged ozone production potential (TOPP) analysis

J. Coates and T. M. Butler

Correspondence to: J. Coates (jane.coates@iass-potsdam.de)

S1 Introduction

This is the supplementary material to the research paper "A Comparison of Chemical Mechanisms using Tagged Ozone Production Potential (TOPP) Analysis" and provides further information about the methodology as well as additional analysis.
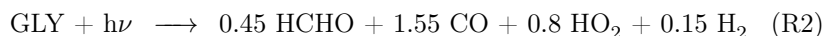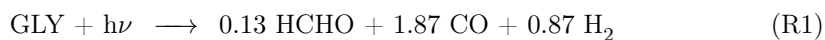
S2 Mechanism Setup

All chemical mechanisms were adapted from their original format into the modularised KPP (Damian et al., 2002) format for use in the MECCA boxmodel (Sander et al., 2005) as modified by (Butler et al., 2011).

The MCM v3.2 (Jenkin et al., 1997, 2003; Saunders et al., 2003; Bloss et al., 2005; Rickard et al., 2015) is the reference mechanism and its approach to dry deposition, photolysis and peroxy radical–peroxy radical reactions were applied to all mechanisms.

S2.1 Photolysis

Photolysis was parameterised as a function of the solar zenith angle following the MCM approach (Saunders et al., 2003). Species from reduced mechanisms with a direct counterpart in the MCM v3.2 were assigned the corresponding MCM v3.2 photolysis rate parameter. Otherwise, the recommended rate parameter in the mechanism determined the appropriate MCM v3.2 photolysis rate parameter. In some cases, the MCM v3.2 photolysis rate parameter closest in magnitude to that specified by the mechanism was used. For example, the organic nitrate species ONIT in RACM2 has a photolysis rate parameter of 1.96×10^{-6} s^{-1} that was compared to the MCM v3.2 organic nitrate photolysis rate parameters ($J_{51} - J_{57}$). The rate parameter J_{54} is the most similar in magnitude and was assigned as the ONIT photolysis rate parameter in RACM2.

Photolysis reactions of a species in reduced mechanisms were sometimes represented by more than one MCM v3.2 photolysis reaction. The product yields of the original mechanism reactions were preserved using combinations of the MCM v3.2 rate parameters. For example, glyoxal photolysis described by (R1) and (R2) in RADM2.

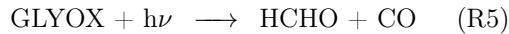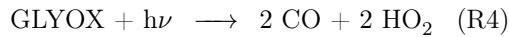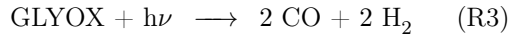$$\text{GLY} + h\nu \longrightarrow 0.13 \text{ HCHO} + 1.87 \text{ CO} + 0.87 \text{ H}_2 \qquad \text{(R1)}$$

$$\text{GLY} + h\nu \longrightarrow 0.45 \text{ HCHO} + 1.55 \text{ CO} + 0.8 \text{ HO}_2 + 0.15 \text{ H}_2 \quad \text{(R2)}$$

	Rate Parameter	MCM v3.2 Products and Yields
(R1)	0.87 J_{31}	1.74 CO + 0.87 H_2
	0.13 J_{32}	0.13 CO + 0.13 HCHO
	0.87 J_{31} + 0.13 J_{32}	1.87 CO + 0.13 HCHO + 0.87 H_2
(R2)	0.15 J_{31}	0.30 CO + 0.15 H_2
	0.45 J_{32}	0.45 CO + 0.45 HCHO
	0.4 J_{33}	0.80 CO + 0.80 HO_2
	0.15 J_{31} + 0.45 J_{32} + 0.4 J_{33}	1.55 CO + 0.45 HCHO + 0.80 HO_2 + 0.15 H_2

Table S1: Calculation of glyoxal MCM v3.2 photolysis rate parameters retaining RADM2 glyoxal photolysis product yields.

Mechanism	Reaction	Rate Constant
MCM v3.2	C2H5O2 = C2H5O	k*RO2*0.6 s^{-1}
	C2H5O2 = C2H5OH	k*RO2*0.2 s^{-1}
	C2H5O2 = CH3CHO	k*RO2*0.2 s^{-1}
MOZART-4	C2H5O2 + CH3O2 = 0.7 CH2O + 0.8 CH3CHO + HO2 + 0.3 CH3OH + 0.2 C2H5OH	2×10^{-13} cm^3 molecules^{-1} s^{-1}
	C2H5O2 + C2H5O2 = 1.6 CH3CHO + 1.2 HO2 + 0.4 C2H5OH	6.8×10^{-14} cm^3 molecules^{-1} s^{-1}
MOZART-4 modified	C2H5O2 = 0.8 CH3CHO + 0.6 HO2 + 0.2 C2H5OH	2×10^{-13}*RO2 s^{-1}

Table S2: Ethyl peroxy radical $(C_2H_5O_2)$ self and cross organic peroxy reactions in MCM v3.2 and MOZART-4 including rate constants. $k = 2(6.6 \times 10^{-27} \exp(365/T))^{\frac{1}{2}}$ molecules^{-1} s^{-1} and RO2 is the sum of all organic peroxy radical mixing ratios.

Whereas in the MCM v3.2, (R3), (R4) and (R5) are prescribed for glyoxal photolysis with the rates J_{31}, J_{32} and J_{33}.

$$\text{GLYOX} + h\nu \longrightarrow 2\text{ CO} + 2\text{ H}_2 \quad \text{(R3)}$$

$$\text{GLYOX} + h\nu \longrightarrow 2\text{ CO} + 2\text{ HO}_2 \quad \text{(R4)}$$

$$\text{GLYOX} + h\nu \longrightarrow \text{HCHO} + \text{CO} \quad \text{(R5)}$$

The product yields in (R1) were retained using a photolysis rate parameter of 0.87 J_{31} + 0.13 J_{32}, whilst for (R2) the rate 0.15 J_{31} + 0.45 J_{32} + 0.4 J_{33} was used. Table S1 illustrates the product yield calculations.

Reactants	Products	Rate Constant
MO2 + MO2	0.74 HO2 + 1.37 HCHO + 0.63 MOH	$9.4 \times 10^{-14} \exp\left(390/T\right)$ cm^3 molecules^{-1} s^{-1}
MO2	0.37 HO2 + 0.685 HCHO + 0.315 MOH	$9.4 \times 10^{-14} \exp\left(390/T\right)$*RO2 s^{-1}
ETHP + MO2	HO2 + 0.75 HCHO + 0.75 ACD + 0.25 MOH + 0.25 EOH	$1.18 \times 10^{-13} \exp\left(158/T\right)$ cm^3 molecules^{-1} s^{-1}
ETHP	0.63 HO2 + 0.065 HCHO + 0.75 ACD + 0.25 EOH	$1.18 \times 10^{-13} \exp\left(158/T\right)$*RO2 s^{-1}

Table S3: Dermination of ETHP pseudo-unimolecular reaction and rate constant in RACM2 including rate constants. RO2 is the sum of all organic peroxy radical mixing ratios.

S2.2 Organic Peroxy Radical Self and Cross Reactions

Reactions of organic peroxy radicals (RO_2) with other organic peroxy radicals are divided into self ($RO_2 + RO_2$) and cross ($RO_2 + R'O_2$) reactions. These reactions are typically represented in chemical mechanisms as bimolecular reactions which would cause ambiguities when implementing the tagging scheme. Namely, which tag to be used for the products of reactions between RO_2 reactants having different tags. The MCM v3.2 approach to self and cross RO_2 reactions (each RO_2 species reacts with the pool of all other RO_2 at a single uniform rate) is used to avoid such ambiguities. The MCM v3.2 approach represents RO_2–RO_2 reactions as a pseudo-unimolecular reaction whose rate constant includes a factor 'RO2' which is the sum of the mixing ratios of all organic peroxy radicals (Saunders et al., 2003).

The pseudo-unimolecular reaction products and their yields were determined by one of two methods. Firstly, by using the $RO_2 + RO_2$ reaction and halving the product yields, demonstrated for the MOZART-4 treatment of the ethyl peroxy radical in Table S2. Alternatively, the $RO_2 + CH_3O_2$ reaction was used to determine the products due to CH_3O_2 and these products are then removed.

Table S3 demonstrates the steps determining the ETHP pseudo-unimolecular reaction in RACM2. First the products due to MO2 (CH_3O_2 in RACM2) are determined as outlined previously using the MO2 + MO2 reaction. The MO2 product yields are subtracted from the ETHP + MO2 reaction. Any products having a negative yield are not included in the

3

54 final pseudo-unimolecular reaction.

The methyl acyl peroxy radical ($CH_3C(O)O_2$) was the exception to the above approach.
56 Although most mechanisms include a $CH_3C(O)O_2 + CH_3C(O)O_2$ reaction, the $CH_3C(O)O_2$
pseudo-unimolecular reaction was derived by subtracting the CH_3O_2 product yields from
58 the $CH_3C(O)O_2 + CH_3O_2$ reaction. This approach was used as the $CH_3C(O)O_2 + CH_3O_2$
reaction is the most significant reaction for $CH_3C(O)O_2$.

60 The rate constant for each pseudo-unimolecular reaction was taken as that of the
$RO_2 + CH_3O_2$ reaction multiplied by an 'RO2' factor, which is the sum of the mixing ratios
62 of all organic peroxy radicals. The $RO_2 + CH_3O_2$ rate constant was chosen as this is the
most likely reaction to occur.

64 Model runs using the original and modified approach to the RO_2–RO_2 reactions for
each mechanism were performed. The resulting O_3 concentration time series were compared
66 and shown in Figure S1.

S2.3 Dry Deposition

68 Dry deposition velocities for individual chemical species are taken from the MCM v3.2. The
MCM v3.2 dry deposition velocities of the same chemical functional group were used for
70 mechanism species without direct MCM v3.2 analogues. For example, the dry deposition
velocity of PAN-like species in all mechanisms was equivalent to that of the PAN species in
72 the MCM v3.2.

S2.4 Negative Product Yield Treatment

74 Some mechanisms include reactions where products have a negative yield. These reactions
were re-written including an operator species with a positive yield as the analysis tools
76 used in this study do not allow negative product yields. The operator species acts as a sink
for the original product by immediately reacting with the original product generating a
78 'NULL' product.

For example, in RADM2 the OH + CSL (cresol) reaction has negative OH yield in (R6)
80 (Stockwell et al., 1990).

$$CSL + OH \longrightarrow 0.1\ HO_2 + 0.9\ XO_2 + 0.9\ TCO_3 - 0.9\ OH \quad (R6)$$

4
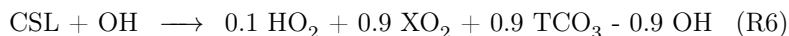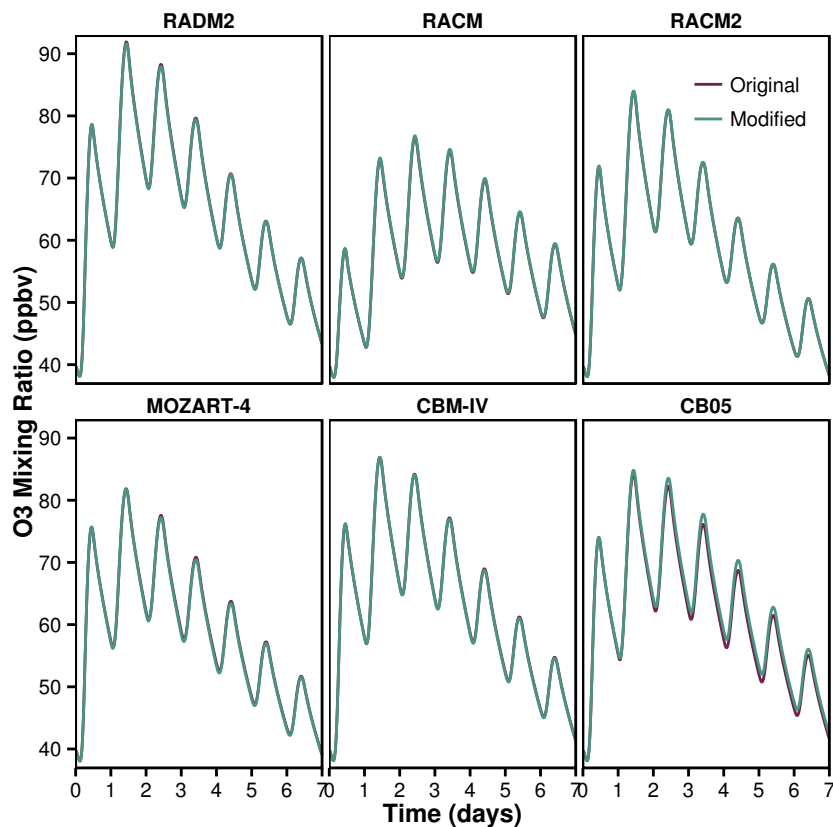
Figure S1: O_3 mixing ratio time series for each reduced mechanism using the original and modified approach to RO_2–RO_2 reactions

82   The negative OH yield was adapted to a positive operator (OHOP) yield in (R7). OHOP then reacts immediately with OH giving a 'NULL' product with a rate constant of

84   8.0×10^{-11} cm^3 s^{-1} (R8). Thus preserving the OH yields from (R6) in RADM2.

$$CSL + OH \quad \longrightarrow \quad 0.1\ HO_2 + 0.9\ XO_2 + 0.9\ TCO_3 + 0.9\ OHOP \quad (R7)$$

$$OHOP + OH \longrightarrow NULL \quad\quad\quad\quad\quad\quad\quad\quad\quad\quad\quad\quad (R8)$$
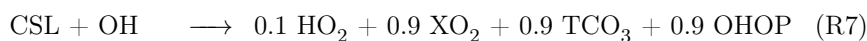
86   ## S3   Mapping Emitted NMVOC to Mechanism Species

The emitted NMVOC are typical of Los Angeles as described in Baker et al. (2008). The

88   MCM v3.2, v3.1 (Jenkin et al., 1997; Saunders et al., 2003; Jenkin et al., 2003) and CRI v2 (Jenkin et al., 2008) explicitly represent all of these NMVOC.

90   The representation of NMVOC in all other mechanisms required mapping the individual NMVOC to specific mechanism species. This mapping followed the recommendations on

the literature of the mechanism; Table S4 describes the mechanism species used for mapping the initial NMVOC. Table 2 of the main article shows the final mapping of each NMVOC to each mechanism species.

S4 Treatment of 2-methylpropene Degradation

Figure 4 of the main article shows the first day TOPP values of the VOC obtained in each reduced mechanism compared to the MCM v3.2. The first day TOPP values of 2-methylpropene in RACM, RACM2, MOZART-4, CBM-IV and CB05 signify differences in its degradation to the MCM v3.2.

The variation between RACM, RACM2 and MCM v3.2 arises from differences in the ozonolysis rate constant of 2-methylpropene. This rate constant is an order of magnitude faster in RACM and RACM2 than in MCM v3.2 as the RACM, RACM2 rate constant is a weighted mean of the ozonolysis rate constants of each VOC represented as OLI (Stockwell et al., 1997; Goliff et al., 2013). The faster rate constant promotes increased radical production leading to more O_x in RACM and RACM2 than the MCM v3.2.

2-methylpropene is represented as BIGENE in MOZART-4. The degradation of BIGENE produces CH_3CHO through the reaction between NO and the 2-methylpropene peroxy radical, whereas no CH_3CHO is produced during 2-methylpropene degradation in the MCM v3.2. CH_3CHO initiates a degradation chain producing O_x involving CH_3CO_3 and CH_3O_2 leading to more O_x in MOZART-4 than MCM v3.2.

CBM-IV and CB05 represent 2-methylpropene as a combination of aldehydes and PAR, the $C-C$ bond (Gery et al., 1989; Yarwood et al., 2005). This representation of 2-methylpropene does not produce the 2-methylpropene peroxy radical, whose reaction with NO is the main source of O_x production in all other mechanisms.

Left columns:

Mechanism	Species	Description
	C2H6	Ethane
	C3H8	Propane
MOZART-4 (Emmons et al., 2010)	BIGALK	Lumped alkanes C >3
	C2H4	Ethene
	C3H6	Propene
	BIGENE	Lumped alkenes C >3
	ISOP	Isoprene
	TOLUENE	Lumped aromatics
	ETH	Ethane
	HC3	OH rate constant (298, 1 atm) between 2.7×10^{-13} and 3.4×10^{-12}
	HC5	OH rate constant (298, 1 atm) between 3.4×10^{-12} and 6.8×10^{-12}
RADM2 (Stockwell et al., 1990)	HC8	OH rate constant (298, 1 atm) greater than 6.8×10^{-12}
	OL2	Ethene
	OLT	Terminal Alkenes
	OLI	Internal Alkenes
	ISO	Isoprene
	TOL	Toluene and less reactive aromatics
	XYL	Xylene and more reactive aromatics
	ETH	Ethane
	HC3	OH rate constant (298 K, 1 atm) less than 3.4×10^{-12} cm^3 s^{-1}
RACM (Stockwell et al., 1997)	HC5	OH rate constant (298 K, 1 atm) between 3.4×10^{-12} and 6.8×10^{-12}
	HC8	OH rate constant (298 K, 1 atm) greater than 6.8×10^{-12}
	ETE	Ethene
	OLT	Terminal alkenes
	OLI	Internal alkenes
	ISO	Isoprene
	TOL	Toluene and less reactive aromatics
	XYL	Xylene and more reactive aromatics

Right columns:

Mechanism	Species	Description
	ETH	Ethane
	HC3	OH rate constant (298 K, 1 atm) less than 3.4×10^{-12} cm^3 s^{-1}
	HC5	OH rate constant (298 K, 1 atm) between 3.4×10^{-12} and 6.8×10^{-12} cm^3 s^{-1}
	HC8	OH rate constant (298 K, 1 atm) greater than 6.8×10^{-12} cm^3 s^{-1}
RACM2 (Goliff et al., 2013)	ETE	Ethene
	OLT	Terminal alkenes
	OLI	Internal alkenes
	ISO	Isoprene
	BEN	Benzene
	TOL	Toluene and less reactive aromatics
	XYM	m-Xylene
	XYO	o-Xylene
	XYP	p-Xylene
	PAR	Paraffin carbon bond C–C
	ETH	Ethene
	OLE	Olefinic carbon bond C=C
CBM-IV (Gery et al., 1989)	ALD2	High molecular weight aldehydes
	ISOP	Isoprene
	TOL	Toluene
	XYL	Xylene
	FORM	Formaldehyde
	ETHA	Ethane
	PAR	Paraffin carbon bond C–C
CB05 (Yarwood et al., 2005)	OLE	Terminal olefin carbon bond R–C=C
	FORM	Formaldehyde
	ISOP	Isoprene
	TOL	Toluene and other monoalkyl aromatics
	XYL	Xylene and other polyalkyl aromatics

Table S4: Description of primary mechanism species used for mapping emitted NMVOCs.

References

Angela K. Baker, Andreas J. Beyersdorf, Lambert A. Doezema, Aaron Katzenstein, Simone Meinardi, Isobel J. Simpson, Donald R. Blake, and F. Sherwood Rowland. Measurements of nonmethane hydrocarbons in 28 United States cities. *Atmospheric Environment*, 42: 170–182, 2008.

C. Bloss, V. Wagner, M. E. Jenkin, R. Vollamer, W. J. Bloss, J. D. Lee, D. E. Heard, K. Wirtz, M. Martin-Reviejo, G. Rea, J. C. Wenger, and M. J. Pilling. Development of a detailed chemical mechanism (MCMv3.1) for the atmospheric oxidation of aromatic hydrocarbons. *Atmospheric Chemistry and Physics*, 5:641–664, 2005.

T. M. Butler, M. G. Lawrence, D. Taraborrelli, and J. Lelieveld. Multi-day ozone production potential of volatile organic compounds calculated with a tagging approach. *Atmospheric Environment*, 45(24):4082–4090, 2011.

V. Damian, A. Sandu, M. Damian, F. Potra, and G.R. Carmichael. The kinetic preprocessor KPP - A software environment for solving chemical kinetics. *Computers and Chemical Engineering*, 26(11):1567–1579, 2002.

L. K. Emmons, S. Walters, P. G. Hess, J.-F. Lamarque, G. G. Pfister, D. Fillmore, C. Granier, A. Guenther, D. Kinnison, T. Laepple, J. Orlando, X. Tie, G. Tyndall, C. Wiedinmyer, S. L. Baughcum, and S. Kloster. Description and evaluation of the Model for Ozone and Related chemical Tracers, version 4 (MOZART-4). *Geoscientific Model Development*, 3: 43–67, 2010.

Michael W. Gery, Gary Z. Whitten, James P. Killus, and Marcia C. Dodge. A photochemical kinetics mechanism for urban and regional scale computer modeling. *Journal of Geophysical Research*, 94(D10):12,925–12,956, 1989.

Wendy S. Goliff, William R. Stockwell, and Charlene V. Lawson. The regional atmospheric chemistry mechanism, version 2. *Atmospheric Environment*, 68:174–185, 2013.

M. E. Jenkin, S. M. Saunders, V. Wagner, and M. J. Pilling. Protocol for the development of the Master Chemical Mechanism, MCM v3 (Part B): Tropospheric degradation of aromatic volatile organic compounds. *Atmospheric Chemistry and Physics*, 3(1):181–193, 2003.

M. E. Jenkin, L. A. Watson, S. R. Utembe, and D. E. Shallcross. A Common Representative
Intermediates (CRI) mechanism for VOC degradation. Part 1: Gas phase mechanism
development. *Atmospheric Environment*, 42:7185–7195, 2008.

Michael E. Jenkin, Sandra M. Saunders, and Michael J. Pilling. The tropospheric
degradation of volatile organic compounds: A protocol for mechanism development.
Atmospheric Environment, 31(1):81–104, 1997.

Andrew Rickard, Jenny Young, and Stephen Pascoe. The Master Chemical Mechanism
Version MCM v3.2. `http://mcm.leeds.ac.uk/MCMv3.2/`, 2015. [Online; accessed
25-March-2015].

R. Sander, A. Kerkweg, P. Jöckel, and J. Lelieveld. Technical Note: The new comprehensive
atmospheric chemistry module MECCA. *Atmospheric Chemistry and Physics*, 5:445–450,
2005.

S. M. Saunders, M. E. Jenkin, R. G. Derwent, and M. J. Pilling. Protocol for the development
of the Master Chemical Mechanism, MCM v3 (Part A): Tropospheric degradation of
non-aromatic volatile organic compounds. *Atmospheric Chemistry and Physics*, 3(1):
161–180, 2003.

William R. Stockwell, Paulete Middleton, Julius S. Chang, and Xiaoyan Tang. The Second
Generation Regional Acid Deposition Model Chemical Mechanism for Regional Air Quality
Modeling. *Journal of Geophysical Research*, 95(D10):16,343–16,367, 1990.

William R. Stockwell, Frank Kirchner, Michael Kuhn, and Stephan Seefeld. A new
mechanism for regional atmospheric chemistry modeling. *Journal of Geophysical Research
D: Atmospheres*, 102(22):25,847–25,879, 1997.

Greg Yarwood, Sunja Rao, Mark Yocke, and Gary Z. Whitten. Updates to the Carbon Bond
Chemical Mechanism: CB05. Technical report, U. S Environmental Protection Agency,
2005.

Chapter 8

Paper II: Variation of the NMVOC Speciation in the Solvent Sector and the Sensitivity of Modelled Tropospheric Ozone

Variation of the NMVOC speciation in the solvent sector and the sensitivity of modelled tropospheric ozone

E. von Schneidemesser [a, *], J. Coates [a], H.A.C. Denier van der Gon [b], A.J.H. Visschedijk [b], T.M. Butler [a]

[a] *Institute for Advanced Sustainability Studies (IASS), Berlinerstrasse 130, 14467 Potsdam, Germany*
[b] *TNO, Netherlands Organization for Applied Scientific Research, Princetonlaan 6, 3584 CB Utrecht, The Netherlands*

HIGHLIGHTS

- The role of NMVOC speciation for ozone production was tested using a box model.
- There is significant variation in NMVOC speciation for solvent sector emissions.
- Results indicate that speciation could have a significant impact on modelled ozone.
- Choice of chemical mechanism also influenced ozone production.

ARTICLE INFO

ABSTRACT

Non-methane volatile organic compounds (NMVOCs) are detrimental to human health owing to the toxicity of many of the NMVOC species, as well as their role in the formation of secondary air pollutants such as tropospheric ozone (O_3) and secondary organic aerosol. The speciation and amount of NMVOCs emitted into the troposphere are represented in emission inventories (EIs) for input to chemical transport models that predict air pollutant levels. Much of the information in EIs pertaining to speciation of NMVOCs is likely outdated, but before taking on the task of providing an up-to-date and highly speciated EI, a better understanding of the sensitivity of models to the change in NMVOC input would be highly beneficial. According to the EIs, the solvent sector is the most important sector for NMVOC emissions. Here, the sensitivity of modelled tropospheric O_3 to NMVOC emission inventory speciation was investigated by comparing the maximum potential difference in O_3 produced using a variety of reported solvent sector EI speciations in an idealized study using a box model. The sensitivity was tested using three chemical mechanisms that describe O_3 production chemistry, typically employed for different types of modelling scales — point (MCM v3.2), regional (RADM2), and global (MOZART-4). In the box model simulations, a maximum difference of 15 ppbv (ca. 22% of the mean O_3 mixing ratio of 69 ppbv) between the different EI speciations of the solvent sector was calculated. In comparison, for the same EI speciation, but comparing the three different mechanisms, a maximum difference of 6.7 ppbv was observed. Relationships were found between the relative contribution of NMVOC compound classes (alkanes and oxygenated species) in the speciations to the amount of Ox produced in the box model. These results indicate that modelled tropospheric O_3 is sensitive to the speciation of NMVOCs as specified by emission inventories, suggesting that detailed updates to the EI speciation information would be warranted. Furthermore, modelled tropospheric O_3 was also sensitive to the choice of chemical mechanism and further evaluation of both of these sensitivities in more realistic chemical-transport models is needed.

1. Introduction

Volatile organic compounds (VOCs) have adverse effects on health, both directly through the toxicity of the VOCs themselves

* Corresponding author.
E-mail address: erika.vons@iass-potsdam.de (E. von Schneidemesser).

(Laurent and Hauschild, 2014) and indirectly as a precursor of secondary air pollutants. Tropospheric ozone (O_3) is a secondary air pollutant formed from the degradation of VOCs in the presence of nitrogen oxides (NOx) and sunlight (Atkinson, 2000). Numerical chemical transport models use emissions of non-methane VOCs (NMVOCs) and NOx, as well as carbon monoxide and methane, to calculate O_3 concentrations. Anthropogenic NMVOC emissions are allocated in emission inventories (EIs) to sectors by source (e.g. industry, solvent use). The type of NMVOCs emitted varies widely from one source to another, with the sectors determining the source profile or speciation of the NMVOCs applied.

The ozone forming potential of NMVOC species differs substantially (Butler et al., 2011). Accurately representing NMVOCs in emission inventories is therefore crucial to be able to reproduce air quality conditions in models, for understanding atmospheric chemistry and the impact of policy measures. As measurements from China have shown, the variation in VOC speciation can vary significantly in different cities and regions, which is crucial for implementing effective policy measures (Shao et al., 2009; Zheng et al., 2009). The challenge of improving NMVOCs in emission inventories and understanding how accurately these inventories represent real-world conditions is compounded by the lack of (long-term) measurements of NMVOCs compounds, limited efforts on updating emission factors, and the variable reactivity of various NMVOC compounds which makes validation of the emission inventories and the assessment of the capacity of models to capture NMVOCs and accurately represent them difficult. In addition, national reporting typically only includes total NMVOC emissions and no information on speciation. Further complicating this issue is a lack of understanding of the relative importance as to whether total NMVOC emissions or NMVOC speciation is more, less, or equally important, including the relative importance of the changes in speciation and total emissions over time.

Despite EIs being critical model input, there are many uncertainties associated with EIs – many of which are not quantified – such as the speciation of NMVOCs and relative contribution of the different sectors to total NMVOC emissions. Significant discrepancies have been documented between the contributions of NMVOC species as represented in EIs and ambient measurements of the NMVOC, with some species being significantly over- or under-represented (Borbon et al., 2013; Coll et al., 2010). The application of protocols developed for a particular country or region (e.g., the US, the UK), which are often adopted in other countries for the development of emission inventories and NMVOC speciation, can also lead to errors and significant differences in NMVOC species between measurements and the emissions estimates (e.g., Chen et al., 2010). EIs also often fail to capture the seasonality in NMVOC emissions (Boynard et al., 2014), for example, because the reporting requires annual total emissions only. In a study comparing emission inventories and datasets for North America and Europe, substantial differences were found for temporal profiles, including the timing of emission release throughout the year and diurnal patterns, noting that owing to possible effects on subsequent atmospheric chemistry further study is warranted (Pouliot et al., 2012).

Furthermore, the current NMVOC speciation applied in many models is based on older data. A global speciation of the NMVOC emissions inventory was developed in the 1990s and made available in 1996 for the base year 1990 in the framework of the EDGAR project (Olivier et al., 2001). Similar NMVOC profiles were also used in the RETRO project, during which an update of the speciation information to the year 1995 for source sub-sector contributions was produced, although no new NMVOC split data were generated or used in RETRO beyond this limited sub-sector contribution reassessment (Schultz et al., 2007). The resulting NMVOC

speciation per sector was released with the EDGAR inventory, providing emissions from 1960 to 2000 and has not been updated significantly since then (Olivier et al., 2005). Other NMVOC speciation recommendations exist, for example, the EMEP model has a default speciation by sector divided into 14 species or categories of species (Simpson et al., 2012), which was derived from work by Passant (2002) based on information from the UK. Reported NMVOC speciation has been shown to change over time. The UK National Atmospheric Emission Inventory provides information on the top 50 NMVOCs by mass to the total NMVOC emissions reported. From 1998 to 2008 the species listed have changed, even among the top 10 (Murrells et al., 2010; NETC, 2000). This indicates that speciation information likely requires regular updating.

In addition, the reported emissions often do not agree with attribution to emission sectors based on measurements. For example, a study conducted in Wuppertal, Germany found that while the German Emission Inventory indicated that 51% of the total NMVOC emissions were attributed to solvent use and only 14% to traffic, measurements indicated a maximum contribution of solvent use to approximately 23% of NMVOCs emissions for the area, and a dominating contribution from traffic sources (Niedojadlo et al., 2007). Similarly, a study in Augsburg, Germany found an overestimation of solvents based on a comparison of measurements and emissions data indicating wider applicability of these results (Mannschreck et al., 2002; Slemr et al., 2002). Further studies have also found that especially for urban areas, vehicles are a major and often dominant source of NMVOC emissions (Borbon et al., 2002, 2013; Boynard et al., 2014; Brulfert et al., 2005; Vega et al., 2000; Warneke et al., 2007). While the majority of studies cited were conducted in developed countries, accurate representation of emissions and sectoral attribution is likely to be an even larger issue in developing nations, where on the whole much less reliable information is available.

Improving an EI requires a large amount of effort due to the diverse sources and variety of inputs used in their construction. Before undertaking such a task, it would be valuable to know whether models are sensitive to changing NMVOC input. In other words, is it worth the effort? In particular, how large are the differences in modelled O_3 using different EIs as model input. In this study we address one aspect of NMVOC EI improvement, specifically, speciation, to better understand the sensitivity of modelled O_3 to different NMVOC speciations with a focus on the solvent sector. In current inventories, the solvent sector is in many cases the largest source of NMVOC emissions. For example, according to data presented by the EEA from the national emissions reported to the Convention on Long-range Transboundary Air Pollution (CLRTAP), the sector 'Solvent and product use' contributed ca. 3.4 million kt of emissions and accounted for 43.10% of the total NMVOC emissions in Europe in 2011. This was higher than all other sectors including 'road transport' (14.60%), and 'commercial, institutional and households' (16.70%), the two next largest sectors (EEA, 2013). Similarly, in the UK (one of the countries providing the most detailed NMVOC speciation as part of their EI) in 2008, 'solvent and other product use' accounted for 42% of the total NMVOC emissions, with the next highest contribution originating in the 'extraction and distribution of fossil fuels' (20%), followed by road transport (14%) (Murrells et al., 2010). Although total emissions of NMVOCs have been reported to be declining over the past decades, since a peak ca. 1990, the large fractional contribution of the solvent sector to total NMVOC emissions is in part owing to the much sharper reductions that have been attributed to NMVOC emissions from the road transport sector, ca. −80% between 1990 and 2011, in comparison to ca. −40% reduction for solvents (EEA, 2013). While this study was limited to the solvent sector for the reasons just discussed, there are a variety of other source sectors, including

those outside of urban areas that could significantly affect ozone production, such as the rapidly developing area of oil and natural gas extraction (Thompson et al., 2014). Recent work has shown that emissions from such sources are likely underestimated in current inventories, including much larger than expected observations of alkanes (Gilman et al., 2013; Pétron et al., 2012).

Finally, previous work evaluating the over- or under-estimation of certain hydrocarbon species in the emission inventories used in chemical transport models found that differences in speciation can have a strong incidence on the representation of the air mass reactivity, resulting in an effect on the ozone production and an impact on peak concentrations (Coll et al., 2010). For these reasons, an investigation into the effect of speciation on ozone production was undertaken. Specifically, the maximum potential difference in modelled O_3 produced by various solvent sector EI NMVOC speciations using an idealized box model setup was investigated.

2. Methods

2.1. Solvent sector NMVOC emission inventories

Through a literature survey a variety of source profiles for the solvent sector were identified, with a focus on Europe. The solvent sector EIs represent a range of case studies, including the European average NMVOC speciation (TNO), from the 'TNO-MACC' inventory widely used in chemical-transport modelling (Builtjes et al., 2002), a model specific speciation (EMEP) providing the basis for the EMEP model (Simpson et al., 2012), a general global anthropogenic speciation often used in global models from the IPCC AR3 (IPCC) (Ehhalt et al., 2001), and country specific profiles for Germany (Friedrich et al., 2002), Greece (Sidiropoulos and Tsilingiridis, 2007) and the UK (Goodwin, 2000; Murrells et al., 2010). Two time-points of the Greek and UK profiles are included to represent the evolution of solvent sector NMVOC emissions over time. Table 1 lists all solvent sector EIs compared in this study and the number of different NMVOCs included in the original profile. Although similar numbers of species may be listed in the Table, even similar numbers of species from the same country do not indicate that the same specific species are included within this group.

To provide a visual comparison of the composition of these different solvent sector speciations, the composition of the profiles was translated to a common basis for comparison based on functional group and carbon number. For this some compounds are 'translated' directly as they exist individually, e.g., ethane, propane, whereas others are grouped or 'lumped' into categories, e.g., alcohols, or higher alkanes. This was necessary because the inventories include differing amounts of detail, with some including only 10 species or groups and others 50, and the 10 or 50 species are often not the same 10 or 50 species or groups. The common basis facilitates comparisons. Fig. 1 shows the percent contribution of each compound or category for all the solvent sector speciations considered in this study. It should be noted that this 'translation' of

the solvent sector speciation was not used as input for the box model, but rather to demonstrate and visualize the difference in speciation. For box model input the original speciation was used and then mapped onto the individual chemical mechanisms. The original speciation information is provided in Tables S1a–g in the Supplemental Information (SI).

2.2. Model description

The MECCA box model (Sander et al., 2005) was used as described in Coates and Butler (2015) without any meteorology or transport processes that are included in 3-D models to focus solely on the photochemical gas-phase processes that produce O_3. Model runs were performed using the detailed gas-phase chemistry of the Master Chemical Mechanism (MCM v3.2) (Bloss et al., 2005; Jenkin et al., 1997, 2003; Rickard et al., 2015; Saunders et al., 2003).

Reduced chemical mechanisms are used by 3-D models for reasons of computational efficiency and these reduced chemical mechanisms typically represent NMVOC by aggregating many VOC into a surrogate mechanism species (lumping). Hence, changing the chemical mechanism in a model also changes the NMVOC input. The sensitivity of modelled O_3 mixing ratios was therefore also determined using the MOZART-4 (Emmons et al., 2010) and RADM2 (Stockwell et al., 1990) mechanisms which are typically used for global and regional modelling studies, respectively. Detailed information on the implementation of MOZART-4 and RADM2 into the MECCA box model can be found in Coates and Butler (2015).

2.3. Model setup and simulations

The model was run under equinoctial conditions representative of 34° north (roughly the city of Los Angeles, USA). CO and O_3 were initialized at 200 ppbv and 40 ppbv and then allowed to evolve freely; methane (CH_4) was fixed at 1.8 ppmv. In each model run (one for each speciation tested), NOx conditions that induced maximum O_3 production were used. This was achieved by emitting the amount of nitric oxide (NO) needed to balance the chemical source of radicals at each time step as described in more detail by Butler et al. (2011). In order to assess whether the different NO sources used in each model run were responsible for the differences in predicted ozone, an additional set of runs was conducted using a 'mean NO source.' For the 'mean NO source' runs, the NO emissions for each time step of the 'tuned NO' runs (one for each speciation tested) was averaged to provide the mean NO emissions for each mechanism.

Model runs were performed using each of the solvent sector EIs of Table 1 using the three gas-phase chemistry schemes (MCM v3.2, MOZART-4 and RADM2). A further set of model runs was performed with each EI after "tagging" each of the chemical mechanisms for the emitted NMVOC. This tagging approach followed Butler et al. (2011) and allowed for attribution of Ox production back to the emitted VOC. As O_3 production is dominated by rapid

Table 1
Solvent sector emission inventories compared in this study. The number of species reflect those originally reported.

| Speciation code	Type	# of Species	References
TNO	European average	23	Builtjes et al. (2002)
IPCC	Global	23	Ehhalt et al. (2001)
EMEP	Model specific	14	Simpson et al. (2012)
DE94	Country specific	10	Friedrich et al. (2002)
GR95	Country specific	32	Sidiropoulos and Tsilingiridis (2007)
GR05	Country specific	32	Sidiropoulos and Tsilingiridis (2007)
UK98	Country specific	50	Goodwin (2000)
UK08	Country specific	50	Murrells et al. (2010)
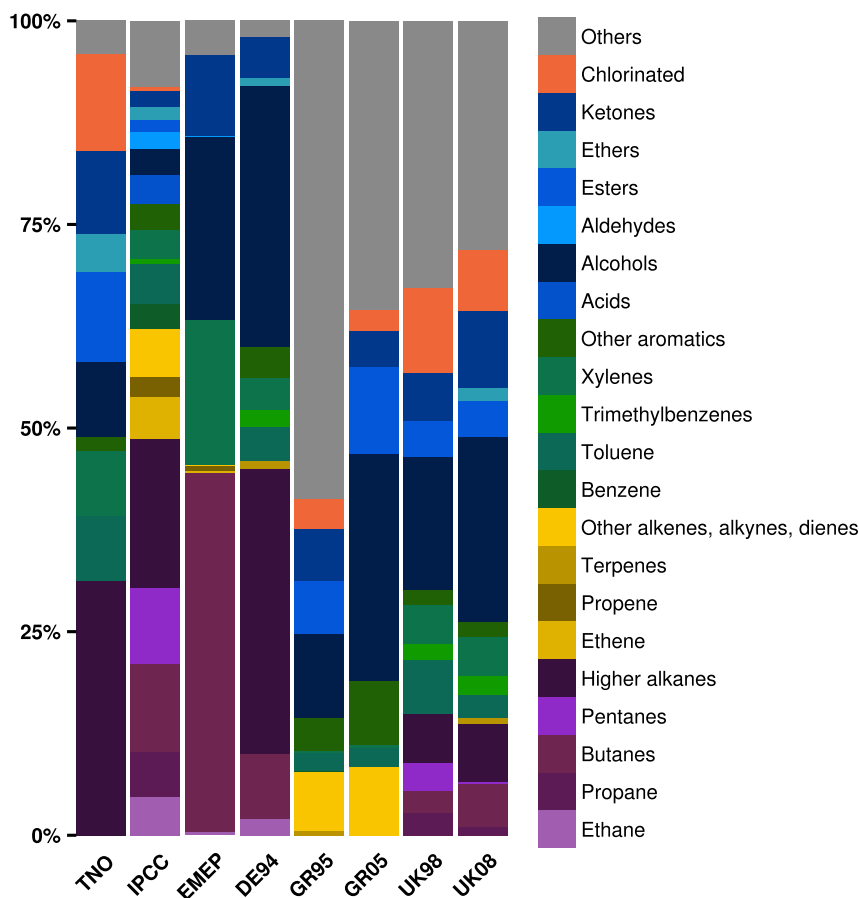
Fig. 1. Solvent sector speciation profiles, as percent contributions by mass, translated to the individual NMVOCs and lumped NMVOC categories used as a common basis for comparison. Similar colors are used to relate compounds by class, e.g., alkanes are grouped and depicted in purples, alkenes and alkynes are grouped and depicted in yellows, etc. See Table 1 for speciation codes and references. (For interpretation of the references to colour in this figure legend, the reader is referred to the web version of this article.)

photochemical cycles, the Ox family was used as a surrogate for O_3 production. For this work, the Ox family was defined as including O_3, NO_2, O, O^1D, NO_3, N_2O_5 and other species that are involved in fast photochemical production and loss cycles with NO_2. This definition of the Ox family implies that Ox production budgets are a measure of the number of NO to NO_2 conversions by peroxy radicals formed during VOC degradation. As all organic peroxy radicals are tagged for the emitted NMVOC, the tag and the reaction rate were used to attribute Ox production back to the emitted VOC. Butler et al. (2011) shows that under the conditions of maximum ozone production as used in this study, the production rate of Ox is closely related to the production rate of ozone, and includes more details of the tagging approach.

2.4. NMVOC initial conditions

This study considered an idealized urban area of 1000 km^2 with total NMVOC emissions of 1000 tons day^{-1} (Warneke et al., 2007). As the solvent sector contributed 43% to total NMVOC emissions (EEA, 2013), the total amount of NMVOC emissions in each model run was 430 tons day^{-1} The total NMVOC emissions were then allocated to the individual NMVOC and groups of NMVOC specified by the EIs in Table 1 that were represented by MCM v3.2 species. Since the MCM is a near explicit mechanism, in many cases lumped species needed to be separated into their individual components for use in this mechanism. For this, an informed allocation was preferred, rather than making different assumptions for different

cases or simply allocating an equal fraction to each species falling under the lumped group. Therefore, Passant (2002) was used to facilitate this allocation, which reports some of the most detailed speciation information available for NMVOC emissions based on detailed profiles from individual activities. The composite profile for Standardized Nomenclature for Air Pollutants (SNAP) category 6 (solvent use sector) with percent contributions from 127 individual NMVOCs specified for SNAP 6 in Passant (2002) was used to provide more explicit speciation information where needed. This is provided in Table S1a. For example, the TNO EI specifies a contribution of 8% from 'xylenes' as a group to the total NMVOC emissions. As the MCM v3.2 represents xylenes not as a group, but as the individual NMVOCs, the relative amounts of the emissions were calculated and attributed to the individual xylene isomers (*m*-, *o*- and *p*-xylene) using the information provided for the solvent sector by Passant (2002) and thereby integrated into the MCM v3.2. The calculation of the attribution of xylenes to individual xylene species is depicted in Table 2. Following the same process, in the case where some NMVOC contribution was attributed to 'others' the NMVOCs listed in the Passant (2002) speciation for solvent use and not already accounted for were used to attribute contributions from the remaining NMVOCs. Finally, in the case of the speciation for Greece, 'white spirit' was included in the speciation profile. Sidiropoulos and Tsilingiridis (2007) also included the composition of white spirit, and therefore the cycloalkanes, paraffins and aromatics represented by the MCMv3.2 having the same carbon numbers as listed by Sidiropoulos and Tsilingiridis (2007) were

Table 2
Example attribution of lumped NMVOC species categories to individual compounds using Passant (2002).

TNO Category	MCM species	Passant % contribution	TNO % contribution	Adjusted % contribution
Xylenes	MXYL (*m*-xylene)	3.2	7.99	5.33 (= 3.2/4.8 × 8)
	OXYL (*o*-xylene)	0.8		1.33 (= 0.8/4.8 × 8)
	PXYL (*p*-xylene)	0.8		1.33 (= 0.8/4.8 × 8)
Total		4.8	7.99	7.99

used to represent NMVOC emissions from white spirit in this study. NMVOC emissions were held constant for the first 6 h of simulations, representing a pulse of NMVOC emissions.

The initial NMVOC emissions and NMVOC species represented by the MCM v3.2 were mapped to the MOZART-4 and RADM2 primary species based on the recommendations from the literature (Emmons et al., 2010; Stockwell et al., 1990). Then the MCM v3.2 species and respective emissions were aggregated into the MOZART-4 and RADM2 species by weighting the MCM v3.2 emissions by the respective carbon numbers. This approach ensured that the amount of emitted reactive carbon was the same in each model run despite the different chemistry schemes.

Two additional sets of runs were done using each solvent sector speciation with each chemical mechanism to evaluate the magnitude of the effect in increasingly realistic conditions, adding (a) emissions for all other anthropogenic emission sectors, followed by (b) biogenic emissions in addition to the anthropogenic emissions of (a). The remaining anthropogenic emissions contributed an additional 570 tons day^{-1} to complete the 1000 tons day^{-1} for the idealized urban area. The relative contributions of each sector were based on the same literature source as the solvent sector contribution (EEA, 2013), and the speciation used for these emissions was a European average provided by TNO (Builtjes et al., 2002). For the biogenics run, all anthropogenic emissions were included, plus an additional 440 tons day^{-1} of biogenic emissions. Specifically 150 tons day^{-1} of isoprene and 290 tons day^{-1} of monoterpene emissions were added to the initial emissions pulse. These values were based on the annual total European emissions information used in the EMEP model (Simpson et al., 2012). The relative contribution of the biogenic (isoprene and monoterpene) emissions to the total anthropogenic NMVOC emissions was calculated and averaged for all of Europe. This average was then related to the hypothetical emissions of 1000 tons day^{-1} used in the box model, to provide a reasonable estimate for biogenic emissions. These runs were done to provide the context for incrementally including more realistic conditions for the box model and estimate the effect of changing the NMVOC speciation of the solvent sector emissions.

3. Results

3.1. Comparison of solvent sector speciation

Fig. 1 presents the comparison of the solvent sector speciations used in this study, translated to the common basis categories to facilitate the comparison, as described in Section 2.1. There is significant variation across the different speciations for the solvent sector. It should be noted that the IPCC speciation is a general speciation that does not distinguish between sectors and therefore if this profile were used in modelling, the solvent sector speciation would equal that of e.g., road transport or agriculture. Even among certain species categories, there are significant variations. For example, the alkanes in the solvent sector are represented completely as higher alkanes in the TNO inventory, whereas the EMEP model solvent speciation represents the vast majority of the

alkanes as butanes with the exception of a small contribution from ethane. The IPCC and UK representations have the alkanes distributed more explicitly across the 4–5 alkane species and groups. Furthermore, the relative contribution of alkanes to the total also varies significantly. For Greece, alkanes are not included in the solvent sector speciation at all, whereas for a number of the other speciations contributions from alkanes are almost 50% of the total. In addition to the diversity in NMVOC speciation likely resulting from different information sources and spatial differences, the multiple years provided for Greece and the UK show differences in the two profiles for the different years, indicating an evolution or change in NMVOC speciation over time. For both the UK and Greece the later profiles show a larger contribution from alcohols and a slight reduction in chlorinated NMVOCs. And in the case of the UK, while the overall amount attributed to alkanes has remained relatively similar, the speciation within the alkanes shifted, being dominated more by butanes and higher alkanes in 2008 than 1998.

In mapping these NMVOC speciation details onto the different chemical mechanisms significant differences result based on what species are lumped or represented explicitly. As discussed in section 2.4, additional information was used from the detailed speciation provided by Passant (2002) where explicit speciation was needed when only lumped categories were provided by the emission inventory used, as in the case of mapping many of the EI onto the MCM v3.2 mechanism. To compare the input emissions speciation of the different mechanisms, the original input speciation as translated for the mechanisms, was again translated further into the common basis categories, to facilitate comparison, as for Fig. 1. This is shown in Fig. 2, with each group of three comparing the speciation of the same EI, as translated for input into each of the three chemical mechanisms used. (The original speciation information is provided in SI for reference, Tables S1a–g.) As the most explicit mechanism included here the MCM v3.2 retains the highest amount of speciation information, and in some cases greater speciation information than the inventory may initially provide (as suggested by the example of xylenes in section 2.4). For example, the MOZART-4 mechanism allows for input of 21 species or NMVOC categories, while the MCM v3.2 allows for ca. 150. For example, in the case of the EMEP speciation, the original speciation of alkanes provided for the solvent sector in the EMEP model, is 0.4% ethane and 44% *n*-butane. When translated onto the respective mechanisms used here, across all mechanisms the alkanes are represented by a small contribution from ethane, but the rest is then represented as butanes in the MCM v3.2, whereas in MOZART-4 butanes are lumped into the 'big alkanes' category, which have a reactivity representative of pentanes for the whole category, and in RADM2, butanes are lumped in the HC3 category, representative of propane. For more details on the mechanisms and their comparison, please see Coates and Butler (2015). This comparison demonstrates that even with the same starting point for input data, significant differences in ozone production may result owing to how these species and their secondary chemistry are represented when translated to different chemical mechanisms.
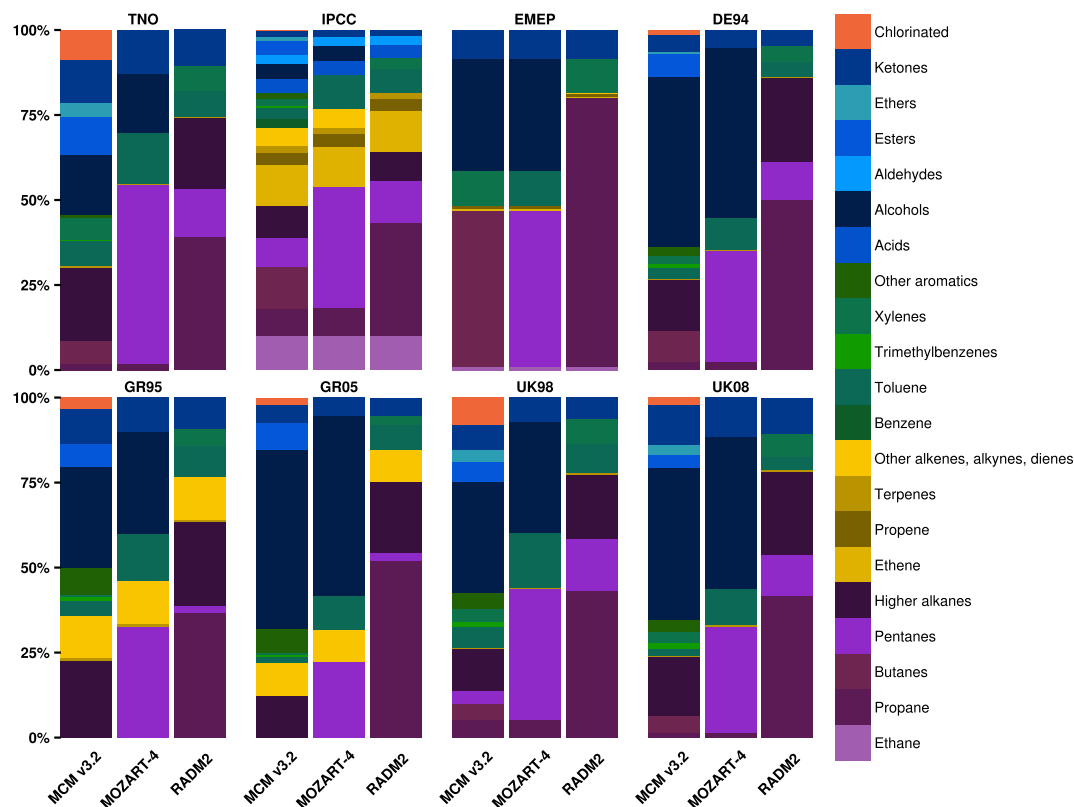
Fig. 2. Solvent sector speciation profiles, as percent contributions by mass, illustrating the differences owing to representation in the different chemical mechanisms, the MCM v3.2, MOZART-4, and RADM2. As in Fig. 1, the profiles were translated to the individual NMVOCs and NMVOC categories that were used as a common basis for comparison. Speciation profiles are grouped by emission inventory, with each group of three stacked bars representing one of the chemical mechanisms used in the box model.

3.2. Sensitivity of O₃ and Ox production budgets

3.2.1. O₃ time series from the eight solvent sector speciations

The sensitivity of modelled O_3 to the NMVOC speciation specified by the EIs listed in Table 1 is shown in Fig. 3 for each chemical mechanism. The top plot in the figure compares the time series of the O_3 mixing ratios obtained in each model run with tuned NO emissions for each speciation, grouped by mechanism. To quantify the differences in the amount of ozone produced by the different speciations, the maximum difference between the speciations at every model time step (20 min) was calculated. The mean and standard deviation of the maximum differences were then calculated for each day and the entire time period. These values indicate the effect that speciation has on ozone levels within one
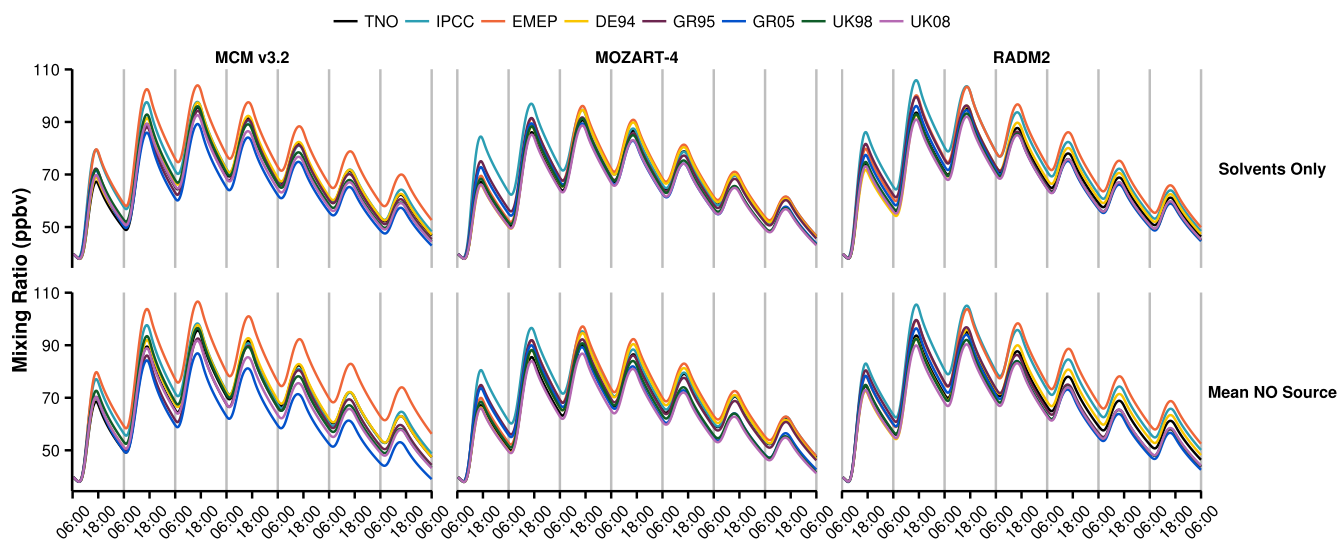
Fig. 3. O_3 mixing ratios produced during the box model run with (top) tuned NO emissions and (bottom) mean NO emissions. The only variation among the runs for each mechanism was the solvent sector speciation and for the tuned NO runs the NO emissions tuned for maximum O_3 production, while for the mean NO runs the same time series of NO emissions was used. The labels reflect the solvent sector speciation EI.

mechanism and are presented in Table 3. The mean maximum difference over the entire simulation (all days) ranged from 7.7 to 12 ppbv O_3 for the three different chemical mechanisms, which is about 11–17% of the mean modelled O_3 mixing ratio. The largest standard deviation in the maximum difference over the entire run (3.7 ppbv O_3) was found for the MOZART-4 mechanism, although this was similar for the MCM v3.2 (2.7 ppbv) and RADM2 (3.5 ppbv). The largest difference in the amount of ozone produced by the different speciations was on the first day for the MOZART-4 runs, but on the second day for the MCM v3.2 and RADM2, with differences decreasing towards the end of the seven days for all mechanisms. In all cases, the standard deviation for the individual days was largest on the first day.

The highest and lowest maxima in O_3 can also be compared, which we did for the second day of the run. In this case, the difference between the highest and lowest maxima of the second day O_3 mixing ratios were 17 ppbv for the MCM v3.2, 12 ppbv in MOZART-4 and 17 ppbv for RADM2. This statistic shows somewhat larger differences relative to the mean maximum difference across the individual time points. In general, the IPCC and EMEP speciations produced the largest O_3 mixing ratios for each chemical mechanism across the 7 days of the run, and in many cases are separated from the group of speciations producing a more similar amount of ozone for one or more days over the course of the run — in some cases for the entire duration of the run.

The results for the 'mean NO' runs were found to be similar to the results of the 'tuned NO' runs, but amplified, as shown in Fig. 3 (bottom) and Table 3. For the 'mean NO' runs the differences in the amount of ozone produced was greater between the different speciations than for the 'tuned NO' runs. This results from some speciations producing less ozone, while others produced similar amounts as in the tuned NO runs. Despite the increased differences in ozone mixing ratios, those speciations that produced the most ozone under 'tuned NO' conditions also produced the most ozone in the 'mean NO' runs and similarly for those speciations that produced lower amounts of ozone.

As an extra sensitivity study to the conditions in the study design, an additional run was done where the square size of the city was increased by a factor of 10, from 1000 sq. km to 10,000 sq. km which is still very much on the order of large cities. This resulted in roughly a factor of 10 decrease in the mean maximum difference observed across the 7 day run, ranging from an average mean maximum difference for all days of 0.9 ± 0.3 to 1.9 ± 0.4 ppbv across the three mechanisms. Interestingly however, the mean modelled ozone mixing ratio only decreased by about half, so the relative contribution of the mean maximum difference observed ranged from ca. 1.5–5.7% of the mean ozone mixing ratios. These results are summarized in Table S2. While the larger area means a smaller effect, this study was set up as an idealized test case. Furthermore,

this study investigates the differences in speciation profiles for only one sector, and from a region of the world where the sector attribution and general data quality are likely more reliable than in many other regions, therefore the results discussed here are likely conservative estimates if all sectors were to be considered and/or data from other regions.

3.2.2. O_3 mixing ratio differences owing to mechanisms

To provide a frame of reference, the amount of ozone produced by the 8 solvent sector speciations was also compared within the three mechanisms used in this study. These results are shown in Fig. 4 and summarized in Table 4. While the differences produced by mechanism choice are significant, the variation tended to be smaller in comparison to the differences observed owing to the different speciations within one mechanism. The largest mean maximum difference among the mechanisms over the model run was found for the EMEP speciation (6.7 ppbv for tuned NO runs and 8.2 ppbv for the mean NO runs). The smallest mean maximum differences were 2.1 ppbv and 3.3 ppbv for the tuned NO and mean NO runs, respectively. As was the case for the differences owing to speciation, the 'mean NO' runs in comparison to the 'tuned NO' runs led to an amplification of the differences observed but followed the same general pattern (Table 4). These results are in line with those from a much more extensive mechanism comparison study, where an 8 ppbv difference in O_3 mixing ratio was observed on the first day among 8 mechanisms (Coates and Butler, 2015).

3.2.3. Attribution of ozone production to individual NMVOCs

In order to understand the differences in modelled O_3 resulting from the different solvent sector speciations, we show both the first day and cumulative (all 7 days) Ox production budgets from the same model run allocated to the TNO EI categories for comparison in Fig. 5 (absolute amounts) and Fig. 6 (relative contribution, without CO and methane for better comparison of the NMVOC species). This allocation is possible using the tagging approach which was previously used in Butler et al. (2011) to allocate Ox production to emitted NMVOC over Los Angeles and Beijing and in Coates and Butler (2015) to compare the Ox produced over Los Angeles by several chemical mechanisms, including MOZART-4 and RADM2, to MCM v3.2.

These figures show that the importance of the different NMVOC classes for Ox production depends on whether a model run of one day or multiple days is considered. On the first day the more reactive species such as alkenes and aromatics produced the most Ox. Whereas at the end of the seven days, alkanes had the largest impact on cumulative Ox production — over half of the total Ox production budget from NMVOCs. The first day vs seven day Ox production could be considered illustrative of the role these species play in urban vs background ozone formation, respectively.

Table 3
Mean and standard deviation of the maximum difference in ozone produced by the different solvent sector speciations (solvent sector emissions only) for the tuned NO and mean NO model runs. The mean ozone mixing ratio across for the entire run is also included. Each day defined as 6am-6am.

|	Tuned NO			Mean NO		
	MCM	MOZART	RADM2	MCM	MOZART	RADM2
Day 1	8.5 ± 4.1	12 ± 6.3	11 ± 5.8	7.5 ± 4.3	9.6 ± 5.4	14 ± 7.9
Day 2	15 ± 2.5	11 ± 1.8	15 ± 1.5	17 ± 3.6	12 ± 0.81	21 ± 2.6
Day 3	14 ± 0.63	6.8 ± 0.81	13 ± 0.92	18 ± 1.2	9.3 ± 0.70	18 ± 1.2
Day 4	12 ± 0.77	6.8 ± 0.85	12 ± 0.99	18 ± 1.6	9.9 ± 1.1	15 ± 0.89
Day 5	12 ± 1.1	6.5 ± 0.56	11 ± 0.84	19 ± 1.9	9.9 ± 0.80	14 ± 1.2
Day 6	12 ± 1.1	5.6 ± 0.45	8.6 ± 0.74	20 ± 1.8	9.0 ± 0.54	13 ± 0.84
Day 7	11 ± 0.94	4.4 ± 0.39	6.4 ± 0.62	19 ± 1.5	7.5 ± 0.42	11 ± 0.63
All days	12 ± 2.7	7.7 ± 3.7	11 ± 3.5	17 ± 4.6	9.5 ± 2.4	15 ± 4.5
Mean O_3 all days	69	67	67	68	67	67
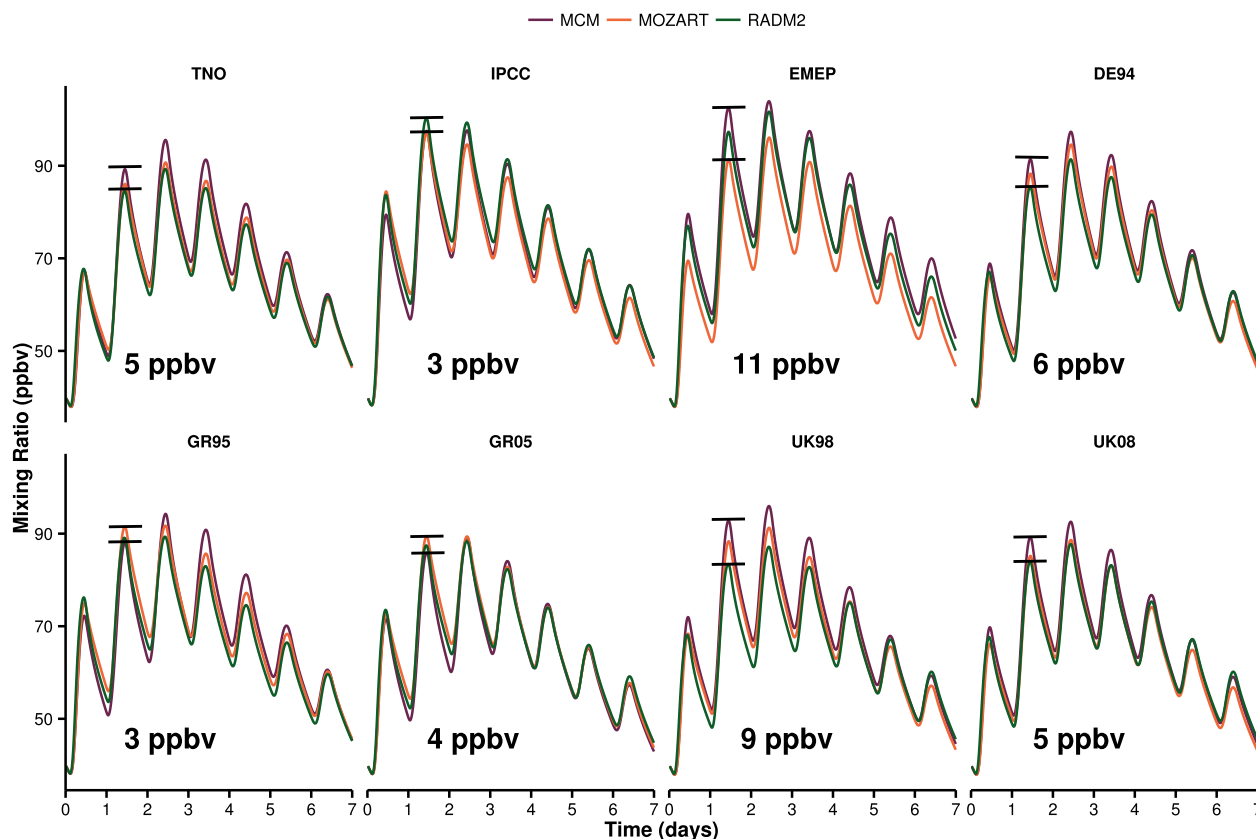
Fig. 4. As for Fig. 3, but grouped by solvent sector speciation, so as to compare the differences among mechanisms.

Table 4
Mean and standard deviation of the maximum difference in ozone produced by the same solvent sector speciation, implemented into the 3 different mechanisms.

	TNO	IPCC	EMEP	DE94	GR95	GR05	UK98	UK08
Tuned NO	3.0 ± 1.6	3.2 ± 1.2	6.7 ± 1.9	2.9 ± 1.4	3.9 ± 1.9	2.1 ± 1.7	4.2 ± 2.3	2.8 ± 1.1
Mean NO	3.3 ± 1.6	4.6 ± 1.9	8.2 ± 2.0	4.4 ± 2.9	5.4 ± 3.1	3.7 ± 2.0	5.3 ± 2.6	4.7 ± 2.1

3.2.4. Correlations between NMVOC compound class and Ox production

Section 3.2.3 showed that alkanes had the largest contribution to Ox production after seven days, whereas aromatics and alkenes have a larger contribution to Ox production in the first day. In this section, we further analyze the impact of the different compound types on Ox production by correlating the total amount of the different compound class of emissions specified in each EI with the total Ox produced during the first day and at the end of the model runs. This correlation between total Ox production at the end of the model run and the percent of total emissions that compound class represents is shown in Fig. 7 (first day results are not shown). The Pearson correlation coefficients in Fig. 7 show that EI speciation profiles specifying more alkane emissions were positively corre-lated with Ox production for the 7 day run, with r values ranging from 0.76 to 0.87 for the three chemical mechanisms. In particular, the IPCC and EMEP EI speciation profiles specify larger alkane emissions than any other EI speciation profile and in turn have the largest Ox production, as was also reflected in their O$_3$ mixing ratios at the top of the group in Fig. 3 for each mechanism. Correlation results for the first day Ox production and alkanes, still showed a positive relationship, although the correlations were less strong, with r values of 0.63 (MCM v3.2), 0.54 (MOZART-4), and 0.23 (RADM2). Given the lower reactivity and greater contributions of

alkanes to Ox production on the longer timescale, these results are in line with those from section 3.2.3.

The inverse is true for solvent sector EI speciation profiles that specify a larger contribution from oxygenated NMVOC groups, such as those for Greece, the UK, or Germany, which led to lower Ox production after seven days than EIs with lesser contributions from oxygenated species. The negative correlation ranged from −0.60 to −0.82, depending on the mechanism. These results were very similar to the first day Ox correlations, with r values ranging from −0.61 to −0.78. For aromatic species there was no consistent correlation across the mechanisms for the first day Ox or the seven day Ox, and the Pearson correlation coefficients were quite low, indicating no strong correlation between the contribution of aro-matic species to the total emissions and the total Ox production. Because not all speciations include alkenes, this correlation analysis was not carried out for alkenes.

3.3. Larger context

To consider conditions approaching more realistic conditions for the box model evaluation of the effect of NMVOC solvent sector speciation, two additional runs were done where (a) emissions for all other non-solvent anthropogenic emission sectors were added, and (b) biogenic emissions were added in addition to the other
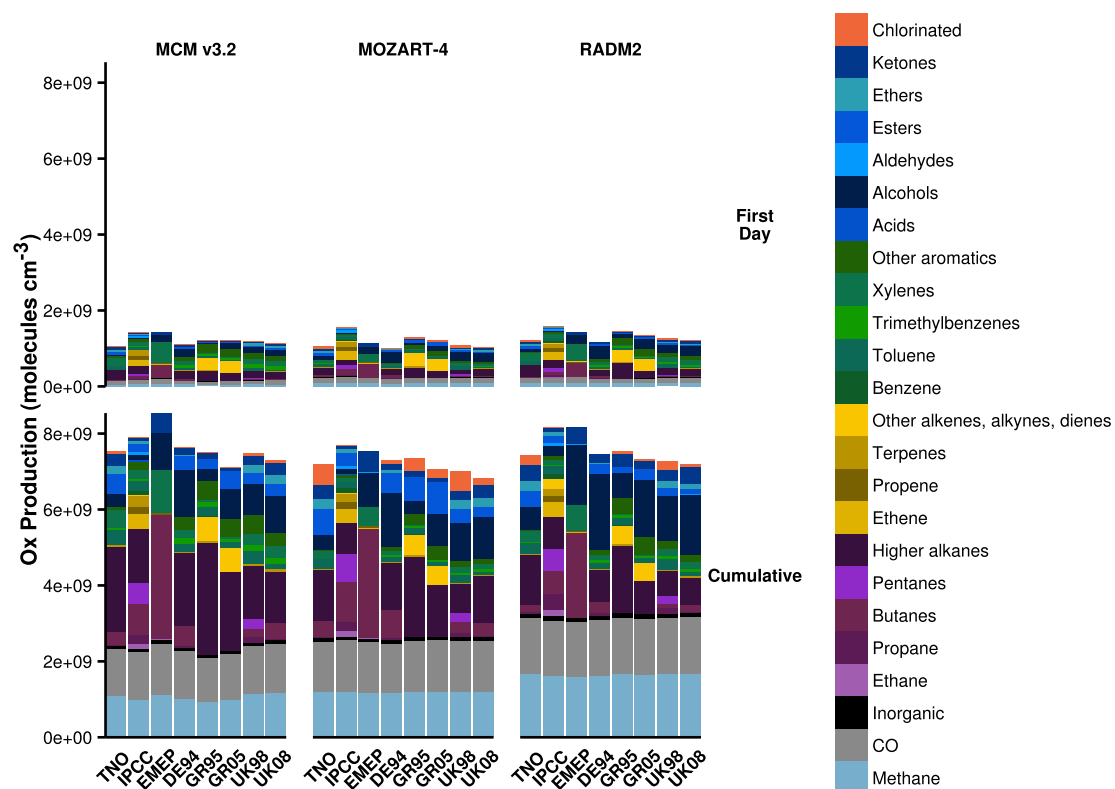
Fig. 5. The total amount of Ox produced during (top) the first day and (bottom) over entire cumulative 7-days included in the model run allocated to the NMVOC species or groups. Translated to the common basis categories for comparison.
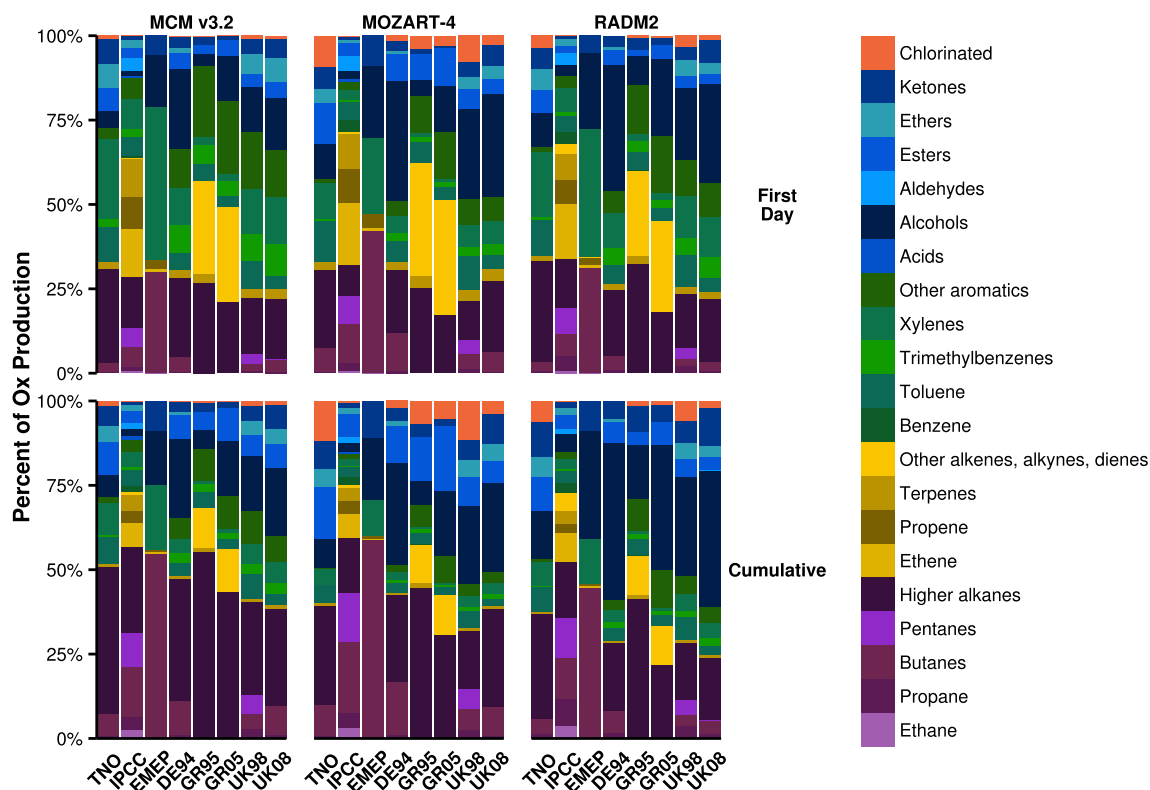
Fig. 6. As Fig. 5 but as percent contributions by mass. Carbon monoxide, methane, and inorganic species were not included in the percent contribution allocations so as to better compare the NMVOC contributions.
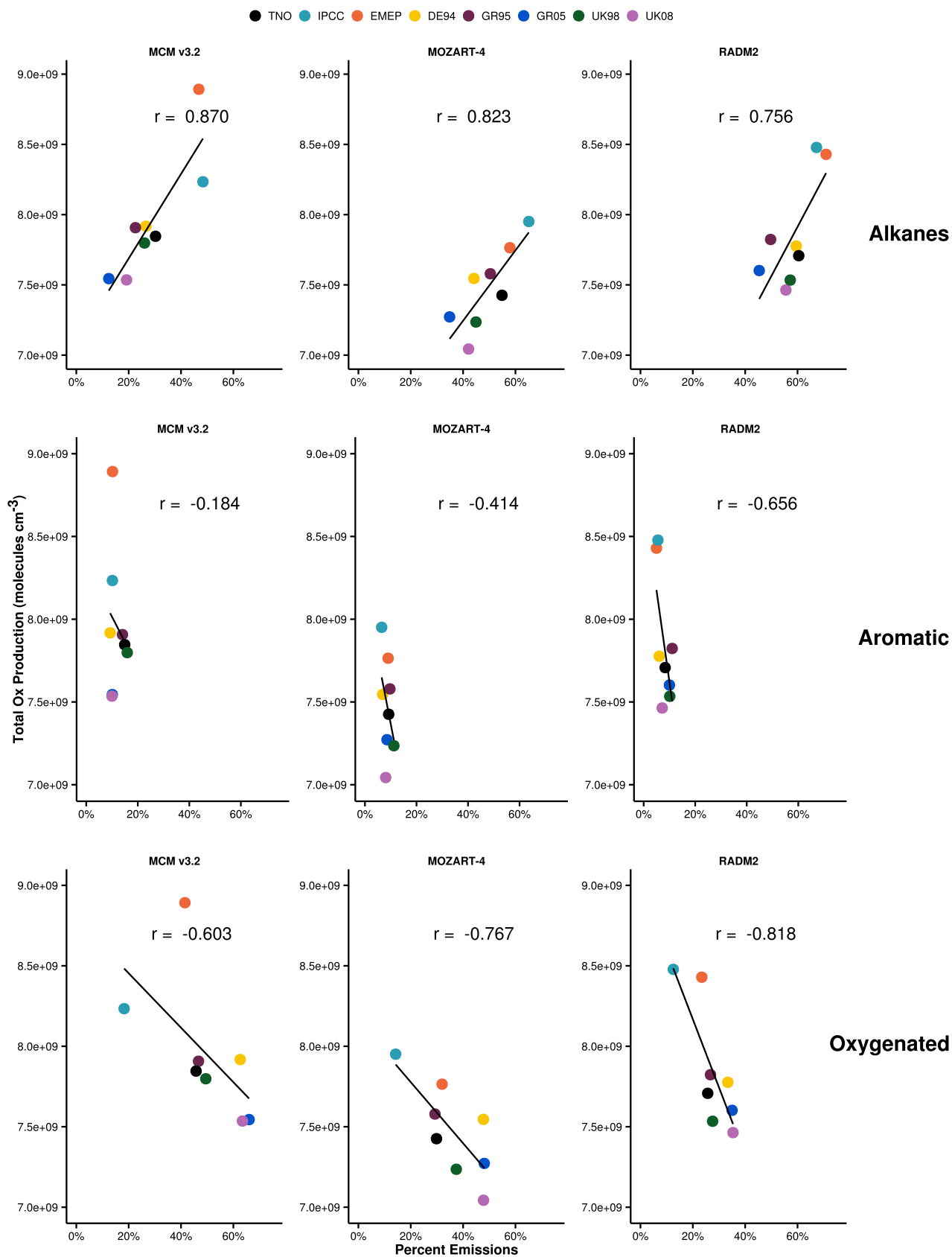
Fig. 7. Correlation of total Ox production (cumulative, 7-day) to the fraction of (top) alkanes, (middle) aromatic, and (bottom) oxygenated NMVOC emissions specified by each EI, presented by mechanism. The Pearson correlation coefficient, r, is given.

anthropogenic emission section emissions of (a). In both cases, the additional emissions were the same across all runs in terms of amount of NMVOC emissions added and speciation attributed. The only parameter varied between the runs was, as previously, the solvent sector speciation. As would be expected, the overall amount of ozone produced increased because of the tuned NO source and increase in NMVOC emissions, but the maximum difference in O_3 owing to the different solvent sector speciations decreased. Specifically, for the added anthropogenic emissions, the maximum difference in O_3 produced over the course of the entire run was 9.2, 6.2, and 7.9 ppbv for the MCM v3.2, MOZART-4, and RADM2, respectively. This implies a reduction of the impact by about ~20—30% (compare Table 5 with Table 3). In the case of the additional anthropogenic emissions plus the biogenic emissions, the maximum difference for the entire run decreased further in the case of the MCM v3.2 and MOZART-4, but remained similar for RADM2. The maximum differences calculated were not significantly different from run (a), in that the maximum differences in O_3 were within the standard deviation among the speciations between the two runs. These statistics are summarized in Table 5. The patterns in the amount of O_3 produced for the different speciations, even with the added emissions, remained the same as those in Fig. 3.

4. Discussion

While there are no studies that evaluate the role of NMVOC speciation on ozone production in the way that it is done in this study, the studies by Coll et al. (2010) and Chen et al. (2010) have significant similarities. Coll et al. (2010) evaluated the ESCOMPTE EI for the Marseille, France area in comparison to measurements for over- or under-estimation of specific hydrocarbons, followed by a model study using a regional chemical-transport model, CHIMERE, to evaluate the degree of sensitivity of the model to the emission profile inputs. The model was run a number of times with perturbations of the non-methane hydrocarbon (NMHC) profile based on the range of uncertainties from the measurement-EI evaluation. Similarly to this study, the variation was in the speciation only and the total mass of NMVOC emissions remained constant. They found that the biases in the inventory could result in differences of 2—10 ppbv in peak O_3 over the study area (Coll et al., 2010), which are quite similar to the effect quantified in the box model runs that included anthropogenic emissions from all sectors and biogenic emissions.

Chen et al. (2010) implemented a sub-mechanism in a regional chemical-transport model that allowed for tracking of all of the photochemical assessment monitoring stations (PAMS) species, which are the suite of NMVOCs measured at US EPA monitoring sites; monitoring of the suite of PAMS species has been adopted by some other countries, e.g., Taiwan. Applied to a case study in Taiwan, emissions of individual species were able to be corrected based on measurement information, with correction factors of 0.06—34, based on calculated correlations of observation and model simulations for each species. The conclusion of the study was that the detailed speciation of the VOCs in EI needs evaluation,

Table 5
Mean and standard deviation of the maximum difference in ozone produced by the different solvent sector speciations over the course of the entire 7 day run including the larger context of all other anthropogenic emissions and these plus biogenic emissions.

	MCM	MOZART	RADM2
+ Anthro emiss	9.2 ± 2.1	6.2 ± 3.4	7.9 ± 1.8
+ Anthro & bio emiss	8.7 ± 2.6	5.0 ± 2.2	8.0 ± 2.1

and that improved speciation information can improve the accurate representation of NMVOCs in models (Chen et al., 2010). While the effect on ozone production was not evaluated as part of that study, a follow-up study did evaluate the effect of improved NMVOC emissions on not only the NMVOCs themselves, but also ozone (Chen et al., 2014). In this case, the total amount of emissions were not kept constant, but increased by ca. 25%, most of which was concentrated in the alkyne and alkane NMVOC species, followed by a lesser increase in the alkene and aromatic species. These changes resulted in a change in the average ozone of 2.9 ppb, and a significant improvement in the model simulations (Chen et al., 2014). These results from Chen et al. (Chen et al., 2010, 2014) and Coll et al. (2010) indicate that, as also observed in the box modelling conducted in this study, NMVOC speciation does have an impact on the modelled ozone concentrations. In such modelling studies, the impact will also depend on whether the area of study is mainly a VOC-limited or NOx-limited ozone regime.

The majority of studies that evaluated EI have done so by comparing with measurements, and/or continue on to assess the NMVOC speciation using ozone formation potentials (OFPs) to suggest target sectors for ozone mitigation action. Such work highlights the differences in NMVOC speciation identified by measurements and source apportionment in comparison to EIs, as outlined in the introduction. These differences and the use of OFPs to inform mitigation actions emphasize the importance of accurate NMVOC speciation in EIs. The Ox production attribution results for the first day from this study (Section 3.2.3) parallel the use of OFPs. For example, Li et al. (2014) compared modelled O_3 produced from different EIs used over East Asia focusing on the representation of individual NMVOC between the EIs. They calculated the ozone formation potential of individual VOCs by multiplying the fractional contributions of the VOC emissions from its source by the Maximum Incremental Reactivity (MIR) of the VOC. MIR values were calculated in Carter (1994) using model runs of one day. This method emphasized the impact of reactive VOC which produce maximum O_3 on the first day at the expense of less-reactive VOC such as alkanes that produce maximum O_3 after the first day. These results are consistent with our first day Ox production budgets (Figs. 5 and 6), however when considering multi-day model runs, less reactive species, such as alkanes, have a higher potential to produce O_3 (Butler et al., 2011; Coates and Butler, 2015) which is also seen in Figs. 5 and 6. This large contribution of alkanes to Ox production during multi-day model runs is also seen in Butler et al. (2011) and Coates and Butler (2015).

Considering the correlation results presented in Fig. 7, when comparing the solvent sector speciations for the two different years each for Greece and the UK, the more recent EI speciations both specify a larger contribution from oxygenated NMVOC and lower contributions from alkanes than the earlier versions of the inventories. This demonstrates that the speciation of the NMVOC emissions change over time, as would be expected given changes in processes, activities, and technology. This demonstrates a need for updating not only the total NMVOC emissions as is done more frequently through yearly reporting, but also the NMVOC speciation in inventories.

A number of studies have evaluated NMVOCs based on methods similar to the first day ozone production potential used in this study, such as OFP or OH reactivity methods. Such methods estimating ozone production potential are often linked to source information and the relative contributions of sources to ozone production to inform mitigation options. For example, in the speciated NMVOC emissions for Asia developed by Li et al. (2014), of the 700 individual NMVOCs evaluated, 30 species with the highest OFPs were considered in greater detail. Of these species, 5 were oxygenated NMVOCs, while only 2 alkanes made the list,

noting that emphasis was placed on the OVOCs and alkenes because of their high contributions to the OFPs, in comparison to their contribution to mass of emissions, which was found to be quite low. Different profiles (speciation) were also evaluated and they found differences in OFP of up to a factor of 3 owing to the different profiles. This emphasizes the sensitivity of OFP to the profiles (speciation) information used (Li et al., 2014). Similarly, Gilman et al. (2009) evaluated measurements of NMVOCs in the Houston and Gavelston Bay area using OH reactivity, which is another way of estimating OFP. Their results attributed the greatest reactivity (ozone formatting potential) to oxygenated VOCs and alkenes, with increases in the OH reactivity in the area attributed to heavy influence from industrial emissions.

These different methods of assessing contribution to O_3 production would likely result in different recommendations as to which sources to focus O_3 mitigation actions on, as alkane dominated sources would not be targeted if first-day OFP methods were used in the assessment. That said, from the mitigation perspective, none of these methods includes consideration of the differences in human toxicology of the NMVOC species, either, instead focusing only on O_3 production. In a study that did consider both aspects, they found that the species contributing significantly to ozone production are often not the same as those with the highest toxicity (Laurent and Hauschild, 2014). Finally, the more reactive species will tend to be more relevant for ozone formation in e.g. urban areas, closer to the emission sources, whereas the less reactive species, such as alkanes, will react on longer timescales more relevant for background conditions.

5. Conclusions

These results show that NMVOC speciation can have a significant effect on the amount of ozone produced in an idealized system, such as a box model. While not directly representative of the real world situation, such a system is a valuable tool to study and understand sensitivities and (inter-) dependencies of a complex atmospheric chemical nature. Significant differences in modelled O_3 were obtained using detailed gas-phase chemistry (MCM v3.2) and simplified chemical mechanisms (MOZART-4 and RADM2). While Ox production is typically dominated by alkenes and aromatics in the first 24 h of the box model runs, after seven days, alkanes had the largest contribution to the total Ox production budget. Furthermore, correlations between the contribution of NMVOC compound classes to the overall NMVOC emissions and the amount of Ox produced were found to be positively correlated to alkanes and negatively correlated to oxygenated species, with no clear relationship observed for aromatics. The correlation between Ox production and amount of alkanes was less for the first day Ox than for the entire 7 days, which would be expected given their lower reactivities. These results indicates that representation of the speciation of NMVOCs in emission inventories will influence the modelled amount of ozone produced, especially when considering that these species are often lumped into compound groups. Therefore, an over- or under-representation of a certain class of compound could result in significant differences in the amount of ozone produced, over the shorter and longer term. While various ozone formation potential factors provide effective estimates as to which species are most crucial to reduce when considered over the short term (1 day), such a study also shows that some of the slower reacting NMVOCs are also important to target if ozone reductions are desired, with implications for which sources and sectors are to be considered and prioritized. This study was not designed to evaluate which solvent sector speciation is most 'correct', and therefore no recommendations are given as to which speciation should be used. An evaluation of activity data, composition of emissions, and comparison with measurements, among other factors would be needed to evaluate the emission inventories to understand which might be the best representation of reality.

One aspect not considered here was the role of NMVOCs in secondary organic aerosol (SOA) formation. In addition to the role as ozone precursors, NMVOCs are also critical precursors to SOA (Hallquist et al., 2009; Jimenez et al., 2009). NMVOC speciation information also plays an important role for understanding and modelling SOA formation, as certain classes of VOCs have been identified as more likely to lead to SOA formation owing to reactivity characteristics and subsequent oxidation products (Hallquist et al., 2009). For example, a study of NMVOC in Santiago de Chile evaluated NMVOC for their role in ozone formation, but also SOA, and found that SOA formation was strongly linked to traffic emissions, and more specifically aromatic compounds (Rappenglück et al., 2005). This aspect should be included in the evaluation of future studies, as it also has a policy relevance related to informing mitigation measures.

This study was an idealized, simplified, first evaluation of the possible effect of NMVOC speciation in emission inventories and the possible consequences for modelled ozone predictions. The simple and transparent approach of the box model studies reported here help put the impact of various parameters in perspective. The maximum impact of the speciation profile on O_3 mixing ratios ranged from 7.7 to 17 ppbv; this was about 10—25% of the average O_3 mixing ratios in the box model runs. The choice of mechanism had about half that impact (3—12%). Both the speciation and the choice of chemical mechanism have an effect on the modelled O_3 concentrations. Given the results of this study where the maximum potential difference in modelled ozone was assessed, further work is recommended to conduct a similar study to evaluate the role of NMVOC speciation under more realistic conditions in a regional and/or global chemical-transport model. Such a study has been initiated by the authors. The result of this study has, and further evaluation will have implications for the necessity of updated NMVOC speciation in emission inventories, as well as the amount of detail appropriate to provide regarding speciation, which could lead to improved capacity of models to capture ambient concentrations of ozone. Current efforts to address the improvement or updating of speciation of NMVOCs in emission inventories and for use in modelling could benefit significantly from regulatory authorities including speciation information along with the emissions reporting, which is currently not the case for the vast majority of countries.

Finally, the combination of a couple of factors could lead to significant changes in the overall NMVOC speciation representation for total NMVOCs in EI. Specifically, the disagreement between the measurements and reported (EI) data as to the contribution of different sectors to NMVOC emissions, as outlined in the introduction and the radically different NMVOC speciation profiles between e.g. the solvent use and road transport sectors. Furthermore, the differences assessed here were based on data from Europe. In regions where data is much sparser and/or less reliable, such as developing nations, the differences are likely to be greater and therefore the results here are likely a conservative estimate in terms of overall ozone impacts. Given the result of this study, which shows significant differences in the amount of O_3 produced for the various speciation profiles available for within one sector, a much greater difference in speciation owing to large shifts in the contributions of different sectors to NMVOC emissions could result in even greater differences in the speciation of NMVOC emissions and thereby atmospheric reactivity, chemistry, and ambient concentrations of O_3, and possibly other species, as they are represented and assessed in models.

Acknowledgements

Appendix A. Supplementary data

Supplementary data related to this article can be found at http://dx.doi.org/10.1016/j.atmosenv.2016.03.057.

References

Atkinson, R., 2000. Atmospheric chemistry of VOCs and NO(x). Atmos. Environ. 34, 2063–2101.

Bloss, C., Wagner, V., Jenkin, M.E., Volkamer, R., Bloss, W.J., Lee, J.D., Heard, D.E., Wirtz, K., Martin-Reviejo, M., Rea, G., Wenger, J.C., Pilling, M.J., 2005. Development of a detailed chemical mechanism (MCMv3.1) for the atmospheric oxidation of aromatic hydrocarbons. Atmos. Chem. Phys. 5, 641–664.

Borbon, A., Gilman, J.B., Kuster, W.C., Grand, N., Chevaillier, S., Colomb, A., Dolgorouky, C., Gros, V., Lopez, M., Sarda-Esteve, R., Holloway, J., Stutz, J., Petetin, H., McKeen, S., Beekmann, M., Warneke, C., Parrish, D.D., De Gouw, J.A., 2013. Emission ratios of anthropogenic volatile organic compounds in northern mid-latitude megacities: observations versus emission inventories in Los Angeles and Paris. J. Geophys. Res. Atmos. 118, 2041–2057.

Borbon, A., Locoge, N., Veillerot, M., Galloo, J.C., Guillermo, R., 2002. Characterisation of NMHCs in a French urban atmosphere: overview of the main sources. Sci. Total Environ. 292, 177–191.

Boynard, A., Borbon, A., Leonardis, T., Barletta, B., Meinardi, S., Blake, D.R., Locoge, N., 2014. Spatial and seasonal variability of measured anthropogenic non-methane hydrocarbons in urban atmospheres: implication on emission ratios. Atmos. Environ. 82, 258–267.

Brulfert, G., Chollet, J.P., Jouve, B., Villard, H., 2005. Atmospheric emission inventory of the Maurienne valley for an atmospheric numerical model. Sci. Total Environ. 349, 232–248.

Builtjes, P., Loon, M.v., Schaap, M., Teeuwisse, S., Visschedijk, A., Bloos, J., 2002. The Development of an Emission Data Base over Europe Adn Further Contributions of TNO-MEP. TNO Environment, Energy and Process Innovation, Apeldoorn, The Netherlands.

Butler, T.M., Lawrence, M.G., Taraborrelli, D., Lelieveld, J., 2011. Multi-day ozone production potential of volatile organic compounds calculated with a tagging approach. Atmos. Environ. 45, 4082–4090.

Carter, W.P.L., 1994. Development of ozone reactivity scales for volatile organic compounds. J. Air Waste Manag. Assoc. 44, 881–899.

Chen, S.-P., Liu, T.-H., Chen, T.-F., Yang, C.-F.O., Wang, J.-L., Chang, J.S., 2010. Diagnostic modeling of PAMS VOC observation. Environ. Sci. Technol. 44, 4635–4644.

Chen, S.-P., Liu, W.-T., Ou-Yang, C.-F., Chang, J.S., Wang, J.-L., 2014. Optimizing the emission inventory of volatile organic compounds (VOCs) based on network observations. Atmos. Environ. 84, 1–8.

Coates, J., Butler, T.M., 2015. A comparison of chemical mechanisms using tagged ozone production potential (TOPP) analysis. Atmos. Chem. Phys. 15, 8795–8808.

Coll, I., Rosseau, C., Barletta, B., Meinardi, S., Blake, D.R., 2010. Evaluation of an urban NMHC emission inventory by measurements and impact on CTM results. Atmos. Environ. 44, 3843–3855.

EEA, 2013. Non-methane Volatile Organic Compounds (NMVOC) Emissions. European Environment Agency (EEA). http://www.eea.europa.eu/data-and-maps/indicators/eea-32-non-methane-volatile-1/assessment-4#toc-2.

Ehhalt, D., Prather, M., Dentener, F., Derwent, R., Dlugokencky, E., Holland, E., Isaksen, I., Katima, J., Kirchhoff, V., Matson, P., Midgley, P., Wang, M., 2001. Atmospheric chemistry and greenhouse gases. In: Houghton, J.T., Ding, Y., Griggs, D.J., Noguer, M., Linden, P.J.v.d., Dai, X., Maskell, K., Johnson, C.A. (Eds.), Climate Change 2001: the Scientific Basis. Contribution of Working Group I to the Third Assessment Report of the Intergovernmental Panel on Climate Change. Cambridge University Press, Cambridge, United Kingdom and New York, NY, USA, p. 881.

Emmons, L.K., Walters, S., Hess, P.G., Lamarque, J.-F., Pfister, G.G., Fillmore, D., Granier, C., Guenther, A., Kinnison, D., Laepple, T., Orlando, J., Tie, X., Tyndall, G., Wiedinmyer, C., Baughcum, S.L., Kloster, S., 2010. Description and evaluation of the model for ozone and related chemical tracers, version 4 (MOZART-4). Geosci. Model Dev. 3, 43–67.

Friedrich, R., Wickert, B., Blank, P., Emeis, S., Engelwald, W., Hassel, D., Hoffmann, H., Michael, H., Obermeier, A., Schäfer, K., Schmitz, T., Sedlmaier, A., Stockhause, M., Theloke, J., Weber, F.-J., 2002. Development of emission models and improvement of emission data for Germany. J. Atmos. Chem. 42, 179–206.

Gilman, J.B., Kuster, W.C., Goldan, P.D., Herndon, S.C., Zahniser, M.S., Tucker, S.C., Brewer, W.A., Lerner, B.M., Williams, E.J., Harley, R.A., Fehsenfeld, F.C., Warneke, C., De Gouw, J.A., 2009. Measurements of volatile organic compounds during the 2006 TexAQS/GoMACCS campaign: industrial influences, regional characteristics, and diurnal dependencies of the OH reactivity. J. Geophys. Res. Atmos. 114, D011525.

Gilman, J.B., Lerner, B.M., Kuster, W.C., De Gouw, J.A., 2013. Source signature of volatile organic compounds from oil and natural gas operations in northeastern Colorado. Environ. Sci. Technol. 47, 1297–1305.

Goodwin, J., 2000. UK Emissions of Air Pollutants 1970 to 1998. DEFRA, Didcot, UK.

Hallquist, M., Wenger, J.C., Baltensperger, U., Rudich, Y., Simpson, D., Claeys, M., Dommen, J., Donahue, N.M., George, C., Goldstein, A.H., Hamilton, J.F., Herrmann, H., Hoffmann, T., Iinuma, Y., Jang, M., Jenkin, M.E., Jimenez, J.L., Kiendler-Scharr, A., Maenhaut, W., McFiggans, G., Mentel, T.F., Monod, A., Prévôt, A.S.H., Seinfeld, J.H., Surratt, J.D., Szmigielski, R., Wildt, J., 2009. The formation, properties and impact of secondary organic aerosol: current and emerging issues. Atmos. Chem. Phys. 9, 5155–5236.

Jenkin, M.E., Saunders, S.M., Pilling, M.J., 1997. The tropospheric degradation of volatile organic compounds: a protocol for mechanism development. Atmos. Environ. 31, 81–104.

Jenkin, M.E., Saunders, S.M., Wagner, V., Pilling, M.J., 2003. Protocol for the development of the Master Chemical Mechanism, MCM v3 (Part B): tropospheric degradation of aromatic volatile organic compounds. Atmos. Chem. Phys. 3, 181–193.

Jimenez, J.L., Canagaratna, M.R., Donahue, N.M., Prevot, A.S.H., Zhang, Q., Kroll, J.H., DeCarlo, P.F., Allan, J.D., Coe, H., Ng, N.L., Aiken, A.C., Docherty, K.S., Ulbrich, I.M., Grieshop, A.P., Robinson, A.L., Duplissy, J., Smith, J.D., Wilson, K.R., Lanz, V.A., Hueglin, C., Sun, Y.L., Tian, J., Laaksonen, A., Raatikainen, T., Rautiainen, J., Vaattovaara, P., Ehn, M., Kulmala, M., Tomlinson, J.M., Collins, D.R., Cubison, M.J., Dunlea, E.J., Huffman, J.A., Onasch, T.B., Alfarra, M.R., Williams, P.I., Bower, K., Kondo, Y., Schneider, J., Drewnick, F., Borrmann, S., Weimer, S., Demerjian, K., Salcedo, D., Cottrell, L., Griffin, R., Takami, A., Miyoshi, T., Hatakeyama, S., Shimono, A., Sun, J.Y., Zhang, Y.M., Dzepina, K., Kimmel, J.R., Sueper, D., Jayne, J.T., Herndon, S.C., Trimborn, A.M., Williams, L.R., Wood, E.C., Middlebrook, A.M., Kolb, C.E., Baltensperger, U., Worsnop, D.R., 2009. Evolution of organic aerosols in the atmosphere. Science 326, 1525–1529.

Laurent, A., Hauschild, M.Z., 2014. Impacts of NMVOC emissions on human health in European countries for 2000-2010: use of sector-specific substance profiles. Atmos. Environ. 85, 247–255.

Li, M., Zhang, Q., Streets, D.G., He, K.B., Cheng, Y.F., Emmons, L.K., Huo, H., Kang, S.C., Lu, Z., Shao, M., Su, H., Yu, X., Zhang, Y., 2014. Mapping Asian anthropogenic emissions of non-methane volatile organic compounds to multiple chemical mechanisms. Atmos. Chem. Phys. 14, 5617–5638.

Mannschreck, K., Klemp, D., Kley, D., Friedrich, R., Kühlwein, J., Wickert, B., Matuska, P., Habram, M., Slemr, F., 2002. Evaluation of an emission inventory by comparison of modelled and measured emission ratios of individual HCs, CO and NOx. Atmos. Environ. 36, S81–S94.

Murrells, T.P., Passant, N.R., Thistlethwaite, G., Wagner, A., Li, Y., Bush, T., Norris, J., Walker, C., Stewart, R.A., Tsagatakis, I., Whiting, R., Conolly, C., Okamura, S., Peirce, M., Sneddon, S., Webb, J., Thomas, J., MacCarthy, J., Choudrie, S., Brophy, N., 2010. UK Emissions of Air Pollutants 1970 to 2008. DEFRA, Didcot, UK.

NETC, 2000. UK Emissions of Air Pollutants 1970 to 1998. National Environmental Technology Centre. http://uk-air.defra.gov.uk/assets/documents/reports/empire/naei/annreport/annrep98/naei98.html. accessed 2014.

Niedojadlo, A., Becker, K.H., Kurtenbach, R., Wiesen, P., 2007. The contribution of traffic and solvent use to the total NMVOC emission in a German city derived from measurements and CMB modelling. Atmos. Environ. 41, 7108–7126.

Olivier, J.G.J., Berdowski, J.J.M., Peters, J.A.H.W., Bakker, J., Visschedijk, A.J.H., Bloos, J.J., 2001. Applications of EDGAR. Including Description of EDGAR 3.0: Reference Database with Trend Data for 1970-1995. RIVM, Bilthoven.

Olivier, J.G.J., Aardenne, J.A.V., Dentener, F.J., Pagliari, V., Ganzeveld, L.N., Peters, J.A.H.W., 2005. Recent trends in global greenhouse gas emissions: regional trends 1970-2000 and spatial distribution of key sources in 2000. Environ. Sci. 2, 81–99.

Passant, N., 2002. Speciation of UK Emissions of Non-methane Volatile Organic Compounds. DEFRA, Oxon, UK.

Pétron, G., Frost, G., Miller, B.R., Hirsch, A.I., Montzka, S.A., Karion, A., Trainer, M., Sweeney, C., Andrews, A.E., Miller, L., Kofler, J., Bar-Ilan, A., Dlugokencky, E.J., Patrick, L., Moore Jr., C.T., Ryerson, T.B., Siso, C., Kolodzey, W., Lang, P.M., Conway, T., Novelli, P., Masarie, K., Hall, B., Guenther, D., Kitzis, D., Miller, J., Welsh, D., Wolfe, D., Neff, W., Tans, P., 2012. Hydrocarbon emissions characterization in the Colorado front range: a pilot study. J. Geophys. Res. Atmos. 117, D016360.

Pouliot, G., Pierce, T., Denier van der Gon, H., Schaap, M., Moran, M., Nopmongcol, U., 2012. Comparing emission inventories and model-ready emission datasets between Europe and North America for the AQMEII project. Atmos. Environ. 53, 4–14.

Rappenglück, B., Schmitz, R., Bauerfeind, M., Cereceda-Balic, F., Von Baer, D., Jorquera, H., Silva, Y., Oyola, P., 2005. An urban photochemistry study in Santiago de Chile. Atmos. Environ. 39, 2913–2931.

Rickard, A., Young, J., Pilling, M., Jenkin, M., Pascoe, S., Saunders, S., 2015. The Master Chemical Mechanism Version MCM v3.2.

Sander, R., Kerkweg, A., Jöckel, P., Lelieveld, J., 2005. Technical note: the new comprehensive atmospheric chemistry module MECCA. Atmos. Chem. Phys. 5, 445–450.

Saunders, S.M., Jenkin, M.E., Derwent, R.G., Pilling, M.J., 2003. Protocol for the development of the Master Chemical Mechanism, MCM v3 (Part A): tropospheric degradation of non-aromatic volatile organic compounds. Atmos. Chem. Phys. 3, 161–180.

Schultz, M.G., Backman, L., Balkanski, Y., Bjoerndalsaeter, S., Brand, R., Burrows, J.P.,

Dalsoeren, S., Vasconcelos, M.d., Grodtmann, B., Hauglustaine, D.A., Heil, A., Hoelzemann, J.J., Isaksen, I.S.A., Kaurola, J., Knorr, W., Ladstaetter-Weißenmayer, A., Mota, B., Oom, D., Pacyna, J., Panasiuk, D., Pereira, J.M.C., Pulles, T., Pyle, J., Rast, S., Richter, A., Savage, N., Schnadt, C., Schulz, M., Spessa, A., Staehelin, J., Sundet, J.K., Szopa, S., Thonicke, K., Bolscher, M.v.h., Noije, T.v., Velthoven, P.v., Vik, A.F., Wittrock, F., 2007. In: Schultz, M.G. (Ed.), REanalysis of the TROpospheric Chemical Composition over the Past 40 Years (RETRO). Max Planck Institute for Meteorology, Jülich/Hamburg, Germany.

Sidiropoulos, C., Tsilingiridis, G., 2007. Composition change of NMVOC emissions from solvent use in greece for the period 1990-2005. Fresenius Environ. Bull. 16, 1108–1112.

Simpson, D., Benedictow, A., Berge, H., Bergström, R., Emberson, L.D., Fagerli, H., Flechard, C.R., Hayman, G.D., Gauss, M., Jonson, J.E., Jenkin, M.E., Nyiri, A., Richter, C., Semeena, V.S., Tsyro, S., Tuovinen, J.-P., Valdebenito, A., Wind, P., 2012. The EMEP MSC-W chemical transport model - technical description. Atmos. Chem. Phys. 12, 7825–7865.

Shao, M., Lu, S., Liu, Y., Xie, X., Chang, C., Huang, S., Chen, Z., 2009. Volatile organic compounds measured in summer in Beijing and their role in ground-level ozone formation. J. Geophys. Res. Atmos. 114, D010863.

Slemr, F., Baumbach, G., Blank, P., Corsmeier, U., Fiedler, F., Friedrich, R., Habram, M., Kalthoff, N., Klemp, D., Kühlwein, J., Mannschreck, K., Möllmann-Coers, M., Nester, K., Panitz, H.J., Rabl, P., Slemr, J., Vogt, U., Wickert, B., 2002. Evaluation of modeled spatially and temporarily highly resolved emission inventories of photosmog precursors for the city of Augsburg: the experiment EVA and its major results. J. Atmos. Chem. 42, 207–233.

Stockwell, W.R., Middleton, P., Chang, J.S., Xiaoyan, T., 1990. The second generation regional acid deposition model chemical mechanism for regional air quality modeling. J. Geophys. Res. 95, 16,343–316,367.

Thompson, C.R., Hueber, J., Helmig, D., 2014. Influence of oil and gas emissions on ambient atmospheric non-methane hydrocarbons in residential areas of Northeastern Colorado. Elem. Sci. Anthr. 2, 1–17.

Vega, E., Mugica, V., Carmona, R.o., Valencia, E., 2000. Hydrocarbon source apportionment in Mexico City using the chemical mass balance receptor model. Atmos. Environ. 34, 4121–4129.

Warneke, C., McKeen, S.A., de Gouw, J.A., Goldan, P.D., Kuster, W.C., Holloway, J.S., Williams, E.J., Lerner, B.M., Parrish, D.D., Trainer, M., Fehsenfeld, F.C., Kato, S., Atlas, E.L., Baker, A., Blake, D.R., 2007. Determination of urban volatile organic compound emission ratios and comparison with an emissions database. J. Geophys. Res. Atmos. 112, D007930.

Zheng, J., Shao, M., Che, W., Zhang, L., Zhong, L., Zhang, Y., Streets, D., 2009. Speciated VOC emission inventory and spatial patterns of ozone formation potential in the Pearl River Delta, China. Environ. Sci. Technol. 43, 8580–8586.

Table S1a. NMVOC Speciation, Composite Profile for SNAP 6 (Solvents), percent contribution by mass to the total (Passant, 2002).

Compound or Group	(%)
ethanol	9.40
methanol	6.40
toluene	5.20
acetone	5.00
butane	4.40
trichloroethene	4.00
m-xylene	3.20
2-butanone	3.00
ethyl acetate	2.80
4-methyl-2-pentanone	2.50
1,1,1-trichloroethane	2.20
dichloromethane	2.00
decane	1.80
1,2,4-trimethylbenzene	1.70
hexane	1.60
2-propanol	1.60
tetrachloroethene	1.50
butyl acetate	1.40
ethylbenzene	1.20
1-butanol	1.20
methylethylbenzene	1.00
nonane	1.00
1-propanol	1.00
undecane	0.90
propane	0.90
2-butanol	0.80
o-xylene	0.80
p-xylene	0.80
2-propyl acetate	0.70
dipentene	0.60
ethyldimethylbenzene	0.60
4-methyldecane	0.50
1,3,5-trimethylbenzene	0.50
1,2,3-trimethylbenzene	0.50
2-methyl-1-propanol	0.50
2-methylpentane	0.40
3-methylnonane	0.40
3-ethyl-2-methylheptane	0.40
2-butoxyethanol	0.40
4-methyl-4-hydroxy-2-pentanone	0.40
2-(2-butoxyethoxy)ethanol	0.40
heptane	0.40
3-methylpentane	0.40
1-methoxy-2-propanol	0.40
cyclohexane	0.40
2-(2-ethoxyethoxy)ethanol	0.40
2-methylnonane	0.40
propylcyclohexane	0.40
unspeciated aromatic hydrocarbons	0.40
2,6-dimethyloctane	0.40
C10 cycloalkanes	0.30
3-methylhexane	0.30
2-methylhexane	0.30
3-methyldecane	0.30
C11 alkanes	0.30
(1-methylpropyl)cyclohexane	0.30
4-methylnonane	0.30
1-methyl-4-isopropylcyclohexane	0.30

propyl acetate	0.30
propylbenzene	0.30
1-ethoxy-2-propanol	0.30
1-methyl-4-isopropylbenzene	0.30
2-methyldecane	0.30
butylcyclohexane	0.30
methylcyclopentane	0.30
styrene	0.30
1,4-dichlorobenzene	0.30
C10 alkanes	0.30
benzyl alcohol	0.30
ethylene glycol	0.30
3-ethyltoluene	0.30
methylpropylbenzene	0.30
1-ethyl-3-methylcyclohexane	0.30
1,2-propanediol	0.20
1-(2-butoxy-1-methyl-ethoxy)-2-propanol	0.20
2,2,4-trimethyl-1,3-pentanediol	0.20
monoisobutyrate	-
tri-n-butyl phosphate	0.20
1,2,3,5-tetramethylbenzene	0.20
1-methoxy-2-propyl acetate	0.20
cyclohexanone	0.20
2-ethoxyethanol	0.20
2-methylpropane	0.20
2-ethoxyethyl acetate	0.20
tetradecane	0.20
dimethylcyclopentane	0.20
(1-methylethyl)cyclohexane	0.20
(2-methylpropyl)cyclohexane	0.20
1-methyl-3-propylbenzene	0.20
2-butoxyethyl acetate	0.20
methylcyclohexane	0.20
1,2,4,5-tetramethylbenzene	0.20
pine oil	0.10
1,2,3-trimethylcyclohexane	0.10
5-methyldecane	0.10
2-[2-(2-ethoxy-ethoxy)-ethoxy]ethanol	0.10
4-methyloctane	0.10
2-methyloctane	0.10
2-(methoxyethoxy)ethanol	0.10
1-ethoxy-2-propyl acetate	0.10
2,5-dimethyloctane	0.10
2-methoxyethanol	0.10
1-(2-methoxy-1-methyl-ethoxy)-2-propanol	0.10
1-(2-ethoxy-1-methyl-ethoxy)-2-propanol	0.10
2-isopropoxyethanol	0.10
3,4-dimethylheptane	0.10
3-methyloctane	0.10
1,2,3,4-tetramethylbenzene	0.10
2,2,3,3-tetramethylhexane	0.10
1-ethyl-4-methylcyclohexane	0.10
dodecane	0.10
dimethyl ether	0.10
4-ethyltoluene	0.10
2-(2-butoxyethoxy)ethyl acetate	0.10
2-(2-ethoxyethoxy)ethyl acetate	0.10
unspeciated hydrocarbons	0.10
(2-methyl-1-propyl)acetate	0.10
2-methoxyethyl acetate	0.10
3,3-dimethyloctane	0.10
ethylcyclohexane	0.10

2-methyl-5-ethyloctane	0.10
3,7-dimethylnonane	0.10
C12 alkanes	0.10
decalin	0.10
2,3-dimethylheptane	0.10
3-ethylheptane	0.10
1-methoxy-2-ethanol	0.10
indan	0.10
unspeciated/other species	6.40

Table S1b. TNO NMVOC Speciation Profile for SNAP 6 (Solvents) in percent contribution by mass, European Average (Builtjes et al. 2002).

Compound or Group	(%)
acids	0
alcohols	9.2
benzene	0
butanes	0
chlorinated HCs	12
esters	11
ethane	0
ethene	0
ethers	4.6
ethyne	0
hexanes&higher alkanes	31
ketones	10
methanal	0
other alk(adi)enes&alkynes	0
other alkanals	0
other aromatics	1.6
others	4.1
pentanes	0
propane	0
propene	0
toluene	8.0
trimethylbenzenes	0
xylene	8.0

Table S1c. IPCC NMVOC speciation profile for all sectors, including solvents, in percent contribution by mass to total (Ehhalt et al., 2001).

Species	(%)
Alcohols	3.2
Ethane	4.7
Propane	5.5
Butanes	10.9
Pentanes	9.4
Higher alkanes	18.2
Ethene	5.2
Propene	2.4
Ethyne	2.2
Other alkenes, alkynes, dienes	3.8
Benzene	3
Toluene	4.9
Xylene	3.6
Trimethylbenzene	0.7
Other aromatics	3.1
Esters	1.4
Ethers	1.7
Chlorinated HC's	0.5
Formaldehyde	0.5
Other aldehydes	1.6
Ketones	1.9

Acids	3.6		
Others	8.1		

Table S1d. NMVOC speciation profile provided in the EMEP model for the solvent sector, in percent contribution by mass to the total (Simpson et al., 2012).

Compound or Group	(%)
Ethane	0.44
n-Butane	44
Ethene	0.24
Propene	0.68
Isoprene	0.008
o-Xylene	18
Methanol	6.1
Ethanol	16
Formaldehyde	0.011
Acetaldehyde	0
Methylethylketone	10
Glyoxal	0
Methylglyoxal	0
Unreacted	4.2

Table S1e. NMVOC speciation profile for the solvent sector for Germany in 1994, in percent contribution by mass to the total (Friedrich et al., 2002).

Compound or Group	(%)
aliphatic hydrocarbons	35
alcohols	25
aromatic compounds	14
esters	8
glycol derivatives	7
ketones	5
halocarbons	2
ethers	1
terpenes	1
Others	2

Table S1f. NMVOC speciation profile for the solvent sector for Greece, in percent contribution by mass to the total (Sidiropoulos and Tsilingiridis, 2007).

Compound or Group	1995	2000	2005
methylenechloride	0.7	0	0.6
tetrachloroethylene	1.5	1.5	1.2
trichloroethylene	1.2	1.5	0.6
1,1,1-trichloroethane	0	-	-
trichlorotrifluoromethane	0	0	-
trichlorofluoromethane	0.2	0	0.2
white spirit	40.9	27.7	34.5
creosote oil	17.7	9.1	0.9
vinyl acetate	7.3	11.6	8.4
ethyl acetate	5.2	8.6	7.7
Acetone	5.5	5.7	4.2
methanol	9.2	15.4	22.6
Benzenes	0.1	0	0
Toluenes	-	0	0
Xylenes	-	-	0
turpentine	0.5	4	0
cyclohexane	0	0	0
Butanone	0.1	0.1	0.1
cyclohexanone	0	0	0
methylisobutylketone	0.9	0.4	0.2
hexylene glycone	0.1	0	0
ethylene glycol	1	2.5	4.8

ethylbenzene	-	0	-
Benzene	-	0	-
Isomers of xylene	0.3	0.4	0.4
o-xylene	-	0	-
Styrene	4	5.6	7.8
Toluene	2.2	2.9	2.3
n-butyl alcohol	0.2	0.3	0.3
diacetone alcohol	0	0.1	0.2
cyclo hexanole	0	0	0
n-butyl acetate	1.2	2.5	2.9

Table S1g. UK National Atmospheric Emission Inventory NMVOC speciation profile for solvent use, in percent contribution by mass to the total, for 1998 (Goodwin, 2000), for 2008 (Murrells et al., 2010).

Compound or Group	1998	2008
Ethanol	10	11
Butane	2.7	5.1
Ethane	0.0	0.0
Propane	2.7	1.0
methanol	0.70	7.8
Toluene	6.6	2.9
Ethylene	0.0	-
Acetone	2.1	4.8
Pentane	3.4	0.12
benzene	0.0	0.00
2-methylbutane	0.0	0.013
m-xylene	3.2	3.1
hexane	1.0	0.67
trichloroethene	4.0	3.3
formaldehyde	0.0	0.0067
2-methylpropane	0.0	0.26
2-butanone	2.4	3.1
dichloromethane	2.0	2.7
decane	2.2	2.1
1,2,4-trimethylbenzene	1.5	1.4
propylene	0.0	0.0
butyl acetate	1.7	2.6
heptane	0.064	0.40
ethylbenzene	1.2	1.2
2-propanol	2.0	2.1
octane	0.092	0.34
ethyl acetate	2.7	1.8
p-xylene	0.78	0.83
o-xylene	0.80	0.77
4-methyl-2-pentanone	1.4	1.5
tetrachloroethene	1.4	1.5
nonane	1.3	1.3
undecane	1.2	1.1
acetylene	0.0	0.0
1-butanol	1.6	1.0
1,3,5-trimethylbenzene	0.57	0.48
1-propanol	1.8	0.92
2-methylpentane	0.0	0.32
2-butoxyethanol	-	0.88
dipentene	-	0.84
1,2,3-trimethylbenzene	-	0.48
1,3-butadiene	0.0	-
1-methoxy-2-propanol	-	0.74
methylethylbenzene	0.0	0.69
2-methylhexane	0.0	0.21
2-butene	0.0	-
4-methyldecane	-	0.64

methyl acetate	0.0	-
methylheptanes	0.0	0.0
1,1,1-trichloroethane	3.0	0.0
2-methylpentane	0.10	0.0
paraffins other	0.0	0.0
3-methylpentane	0.090	0.0
3-ethyltoluene	0.40	0.0
4-ethyltoluene	0.20	0.0
1-butene	0.0	0.0
2-pentene	0.0	0.0
other VOCs	28	24
other grouped species	-	2.0
Unspeciated VOCs	5.3	2.1

Table S2. Mean and standard deviation of the maximum difference in ozone produced by the different solvent sector speciations (solvent sector emissions only) with tuned NO and a 10,000 sq. km area model runs. The mean ozone mixing ratio across for the entire run is also included. Each day defined as 6am-6am.

	MCMv3.2	MOZART-4	RADM2
Day 1	1.3±0.7	1.2±0.6	1.2±0.6
Day 2	2.1±0.2	1.2±0.2	1.7±0.2
Day 3	2.0±0.2	1.1±0.1	1.5±0.1
Day 4	2.1±0.2	1.0±0.1	1.3±0.1
Day 5	2.1±0.2	0.8±0.1	1.1±0.1
Day 6	1.9±0.1	0.6±0.1	0.8±0.1
Day 7	1.5±0.1	0.6±0.0	0.6±0.1
Entire Run	1.9±0.4	0.9±0.3	1.2±0.4
Mean O3 all days	37	36	40

Chapter 9

Paper III: The Influence of Temperature on Ozone Production under varying NO$_x$ Conditions – a modelling study

Chapter 10

Publication List

10.1   Scientific Articles

J. Coates and T. M. Butler. A comparison of chemical mechanisms using tagged ozone production potential (TOPP) analysis. *Atmospheric Chemistry and Physics*, 15(15):8795–8808, 2015.

E. von Schneidemesser, J. Coates, H. D. van der Gon, A. Visschedijk, and T. Butler. Variation of the NMVOC speciation in the solvent sector and the sensitivity of modelled tropospheric ozone. *Atmospheric Environment*, 135:59 – 72, 2016.

J. Coates, K. A. Mar, N. Ojha, and T. M. Butler. The influence of temperature on ozone production under varying NO_x conditions – a modelling study. *Atmospheric Chemistry and Physics Discussions*, Submitted, 2016.

10.2   Presentations

J. Coates and T. M. Butler, Comparing chemical mechanisms using Tagged Ozone Production Potentials. 2013 American Geophysical Union Fall Meeting, 10th December 2013.

J. Coates and T. M. Butler, Comparing how chemical mechanisms treat VOC degradation and impact on ozone production. 2014 PhD Conference on Earth System Science, 13th March 2014.

J. Coates and T. M. Butler, The influence of atmospheric conditions on the production

of ozone during VOC oxidation. 2015 American Geophysical Union Fall Meeting, 15th December 2015.

10.3   Posters

J. Coates and T. M. Butler, Comparing how chemical mechanisms treat VOC degradation and impact on ozone production. 2014 PhD Conference on Earth System Science, 13th March 2014.

J. Coates and T. Butler, Understanding ozone pollution: a comparison of chemical mechanisms. 2014 Our Climate Our Future Conference, 7th October 2014.

Appendix

Contribution to Paper I:

The experimental setup was designed by Tim Butler, the tagging of all chemical mechanisms and all model simulations performed by myself at the IASS. All analysis and graphical plotting of the model output data was performed by myself. The paper was written by myself assisted by Tim Butler.

Contribution to Paper II:

The experimental setup was formulated by Erika von Schneidemesser, Tim Butler and myself. Translating the NMVOC emissions into chemical mechanism species was performed by myself aided by Erika von Schneidemesser and colleagues at TNO. All model simulations and analysis of model data was performed by myself at the IASS. I prepared an initial draft of the paper which was further updated by Erika von Schneidemesser and the other co-authors.

Contribution to Paper III:

The experimental setup was designed by Tim Butler any myself. I updated the box model setup to include vertical mixing and a diurnal PBL height, and performed all model simulations at the IASS. Observational data was provided by Noelia Otero Felipe and WRF-Chem model output by Kathleen A. Mar and Narendra Ojha. Analysis and graphical plotting of the box model output data was performed by myself. The paper was written by myself aided by the co-authors.